THE NIKIFOROV-UVAROV METHOD IN THE STUDY OF THERMODYNAMIC PROPERTIES OF DIATOMIC MOLECULES

BY

MORRIS RAMANTSWANA

THE NIKIFOROV-UVAROV METHOD IN THE STUDY OF THERMODYNAMIC PROPERTIES OF DIATOMIC MOLECULES

by

MORRIS RAMANTSWANA

submitted in accordance with the requirements
for the degree of

DOCTOR OF PHILOSOPHY

in the subject

PHYSICS

at the

UNIVERSITY OF SOUTH AFRICA

SUPERVISOR : PROF. G. J. RAMPHO
JOINT SUPERVISOR : PROF. A. N. IKOT

FEBRUARY 2024

Declaration

Student : M. Ramantswana

Student No. : 5361 4593

I declare that **"THE NIKIFOROV-UVAROV METHOD IN THE STUDY OF THERMODYNAMIC PROPERTIES OF DIATOMIC MOLECULES"** is my own work and that all the sources that I have used or quoted have been indicated and acknowledged by means of complete references.

SIGNATURE DATE

Acknowledgements

I would like to thank the following individuals for encouragement and informative discussions related to this the work :

- Prof. G. J. Rampho for his encouragement, support, guidance and availability for discussions.
- Prof. A. N. Ikot (University of Port Harcourt, Nigeria) for his expert guidance and inspiration during this work.
- M. O. Tshikororo, my partner for the patience and incredible support throughout this work.
- M. S. Ramantswana, my mother for support and encouragement.
- Members of the Department of physics at Unisa for their support.

Publications

This thesis is based on the following publications:

- M. Ramantswana, G. J. Rampho, C. O. Edet, A. N. Ikot, U. S. Okorie, K. W. Qadir, H. Y. Abdullah, Determination of thermodynamic properties of CrH, NiC and CuLi diatomic molecules with the linear combination of Hulthen-type potential plus Yukawa potential, Physics Open 14 (2023) 100135.

- M. Ramantswana, A. N. Ikot, G. J. Rampho, C. O. Edet, U. S. Okorie, Thermodynamic Functions of Manning-Rosen plus a class of Yukawa potential using Euler MacLaurin Formula, Revista Mexicana de Física E 19 (2022) 020204.

- U. S. Okorie, A. N. Ikot, M. E. Udoh, M. Ramantswana, G. J. Rampho, A. Abdel-Aty and R. Sever, A statistical analysis of combined perturbed Yukawa and deformed Hulthen (PYDH) potentials in D-dimentions, SSRN 4235120.

- N. Ibrahim, U. S. Okorie, N. Sulaiman, G. J. Rampho, M. Ramantswana, Solutions of Schrödinger equation of shifted screened Kratzer potential and its thermodynamic functions using extended NU method, Frontiers in Physics 10 (2022) 988279.

- A. N. Ikot, C. O. Edet, U. S. Okorie, M. Ramantswana, G. J. Rampho, R. Horchani, H. Y. Abdullah, H. Y. Zahran, L. E. Obagboye, A.-H. Abdel-Aty, S. Kaya, Eigenfunction, uncertainties and thermal properties of the Schrödinger equation with Screened modified Kratzer potential for diatomic molecules, Indian Journal of Physics 96 (2022) 3429.

- U.S. Okorie, A.N. Ikot, G.J. Rampho, M.C. Onyeaju, M.U. Ibezim-Ezeani, Abdel-Haleem Abdel-Aty, M. Ramantswana, Bound and scattering states of the Klein-Gordon equation for shifted Tietz-Wei potential with applications to diatomic molecules, Mol. Phys. 119 (2021) e1922773.

- P. Nwabuzor, C. O. Edet, A. N. Ikot, U. S. Okorie, M. Ramantswana, R. Horchani, A.-H. Abdel-Aty, G. J. Rampho, Analyzing the Effects of Topological Defect (TD) on the Energy Spectra and Thermal Properties of LiH, TiC and I 2 Diatomic Molecules, Entropy 23 (2021) 1060.

- A. N. Ikot, C. O. Edet, U. S. Okorie, A. -H. Abdel-Aty, M. Ramantswana, G. J. Rampho, N. A. Alshehri, S. K. Elagan, S. Kaya, Solutions of the 2D Schrodinger equation and its thermal properties for improved ultra-generalized exponential hyperbolic potential (IUGE-HP), The European Physical Journal Plus 136 (2021) 434.

- C. O. Edet, A. N. Ikot, U. S. Okorie, G. J. Rampho, M. Ramantswana, R. Horchani, H. Abdullah, J. A. Vinasco, C. A. Duque, Abdel-Haleem Abdel-Aty, Persistent Current, Magnetic Susceptibility, and Thermal Properties for a Class of Yukawa Potential in the Presence of External Magnetic and Aharanov–Bohm Fields, International Journal of Thermophysics 42 (2021) 138.

Summary

Transition metal hydrides, including CrH and others, have a significant impact on chemical synthesis, serving as intermediates and in solid matrix samples for infrared spectroscopy. Moreover, the CuLi molecule provides insights into the bonding characteristics of mixed transition metal lithides. Additionally, the study of transition metal carbide molecules like TiC, NiC, and others is currently a highly active research area, driven by the necessity for accurate measurement of their chemical bonding.

This thesis explores the solution of the Schrödinger equation for the Manning-Rosen potential alongside a class of Yukawa and the Hulthén plus Yukawa potential models using the Nikiforov-Uvarov method. It obtains the energy eigenvalues and corresponding eigenfunctions in closed form. Subsequently, the partition function is computed, and various thermodynamic functions such as Helmholtz free energy, mean energy, entropy, and specific heat capacity of the system are evaluated.

Furthermore, the Schrödinger equation for the Hulthén plus Yukawa potential model is solved under the influence of magnetic and Aharonov-Bohm flux fields using the exact quantization rule. Closed-form expressions for the energy eigenvalues are derived and utilized to compute the partition function and other thermo-magnetic functions such as Helmholtz free energy, mean energy, entropy, specific heat, magnetization, and magnetic susceptibility for CuLi, CrH, and NiC diatomic molecules. These findings are relevant in condensed matter physics, chemical and molecular physics, and various other areas of physics.

Keywords: Aharonov-Bohm flux, Diatomic molecules, Hulthén potential, Magnetic fields, Manning-Rosen potential, Nikiforov-Uvarov method, Partition function, Schrödinger equation, Thermodynamic properties, Yukawa potential

Contents

1 Introduction **1**

1.1 Molecular potential models 1

1.2 Solution methods 3

1.3 The objective of this thesis 7

1.4 Structure of the thesis 9

2 Diatomic Molecules **10**

2.1 Schrödinger equation in spherical coordinates 10

2.2 The Nikiforov-Uvarov method 15

2.3 Thermo-magnetic properties. 19

2.3.1 Thermodynamic properties 19

2.3.2 Magnetic properties 24

3 Thermo-magnetic Functions **27**

3.1 Diatomic Molecular Potentials 27

3.2 Eigensolutions and thermodynamic functions with the MRCYP 32

3.2.1 Bound solutions for the MRCYP 32

3.2.2 Thermodynamic functions for the MRCYP 36

3.3 Eigensolutions and thermodynamic functions for the HYP 41

3.3.1 Bound solutions for the HYP 41

3.3.2 Thermodynamic functions for the HYP 45

3.3.3 Bound solutions for the HYP with the magnetic and AB flux fields 50

3.3.4 Thermo-magnetic functions with the HYP 54

4 Results and Discussion **58**

4.1 Results with the MRCYP 58

4.2 Results with the HYP. 68

4.2.1 Calculations without magnetic and AB flux fields 68

4.2.2 Calculations with magnetic and AB flux fields 73

5 Concluding Remarks **82**

Bibliography **85**

List of Tables

4.1 Energy eigenvalues of the MRCYP for different screening parameters δ and quantum states n and ℓ. 59

4.2 Spectroscopic parameters for CuLi, CrH, and NiC diatomic molecules. . 68

List of Figures

3.1 Comparison of the MRCYP $V(r)$ and its approximation $V'(r)$ against the separation distance r for (a) $\delta = 0.0001$; (b) $\delta = 0.001$; (c) $\delta = 0.01$. 29

3.2 Comparison of the HYP $V(r)$ and its approximation $V'(r)$ against the separation distance r for (a) CuLi diatomic molecule; (b) CrH diatomic molecule; (c) for NiC diatomic molecule. 30

3.3 The difference $\Delta V(r)$ between $V'(r)$ and $V(r)$ against the separation distance r for (a) the MRCYP; (b) the HYP. 31

3.4 Comparison between the Centrifugal term $1/r^2$ with the Greene-Aldrich approximation against the separation distance r for $\delta = 0.0001$ for the Manning-Rosen plus the class of Yukawa potential. 32

4.1 (a) Energy spectra $E_{n\ell}$ as a function of δ for various quantum states n and ℓ. (b) Energy spectra $E_{n\ell}$ as a function of potential strength V_0 for various quantum states n and ℓ. 60

4.2 (a) Energy spectra $E_{n\ell}$ as a function of μ for various quantum states n and ℓ. (b) Energy spectra $E_{n\ell}$ as a function of n for various angular momentum quantum states ℓ. 61

4.3 Energy spectra $E_{n\ell}$ as a function of ℓ for various principal quantum states n. 62

4.4 Variation of the vibrational partition function $Z(T)$ with temperature T for different values of (a) screening parameter δ; and (b) quantum states n and ℓ. 63

4.5 Variation of the vibrational free energy $F(T)$ with temperature T for different values of (a) screening parameter δ; and (b) quantum states n and ℓ. 64

4.6 (a) Variation of the vibrational mean energy $U(T)$ with temperature for different values of (a) screening parameter δ; and (b) quantum states n and ℓ. 65

4.7 (a) Variation of the vibrational entropy $S(T)$ with temperature T for different values of (a) screening parameter δ; and (b) quantum states n and ℓ. 66

4.8 Variation of the specific heat capacity $C(T)$ with temperature T for different values of (a) screening parameter δ; and (b) quantum states n and ℓ. 67

4.9 Energy spectra variation of the Hulthén plus Yukawa potential with (a) angular momentum quantum number ℓ, (b) principal quantum number n, for various diatomic molecules 69

4.10 Variation of vibrational partition function $Z(\beta)$, (b) vibrational free energy $F(\beta)$ and (c) vibrational mean energy energy $U(\beta)$, with changing temperature $\beta(K^{-1})$, for different diatomic molecules with the Hulthén plus Yukawa potential. 70

4.11 Variation of vibrational entropy $S(\beta)$ and (b) vibrational specific heat capacity energy $C(\beta)$, with changing temperature $\beta(K^{-1})$, for different diatomic molecules with the Hulthén plus Yukawa potential. 71

4.12 Variation of vibrational partition function $Z(\beta)$, (b) vibrational free energy $F(\beta)$ and (c) vibrational mean energy energy $U(\beta)$, with changing maximum quantum number $n_{\max}$, for different diatomic molecules with the Hulthén plus Yukawa potential. 72

4.13 Variation of vibrational entropy $S(\beta)$ and (b) vibrational specific heat capacity energy $C(\beta)$, with changing maximum quantum number $n_{\max}$, for different diatomic molecules with the Hulthén plus Yukawa potential. 73

4.14 Variation of (a) vibrational partition function $Z(\beta, \boldsymbol{B}, \Phi_{AB})$, (b) vibrational free energy $F(\beta, \boldsymbol{B}, \Phi_{AB})$ and (c) vibrational mean energy energy $U(\beta, \boldsymbol{B}, \Phi_{AB})$, with changing temperature $\beta(K^{-1})$, for different diatomic molecules with the Hulthén plus Yukawa potential. 74

4.15 Variation of vibrational entropy $S(\beta, \boldsymbol{B}, \Phi_{AB})$ and (b) vibrational specific heat capacity energy $C(\beta, \boldsymbol{B}, \Phi_{AB})$, with changing temperature $\beta(K^{-1})$, for different diatomic molecules with the Hulthén plus Yukawa potential. 75

4.16 Variation of (a) vibrational partition function $Z(\beta, \boldsymbol{B}, \Phi_{AB})$, (b) vibrational free energy $F(\beta, \boldsymbol{B}, \Phi_{AB})$ and (c) vibrational mean energy energy $U(\beta, \boldsymbol{B}, \Phi_{AB})$, with changing magnetic field $\boldsymbol{B}$, for different diatomic molecules with the Hulthén plus Yukawa potential. 76

4.17 Variation of vibrational entropy $S(\beta, \boldsymbol{B}, \Phi_{AB})$ and (b) vibrational specific heat capacity energy $C(\beta, \boldsymbol{B}, \Phi_{AB})$, with changing magnetic field $\boldsymbol{B}$, for different diatomic molecules with the Hulthén plus Yukawa potential. 77

4.18 Variation of (a) vibrational partition function $Z(\beta, \boldsymbol{B}, \Phi_{AB})$, (b) vibrational free energy $F(\beta, \boldsymbol{B}, \Phi_{AB})$ and (c) vibrational mean energy energy $U(\beta, \boldsymbol{B}, \Phi_{AB})$, with changing AB field ξ, for different diatomic molecules with the Hulthén plus Yukawa potential. 78

4.19 Variation of vibrational entropy $S(\beta, \boldsymbol{B}, \Phi_{AB})$ and (b) vibrational specific heat capacity energy $C(\beta, \boldsymbol{B}, \Phi_{AB})$, with changing AB field ξ, for different diatomic molecules with the Hulthén plus Yukawa potential. . 79

4.20 The magnetization $M(\beta, \boldsymbol{B}, \Phi_{AB})$ of the Hulthén plus Yukawa potential with (a) temperature $\beta(K^{-1})$, (b) magnetic field $\boldsymbol{B}(T)$ (c) AB field ξ, for different diatomic molecules. 80

4.21 The variation of the magnetic susceptibility $\chi_m(\beta, \boldsymbol{B}, \Phi_{AB})$ of the Hulthén plus Yukawa potential with (a) temperature $\beta(K^{-1})$, (b) magnetic field $\boldsymbol{B}(T)$, (c) AB field ξ, for different diatomic molecules. 81

Chapter 1

Introduction

The exact accurate solution of the Schrödinger equation (SE) holds great significance in physics and chemistry, as it allows for the determination of both the energy spectrum and the wave function. These fundamental elements contain essential information about the physical properties of quantum mechanical systems [1, 2]. In both relativistic and non-relativistic quantum mechanics, various equations such as the Schrödinger, Klein-Gordon, and Dirac equations are utilized to understand physical systems, employing potential models to describe particle interactions. However, only a limited number of potential models enable accurate closed-form solutions of their quantum mechanical equations. Notable among these models are the harmonic oscillator, pseudoharmonic, Kratzer, Mie-type, and Coulomb potentials. For all other potential models, only approximate solutions can be derived [3, 4].

1.1 Molecular potential models

Over the years, several potential models have been developed in chemistry and molecular physics to analyze diatomic and polyatomic structures using quantum mechanical equations. The harmonic oscillator potential stands out as a commonly utilized model for understanding diatomic molecular dynamics due to its mathematical convenience. However, recognizing the anharmonic nature of diatomic molecules' vibrations, the Morse potential function emerged in 1929 as a more suitable approximation [5–7]. This potential has widespread application across physics and chemistry, making it one of the most utilized models. Akanbi et al. provided eigenvalues and eigenfunctions

for the modified Morse potential, along with thermodynamic properties for molecules like caesium and tin carbide [8]. Recently, Nwabuzor and collaborators analyzed how topographical defects affect the energy spectra and thermal properties of LiH using the Morse potential [5].

In the realm of molecular physics, the Manning-Rosen potential model has received significant attention as a mathematical tool for describing diatomic molecule vibrations [9, 10]. While effective in various physics disciplines such as condensed matter, atomic, particle, and nuclear physics, this model notably overlooks major relativistic effects [11]. Jia and colleagues provided analytical formulas for several vibrational properties of diatomic molecules [12]. Additionally, Heman et al. made predictions on the thermodynamic properties of hydrogen chloride formation using the Manning-Rosen potential [13].

In 1933, Pöschl and Teller introduced the Pöschl-Teller potential for studying diatomic molecule vibrations in nuclear and molecular physics [14]. This model is particularly suited for quantum systems involving excitons, quantum conductors, and quantum dots. Several studies have derived solutions for the Schrödinger and Klein-Gordon equations, along with corresponding thermodynamic functions, for the Pöschl-Teller potential [15–17].

The Deng-Fan oscillator potential, also known as the generalized Morse potential, has been utilized since its proposal in 1957 to describe nucleon dynamics in diatomic molecules [18, 19]. Hassanabadi et al. computed energy spectra and eigenfunctions of the Klein-Gordon equation under asymmetric vector and scalar potentials [20], while Nath and Roy employed the Nikiforov-Uvarov (NU) approach to solve the Schrödinger equation using the Deng-Fan potential [21].

The Yukawa potential, known as the screened Coulomb potential in atomic physics and Debye-Hückel potential in plasma physics, finds applications across various branches

of physics [22]. Napsuciale et al. presented an analytical solution to the quantum problem of a particle in the Yukawa potential using supersymmetry [24]. The Hulthén potential, introduced in 1942, is widely used for investigating vibrational properties in diatomic molecules [25,26]. Ahmadov provided analytical solutions for the Schrödinger equation of the Hulthén potential using the supersymmetry technique [29].

Researchers have also explored combined potential models, such as Manning-Rosen plus Yukawa, and Hulthén plus Yukawa, for studying diatomic molecules' interactions [11,30]. These combined models offer a comprehensive understanding of physical properties in both continuum and bound states of interacting systems. However, research on the solution of the Schrödinger equation and associated thermodynamic properties using these combined potential models within the Nikiforov-Uvarov framework remains scarce [11,33].

1.2 Solution methods

Various methods have been utilized to solve equations such as the Schrödinger, Klein-Gordon, and Dirac equations. These methods encompass the functional analysis approach (FAA) [34], asymptotic iteration method (AIM) [35, 36], Laplace transformation (LTM) [37], supersymmetry of quantum mechanics (SUSYQM) method [38–41], algebraic methods (AM) [42], proper and exact quantization rules (PEQR) [43], and Nikiforov-Uvarov functional analysis method (NUFA) [44].

Witten, Copper, and Freedman initially proposed the SUSYQM method [45, 46] to verify non-perturbative approaches in quantum field theory for understanding SUSY breaking. Recently, the Nikiforov-Uvarov approach, among others, has been utilized in conjunction with SUSYQM to generate supersymmetric solutions for the Schrödinger equation with central confining potentials [47]. SUSYQM considers the supersymmetry algebra used by fermionic and bosonic operators. The commutation of fermionic oper-

ators with the Hamiltonian establishes a relationship between the energy eigenvalues, eigenfunctions, and S-matrix components of the complete supersymmetry Hamiltonian. Infeld and Hull utilize this correlation in their factorization approach to categorize potential problems that can be resolved analytically [48].

Ciftci and his colleagues developed the asymptotic iteration method to analyze relativistic equations [49,50]. When a direct solution to the differential equation is absent, the eigenvalue problem is solved via asymptotic iteration. Unlike other methods, AIM can effectively solve the eigenvalue problem for large n [51,52]. Hamzavi and colleagues achieved an accurate solution for the Dirac equation with pseudospin symmetry in the presence of a spatially varying mass Coulomb potential and a Coulomb-like tensor interaction using this method [53]. Olgar and his colleagues conducted a study on the Dirac-Coulomb issue, specifically focusing on a solution with a bound state that has a mass that varies in space. They employed the asymptotic iteration method for their analysis [54]. Sous also used the AIM method to report the energy eigenvalues for a complex potential in a correlated manner [55]. In another work, Ikot and his co-workers recently employed the AIM technique to accurately calculate the bound state energy spectrum of the Schrödinger equation. This was done for CO, NO, O_2, and I_2, using the energy-dependent molecular Kratzer potential [56].

Erwin Schrödinger introduced the Laplace transformation method to solve the eigenvalue problem and determine the radial wave function of the hydrogen atom [57]. This approach transforms a second-order Schrödinger equation into a first-order differential equation. Englefield then also resolved the Coulomb, oscillator, exponential, and Yamaguchi potentials by employing LTM [58]. Miraboutalebi and Rajaei presented an analytical solution for the N-dimensional Schrödinger equation with the Morse potential using this methodology [59]. Additionally, Miraboutalebi obtained precise solutions of the Klein-Gordon equation for the Mie-type potential while considering the existence of a vector potential field that has a non-zero spatial component [60]. However, the

approach cannot be used for extremely short separation distances when dealing with greater radial and orbital momentum quantum numbers. Furthermore, the approach is solely efficacious in addressing several forms of spherically symmetrical potentials [57].

In 1981, Iachello utilized Lie algebraic methods to define the rotational vibration spectra of diatomic molecules, based on the second quantization of the Schrödinger equation [61]. Algebraic methods, which are also used to manage systems with dynamical symmetry, accurately describe both Dunham-type expansions and force-field variational approaches [62]. Over the years, there has been an interest in using algebraic techniques to study polyatomic molecules as well [63, 64]. Using a one-dimensional algebraic model, the stretching vibrational spectra of certain AB_4 tetrahedral molecules up to the first overtone are reported for the first time by Choudhury [65]. Setare and Karimi investigated the Schrödinger equation with the Kratzer potential using the algebraic technique as well [42]. However, the algebraic method has not been fully employed to address the treatment of scattering states, even though it has previously been applied to investigate bound solutions [66].

The exact quantization rule proposed by Ma and Xu in 2005 yields accurate eigenvalues for quantum systems that can be exactly solved [67, 68]. This is achieved by incorporating a correction to the well-established JKWB quantization condition. The integral correction accommodates the solution to the Riccati equation, which is correlated to the Schrödinger equation for the lowest energy state. To this end, Dong and his collaborators derived analytical solutions of the Schrödinger equation for the deformed harmonic oscillator in one dimension with the Kratzer potential and pseudoharmonic oscillator in three dimensions, by applying the exact quantization rule [69]. A recent study by Kumar and Dong introduced a quantization rule for determining the energy spectrum of bound states in non-relativistic quantum mechanics. This rule is based on the parametric Nikiforov-Uvarov approach [70].

The functional analysis approach, alternatively referred to as the modified factorization method, transforms the second-order differential equation into a hypergeometric equation through the suitable application of a transformation [71]. The energy eigenvalues and corresponding eigenfunctions of diatomic molecules, which are characterized by the Morse-Rosen potential model, were computed using this approach [72]. Ikot and his collaborators recently utilized the Nikiforov-Uvarov functional analysis method to successfully solve the Klein-Gordon equation. They employed the improved screened Kratzer potential (ISKP) model [73].

The Nikiforov-Uvarov method, introduced by Nikiforov and Uvarov in 1988 [5, 74], stands as a highly effective technique for solving equations akin to Schrödinger's in spherical dimensions. It is an analytical approach relying on specific solutions of orthogonal second-order linear differential equations. This method transforms the Schrödinger equation into a generalized hypergeometric equation through appropriate coordinate transformations. Numerous researchers have explored Schrödinger, Dirac, and Klein-Gordon equations using this method across various potential models. The Nikiforov-Uvarov method offers a more accurate, straightforward solution to the radial Schrödinger equation compared to conventional methods [5, 74]. Utilizing this approach, Edet et al. derived an approximation of the Schrödinger equation for the modified Kratzer potential plus screened Coulomb potential model [75]. Additionally, the Nikiforov-Uvarov method has been employed to approximate bound state solutions of the Schrödinger equation within non-relativistic quantum mechanics, focusing specifically on the Coshine Yukawa potential (CYP) [76].

Recently, Ikot and colleagues proposed the Nikiforov-Uvarov functional analysis approach to solve second-order differential equations of hypergeometric type [44]. NUFA utilizes the parametric Nikiforov-Uvarov method and functional analysis to determine energy eigenvalues and corresponding eigenfunctions of bound states. This functional analysis offers a direct and efficient approach, bypassing the need for complex

algebraic transformations required by alternative techniques [44]. The Schrödinger equation featuring the Deng-Fan-Eckart potential (DFEP) is analytically solved using the Nikiforov-Uvarov-Functional Analysis method to derive thermodynamic properties for diatomic molecules such as H_2, CO, ScN, and ScF [77]. In a separate study, Udoh and colleagues successfully resolved the radial Schrödinger equation by employing the Nikiforov-Uvarov functional analysis method with the shifted Morse potential model [78].

1.3 The objective of this thesis

Numerous attempts have been made to acquire explicit expressions of partition functions for molecular potential energy models in diatomic and polyatomic molecules. In this context, and also in the non-relativistic case, investigating the thermodynamic functions of different potential models through a partition function and its derivatives with respect to temperature was an important development. Moreover, research on the significance of molecular vibrations and rotational spectroscopy is ongoing in scientific disciplines such as biology and environmental science [79]. Using the Asymptotic Iteration Method, Ikot et al. presented energy eigenvalues with the general molecular potential (GMP) and thermodynamic properties of the $X^1\Sigma_g^+$ of K_2 diatomic molecules [80]. Via the Euler-Maclaurin formula, Chabi and Boumali recently determined eigensolutions of the Schrödinger equation with the three-dimensional Morse potential and calculated thermal properties of H_2, HCl, and LiH diatomic molecules [81].

Moreover, literature highlights the increasing significance of magnetic field effects, such as the Zeeman, Rashba, and Dresselhaus effects, in altering the behaviour of quantum systems [82–84]. These effects play a crucial role in eliminating degeneracy within systems [85]. Additionally, recent discoveries have shown that introducing the Aharonov-Bohm (AB) field to a system can also serve this purpose [86,87]. Ikhadir et al. employed the wave function ansatz technique to examine the energy eigenvalues and wave func-

tions for any arbitrary m-state within the two-dimensional Schrödinger wave equation. This was done under the influence of various power interaction potentials, within constant magnetic fields and Aharonov–Bohm flux fields perpendicular to the confined particle plane [88]. Quite recently, Ikot et al. investigated the use of the factorization method to analyze the Schrödinger equation, which includes a screened Kratzer potential (SKP), as well as external magnetic and AB flux fields [85].

This thesis employs the Nikiforov-Uvarov method to solve the Schrödinger equation for two combined potential models: the Manning-Rosen combined with a Yukawa potential (MRCYP), and the Hulthén combined with a Yukawa potential (HYP). These models were chosen because previous studies have successfully determined energy levels and wave functions using them. However, no exploration has been done on their solutions to the Schrödinger equation and the associated thermodynamic properties. These combined potentials are known for accurately representing energy in both bound and continuum states of interacting systems, as well as physical characteristics of wave functions. Using the energy eigenvalues obtained, we then determine the vibrational partition function and various thermodynamic properties (such as vibrational free energy, internal energy, entropy, and specific heat capacity) for different diatomic molecules.

For the Hulthén plus Yukawa potential model, we focus on the diatomic molecules CuLi, CrH, and NiC. These selections are advantageous due to the significance of transition metal hydrides (e.g., ScH, TiH, VH, CrH, MnH) in chemical synthesis as intermediates and in solid matrix samples for infra-red spectroscopy. Additionally, CuLi, comprising copper (Cu) and lithium (Li), serves as a supplementary diatomic molecule to elucidate bonding characteristics in mixed transition metal lithides. Furthermore, the study of transition metal carbide molecules like TiC and NiC is of great interest due to the necessity of comprehending their chemical bonding [89]. The ongoing research in this area emphasizes the need to investigate their thermo-magnetic properties, particularly at higher temperatures, and other significant traits, thus warranting further exploration.

To address this, we also explore the effects of the external magnetic and Aharanov-Bohm flux fields on thermodynamic properties by solving the 2-D Schrödinger equation with the Hulthén plus Yukawa potential model using the exact quantization rule (EQR). The energy spectra obtained are then utilized to calculate the vibrational partition function and other thermo-magnetic properties (including vibrational free energy, internal energy, entropy, specific heat capacity, magnetization, and magnetic susceptibility) for CuLi, CrH, and NiC diatomic molecules.

1.4 Structure of the thesis

This thesis is outlined as follows: Chapter 2 introduces the Nikiforov-Uvarov method and obtains thermodynamic properties for diatomic molecules. Chapter 3 presents mathematical solutions to the Schrödinger equation with specific potentials, along with the computation of thermodynamic properties for diatomic molecules. Chapter 4 focuses on the results and discussions, while Chapter 5 offers concise concluding remarks.

Chapter 2

Diatomic Molecules

2.1 Schrödinger equation in spherical coordinates

Here, we develop a formula for solving the radial Schrödinger problem in spherical dimensions based on the citation from [5]. Within the realm of quantum mechanics, solving the Schrödinger equation for a given physical system holds significance as it provides insight into the wave function $\Psi(\boldsymbol{r}, t)$ and energy E, encapsulating essential information about the system's physical properties. The information provided encompasses various attributes of the particle, including its energy, momentum, and coordinates, alongside its wave properties such as frequency and wavelength. The quantum mechanical system is delineated by the probability amplitude $|\Psi(\boldsymbol{r}, t)|^2$ and its accompanying phase [94]. Moreover, the wave function $\Psi(\boldsymbol{r}, t)$ denotes the particle's state concerning the potential $V(\boldsymbol{r})$, with $\boldsymbol{r}$ indicating the particle's spatial position. In a system consisting of a single particle moving along a one-dimensional path and described using Cartesian coordinates, the wave function $\Psi(r, t)$ can be expressed as $\Psi(x, t)$, while the potential energy function $V(\boldsymbol{r})$ can be denoted as $V(x)$. Alternatively, in a three-dimensional system with spherical coordinates containing only one particle, the wave function can be represented as $\Psi(\boldsymbol{r}, t) = \Psi(r, \theta, \phi, t)$ and the potential as $V(\boldsymbol{r}) = V(r, \theta, \phi)$. In quantum mechanics, predicting the future state $\Psi(\boldsymbol{r}, t)$ of a particle's system over time requires referencing its initial state $(\boldsymbol{r}, t = 0)$. To achieve this, we employ the equation proposed by Erwin Schrödinger

$$i\hbar \frac{\partial \Psi(\boldsymbol{r}, t)}{\partial t} = -\frac{\hbar^2}{2\mu} \nabla^2 \Psi(\boldsymbol{r}, t) + V(\boldsymbol{r}) \Psi(\boldsymbol{r}, t), \tag{2.1}$$

as cited in various works [75, 80, 95–101]. Here, μ represents the reduced mass, $\hbar$ represents the reduced Planck's constant which is defined as $h/2\pi$, and ∇^2 represents the Laplacian operator

$$\nabla^2 = \frac{\partial^2}{\partial x^2} + \frac{\partial^2}{\partial y^2} + \frac{\partial^2}{\partial z^2}, \tag{2.2}$$

in Cartesian coordinates. Equation (2.1) is commonly known as the time-dependent Schrödinger equation and can easily be converted into the time-independent form by using a wave function

$$\Psi(\boldsymbol{r}, t) = e^{-iEt/\hbar}\psi(\boldsymbol{r}), \tag{2.3}$$

that corresponds to states with a constant value of E. In addition, the probability density

$$|\Psi(\boldsymbol{r}, t)|^2$$

for states

$$\Psi(\boldsymbol{r}, t) = e^{-iEt/\hbar}\psi(\boldsymbol{r})$$

is equal to $|\psi(\boldsymbol{r})|^2$. This probability density is independent of the state and remains constant throughout time. Therefore, we may now designate states as "stationary states" when they are primarily focused on energy states that remain constant [102]. By substituting the wave function from equation (2.3) into equation (2.1), we obtain the time-independent Schrödinger equation

$$-\frac{\hbar^2}{2\mu}\nabla^2\psi(\boldsymbol{r}) + V(\boldsymbol{r})\psi(\boldsymbol{r}) = E\psi(\boldsymbol{r}). \tag{2.4}$$

For simplicity, we'll denote equation (2.4) as the Schrödinger equation. The solution to the SE not only relies on the potential energy function $V(\boldsymbol{r})$ but also on the chosen coordinate system. While many quantum mechanical systems can be addressed by solving the one-particle, one-dimensional SE using Cartesian coordinates, our focus here is on the one-particle, three-dimensional SE using spherical coordinates. Hence, in this thesis, we will address any one-particle issue with a spherically symmetric potential energy function $V(r)$, where we assume that $V(r)$ depends solely on the radial variable

r in spherical coordinates, i.e.,

$$V(\boldsymbol{r}) = V(r, \theta, \phi) \equiv V(r).$$

Additionally, the stationary-state wave function $\psi(\boldsymbol{r})$ takes the form

$$\psi(r, \theta, \phi) = \mathcal{R}(r)Y(\theta, \phi),$$

where $\mathcal{R}(r)$ represents the unknown radial wave function and $Y(\theta, \phi)$ denotes the spherical harmonics.

Central potentials, as utilized within the Schrödinger equation, are characterized by their exclusive dependence on the radial distance between a particle. In spherical coordinates, a point in space is defined by its radial distance r from the origin, alongside two angles: the zenith angle θ and the azimuthal angle ϕ. To ensure a unique assignment of spherical coordinates to each point, it's imperative to constrain their ranges. The permissible ranges are $r \geq 0$, $0 \leq \theta \leq \pi$, and $0 \leq \phi \leq 2\pi$. Notably, the necessity of employing spherical coordinates for solving the Schrödinger equation for a particle influenced by a potential function can be subject to questioning.

Solving the Schrödinger equation in spherical coordinates for realistic potentials in physics involves separating the wave function into independent components. Consequently, the motion of a rotating molecule or an electron orbiting an atomic nucleus can be accurately depicted using a single coordinate in spherical coordinates. A prime example illustrating this concept is the Coulomb potential, which describes the electromagnetic interaction between an electron and a proton expressed in Cartesian coordinates as

$$V(x, y, z) = \frac{-e'^2}{\sqrt{x^2 + y^2 + z^2}},$$

where $e' = \frac{e}{\sqrt{4\pi\varepsilon_0}}$, with e denoting the elementary electric charge and ε_0 representing the electric permittivity of free space.

Solving the Schrödinger equation with the potential $V(x, y, z)$ can pose challenges due

to the presence of non-separable variables in Cartesian coordinates, even if the wave function becomes separable. Converting from Cartesian to spherical coordinates would streamline the solution of the Schrödinger equation. In spherical coordinates, the potential $V(x, y, z)$ is represented as $V(r) = e'^2/r$, where it solely relies on the radial distance r. The transformation utilized for this conversion is given by the formula

$$r = \sqrt{x^2 + y^2 + z^2}.$$

Furthermore, the variables (x, y, z) in Cartesian coordinates can be correlated with the variables (r, θ, ϕ) in spherical coordinates as follows:

$$x = r\sin\theta\cos\phi, \quad y = r\sin\theta\sin\phi, \quad z = r\cos\theta, \quad \theta = \cos^{-1}\left(\frac{z}{r}\right), \quad \phi = \tan^{-1}\left(\frac{y}{x}\right). \tag{2.5}$$

Now, let's examine the variables that can be isolated in spherical coordinates. By taking into account the Schroedinger equation in equation (2.4), we'll derive the SE in the same coordinate system by using the relationship given in equation (2.5) and the Laplacian operator

$$\nabla^2 = \frac{1}{r^2}\frac{\partial}{\partial r}\left(r^2\frac{\partial}{\partial r}\right) + \frac{1}{r^2\sin\theta}\frac{\partial}{\partial\theta}\left(\sin\theta\frac{\partial}{\partial\theta}\right) + \frac{1}{r^2\sin^2\theta}\frac{\partial^2}{\partial\phi^2}, \tag{2.6}$$

in spherical coordinates to obtain

$$\left[-\frac{\hbar^2}{2\mu}\left(\frac{1}{r^2}\frac{\partial}{\partial r}\left(r^2\frac{\partial}{\partial r}\right) + \frac{1}{r^2\sin\theta}\frac{\partial}{\partial\theta}\left(\sin\theta\frac{\partial}{\partial\theta}\right) + \frac{1}{r^2\sin^2\theta}\frac{\partial^2}{\partial\phi^2}\right) + V(r)\right]\psi(r,\theta,\phi) = E\psi(r,\theta,\phi). \tag{2.7}$$

Our aim is to discover a solution to the Schrödinger equation (2.7) that can be decomposed into the structure

$$\psi(r, \theta, \phi) = \mathcal{R}(r)Y(\theta, \phi).$$

By employing the proposed wave function $\psi(r, \theta, \phi)$, the Schrödinger equation can be expressed as

$$\frac{1}{\mathcal{R}(r)}\frac{d}{dr}\left(r^2\frac{d\mathcal{R}(r)}{dr}\right) + \frac{2\mu}{\hbar^2}r^2\left(E - V(r)\right) = \frac{1}{Y(\theta,\phi)}\left[\frac{1}{\sin\theta}\frac{\partial}{\partial\theta}\left(\sin\theta\frac{\partial Y(\theta,\phi)}{\partial\theta}\right) + \frac{1}{\sin^2\theta}\frac{\partial^2 Y(\theta,\phi)}{\partial\phi^2}\right]. \tag{2.8}$$

The two sides of this equation are contingent upon separate variables, hence they can only be equivalent if they are equal to a fixed value. Hence, it is necessary for both of the following equations to hold concurrently

$$\frac{1}{\sin\theta}\frac{\partial}{\partial\theta}\left(\sin\theta\frac{\partial Y(\theta,\phi)}{\partial\theta}\right)+\frac{1}{\sin^2\theta}\frac{\partial^2 Y(\theta,\phi)}{\partial\phi^2}+\mathcal{L}Y(\theta,\phi)=0. \tag{2.9}$$

$$\frac{1}{\mathcal{R}(r)}\frac{d}{dr}\left(r^2\frac{d\mathcal{R}(r)}{dr}\right)+\left[\frac{2\mu}{\hbar^2}r^2\left(E-V(r)\right)-\frac{\mathcal{L}}{r^2}\right]\mathcal{R}(r)=0, \tag{2.10}$$

Since we have two distinct equations, we can address each one individually. Equation (2.10) pertains solely to radial variables, while equation (2.9) solely pertains to angular variables. The solution to the angular component in equation (2.9) is evidently straightforward as it lacks a potential or energy term. Hence, we can once again utilize the method of separating variables by assuming the angular function

$$Y(\theta,\phi)=\Theta(\theta)\Phi(\phi).$$

It is crucial to note that equation (2.9) can be decomposed using the substitution

$$Y(\theta,\phi)=\Theta(\theta)\Phi(\phi).$$

To achieve this, the functions $\Theta(\theta)$ and $\Phi(\phi)$ must satisfy the subsequent differential equations:

$$\frac{1}{\Phi(\phi)}\frac{d^2\Phi(\phi)}{d\phi^2}\left(r^2\frac{d\mathcal{R}(r)}{dr}\right)=-m^2. \tag{2.11}$$

$$\frac{1}{\sin\theta}\frac{d}{d\theta}\left(\sin\theta\frac{d\Theta(\theta)}{d\theta}\right)+\left(\mathcal{L}-\frac{m^2}{\sin^2\theta}\right)\Theta(\theta)=0, \tag{2.12}$$

Presently, we are certain that solving these equations can be accomplished effortlessly. However, our attention will be directed solely towards $\mathcal{L}$ and m, examining their respective physical implications. The separable constant m needs to be an integer, whether positive or negative. Specifically, m can assume values of $0, \pm1, \pm2, ...$, and is typically referred to as the magnetic quantum number. Through the substitution of the variable θ with $\omega = \cos\theta$, we can reformulate equation (2.12), which becomes more intricate as:

$$\frac{d}{d\omega}\left[\left(1-\omega^2\right)\frac{dP(\omega)}{d\omega}\right]+\left(\mathcal{L}-\frac{m^2}{1-\omega^2}\right)P(\omega)=0, \tag{2.13}$$

where polynomial $P(\omega)$ denotes the Legendre polynomial. Typically, equation (2.13) yields two distinct solutions, both becoming infinite when $\omega = \pm 1$. We investigate solutions of the Schrödinger equation representing particles in bound states. These solutions, known as wave functions, must adhere to the boundary conditions specified in equation (2.13) while remaining finite and single-valued throughout space. However, if the constant $\mathcal{L}$ can be expressed as $\mathcal{L} = \ell(\ell+1)$, where ℓ denotes the orbital quantum number taking values $\ell = 0, 1, 2, 3, ...$, for such ℓ, one of the solutions remains finite for all possible ω values.

Since Legendre polynomials are of order ℓ, with $|m| = 0, 1, 2, 3, ... \leq \ell$, the magnetic quantum number m must be limited to values less than or equal to ℓ in the definition of the associated Legendre function. Alternatively, there are $(2\ell + 1)$ valid options for m, implying that $-\ell \leq m \leq \ell$. By substituting $\mathcal{L} = \ell(\ell + 1)$ into equation (2.10), we find that the radial wave function $\mathcal{R}(r)$ and the eigenvalues E of the Schrödinger equation depend on the quantum number ℓ and satisfy the equation

$$\frac{d^2\mathcal{R}(r)}{dr^2} + \frac{2}{r}\frac{d\mathcal{R}(r)}{dr} + \frac{2\mu}{\hbar^2}\left[E - V(r) - \frac{\hbar^2\ell(\ell+1)}{2\mu r^2}\right]\mathcal{R}(r) = 0. \tag{2.14}$$

The given equation can be restated as an ordinary differential equation, which includes a variable-dependent coefficient. Standard techniques outlined in quantum mechanics textbooks can be utilized for its resolution. The solution to equation (2.14) can be achieved using analytical methods, depending on the specific characteristics of the potential function $V(r)$ [103].

2.2 The Nikiforov-Uvarov method

The Nikiforov-Uvarov (NU) approach is based on the solution of second-order hypergeometric differential equations using specific orthogonal functions [104]. By utilizing a suitable coordinate transformation $r \longrightarrow s$, the Schrödinger-like equations expressed in spherical coordinates, along with a given potential $V(r)$, can be simplified to a gen-

eralized equation with hypergeometric characteristics. These equations can be solved methodically to obtain accurate and precise solutions. The principles of the Nikiforov-Uvarov approach were deduced from Chapter 11 in the cited text [5]. The central equation closely associated with the methodology is as follows:

$$\mathcal{R}''(s) + \frac{\tilde{\tau}(s)}{\sigma(s)}\mathcal{R}'(s) + \frac{\tilde{\sigma}(s)}{\sigma(s)}\mathcal{R}(s) = 0, \tag{2.15}$$

The wave function $\psi(s)$ is a hypergeometric-type function, characterized by $\tilde{\sigma}(s)$ and $\sigma(s)$, which are polynomials of degree two or less, and $\tilde{\tau}(s)$, which is a polynomial of degree one or less. By making the assumption that the equation

$$\mathcal{R}(s) = \phi(s)y_n(s), \tag{2.16}$$

holds and choosing a suitable function $\phi(s)$, equation (2.15) may be simplified to;

$$y'' + \left(\frac{2\phi'(s)}{\phi(s)} + \frac{\tilde{\tau}(s)}{\sigma(s)}\right)y'(s) + \left(\frac{\phi''}{\phi(s)} + \frac{\phi'(s)}{\phi(s)}\frac{\tilde{\tau}(s)}{\sigma(s)} + \frac{\tilde{\sigma}(s)}{\sigma^2(s)}\right)y(s) = 0. \tag{2.17}$$

The coefficient of $y'(s)$ is determined by the quotient of $\tau(s)$ and $\sigma(s)$, where $\tau(s)$ is a polynomial with a maximum degree of one. The equation is represented as follows:

$$\frac{\tau(s)}{\sigma(s)} = \frac{2\phi'(s)}{\phi(s)} + \frac{\tilde{\tau}(s)}{\sigma(s)}, \tag{2.18}$$

with the regular expression obtained as

$$\frac{\pi(s)}{\sigma(s)} = \frac{\phi\prime(s)}{\phi(s)}, \tag{2.19}$$

where

$$\pi(s) = \frac{1}{2}[\tau(s) - \tilde{\tau}(s)]. \tag{2.20}$$

The most effective illustration of equation (2.18) is

$$\tau(s) = \tilde{\tau}(s) + 2\pi(s). \tag{2.21}$$

The recently proposed parameter $\pi(s)$ is a polynomial of degree one at most. Furthermore, the expression $\phi''(s)/\phi(s)$, present in the coefficient of $y(s)$ in equation ((2.17)), can be written in the following form:

$$\frac{\phi''}{\phi(s)} = \left(\frac{\phi'(s)}{\phi(s)}\right)' + \left(\frac{\phi'(s)}{\phi(s)}\right)^2 = \left(\frac{\pi(s)}{\sigma(s)}\right)' + \left(\frac{\pi(s)}{\sigma(s)}\right)^2. \tag{2.22}$$

$$\frac{\sigma(s)}{\sigma^2(s)} = \frac{\phi''}{\phi(s)} + \frac{\phi'(s)}{\phi(s)}\frac{\tilde{\tau}(s)}{\sigma(s)} + \frac{\tilde{\sigma}(s)}{\sigma^2(s)}, \tag{2.23}$$

where

$$\sigma(s) = \tilde{\sigma}(s) + \pi^2(s) + \pi(s)\left[\tilde{\tau}(s) - \sigma'(s)\right] + \pi'(s)\sigma(s). \tag{2.24}$$

By substituting the right-hand sides of equations (2.18) and (2.23) into equation (2.17), we obtain the following hypergeometric equation:

$$y''(s) + \frac{\tau(s)}{\sigma(s)}y'(s) + \frac{\bar{\sigma}(s)}{\sigma^2(s)}y(s) = 0. \tag{2.25}$$

As a result of the algebraic modifications mentioned above, equation (2.15) is consistently maintained in its functional form. If the polynomial $\bar{\sigma}(s)$ in equation (2.25) is a multiple of $\sigma(s)$, then it can be written as

$$\bar{\sigma}(s) = \lambda\sigma(s), \tag{2.26}$$

where λ is a constant. In this case, equation (2.25) is simplified to an equation of hypergeometric-type, and can be written as

$$\sigma(s)y''(s) + \tau(s)y'(s) + \lambda y(s) = 0. \tag{2.27}$$

The solution to this equation is expressed as a hypergeometric-type function. In order to determine the polynomial $\pi(s)$, equation (2.24) is compared with equation (2.26), resulting in the derivation of a quadratic equation for $\pi(s)$ given below:

$$\pi^2(s) + \pi(s)\left[\tilde{\sigma}(s) - \sigma'(s)\right] + \tilde{\sigma}(s) + k\sigma(s) = 0, \tag{2.28}$$

$$\lambda = k + \pi'(s). \tag{2.29}$$

The following equality, results from solving this quadratic equation (2.28) for $\pi(s)$:

$$\pi(s) = \frac{\sigma'(s) - \tilde{\tau}(s)}{2} \pm \sqrt{\left(\frac{\sigma'(s) - \tilde{\tau}(s)}{2}\right)^2 - \tilde{\sigma}(s) + k\sigma(s)}. \tag{2.30}$$

To determine the potential solutions based on the positive and negative signs of equation (2.30), the parameter k inside the square root must be explicitly known. In order

to fulfil this condition, the expression within the square root must be the result of squaring a polynomial, as $\pi(s)$ is a polynomial with a maximum degree of one. For this situation, there exists a quadratic equation form that can be used to represent the constant k.

By equating the discriminant of this quadratic equation to zero, the value of the constant k may be unambiguously determined. Once the value of k is determined, the polynomial $\pi(S)$ is derived from equation (2.30). Subsequently, equations (2.20) and (2.29) are employed to yield $\tau(s)$ and λ, respectively. A prevalent approach in generalizing the solutions of equation (2.27) is to demonstrate that all the derivatives of hypergeometric-type functions also possess the characteristic of being hypergeometric-type. To achieve this objective, equation (2.27) is differentiated utilizing the notation $\upsilon_1(s) = y''(s)$, resulting in

$$\sigma(s)\upsilon_1''(s) + \tau_1(s)\upsilon_1'(s) + \mu_1\upsilon_1(s) = 0. \tag{2.31}$$

Here, $\tau_1(s) = \tau(s) + \sigma'(s)$ and $\mu_1 = \lambda + \tau'(s)\tau_1(s)$ is a polynomial of degree at most one and μ_1 is a parameter that is independent of the variable s. Equation (2.31) is evidently a hypergeometric-type equation. By using $\upsilon_2(s) = y''(s)$ as an alternative form, the second derivative of equation (2.27) can be expressed as

$$\sigma(s)\upsilon_2''(s) + \tau_2(s)\upsilon_2'(s) + \mu_2\upsilon_2(s) = 0, \tag{2.32}$$

where

$$\tau_2(s) = \tau_1(s) + \sigma'(s) = \tau(s) + 2\sigma'(s), \tag{2.33}$$

$$\mu_2 = \mu_1 + \tau_1'(s) = \lambda + 2\tau'(s) + \sigma''(s). \tag{2.34}$$

Similarly, a general hypergeometric-type equation will have its solution constructed by using $\upsilon_n(s) = y^n(s)$ and takes the form

$$\sigma(s)\upsilon_n''(s) + \tau_n(s)\upsilon_n'(s) + \mu_n\upsilon_n(s) = 0. \tag{2.35}$$

The following are general recurrence relations for $\tau_n(s)$ and μ_n:

$$\tau_n(s) = \tau(s) + n\sigma'(s), \tag{2.36}$$

and

$$\mu_n = \lambda + n\tau'(s) + \frac{n(n-1)}{2}\sigma''(s), \tag{2.37}$$

respectively. when $\mu_n = 0$, equation (2.37) is reduced to

$$\lambda_n = -n\tau'(s) - \frac{n(n-1)}{2}\sigma''(s), \quad (n = 0, 1, 2...). \tag{2.38}$$

Hence, equation (2.35) possesses a solution in the form of $y(s) = y_n(s)$, which is a polynomial of degree n. To achieve an eigenvalue solution using the NU approach, it is necessary to establish the relationship between and n by utilizing Equations (2.29) and (2.38). Here, $y_n(s)$ is a hypergeometric function whose polynomial solutions are determined by the Rodrigues relation

$$y_n(s) = \frac{B_n}{\rho(s)}\frac{d^n}{ds^n}\left[\sigma^n(s)\rho(s)\right], \tag{2.39}$$

where B_n is the normalization constant, and the weight function $\rho(s)$ must satisfy the following condition:

$$\frac{d}{ds}\left[\sigma(s)\rho(s)\right] = \tau(s)\rho(s). \tag{2.40}$$

2.3 Thermo-magnetic properties.

2.3.1 Thermodynamic properties

As previously mentioned, the primary aim of this study is to examine the thermodynamic properties such as free energy, average energy, entropy, and specific heat capacity for selected diatomic molecules using the Nikiforov-Uvarov method. Before presenting expressions for these thermodynamic properties, let us now provide a brief description of each property.

The Helmholtz free energy

The Helmholtz free energy, denoted as F, serves as an approximation of the useful work obtainable from a closed thermodynamic system maintained at a constant temperature [105].

Mean energy

The average energy of a thermodynamic system represents its internal energy. For an isolated system, the average energy remains constant. It signifies the energy required to establish or maintain the system's current internal state, encompassing the kinetic energy of its particles but excluding the overall kinetic energy of the system. It monitors the energy exchanges within the system resulting from alterations in its internal state [106].

Entropy

Entropy denotes the amount of thermal energy per unit temperature within a system that is unavailable for useful work. As work arises from the ordered motion of molecules, entropy can be conceptualized as a measure of the molecular disorder or unpredictability within the system. Understanding entropy provides insights into the spontaneous changes observed in a wide array of everyday phenomena [107].

Specific heat capacity

Specific heat capacity, also known as massic heat capacity in thermodynamics, is determined by dividing the heat capacity of a material by its mass. It represents the amount of heat required to raise the temperature of one unit mass of the substance by one unit. Specific heat capacity is contingent upon temperature and the state of the material material [108, 109].

Next, let us commence the derivation of thermodynamic functions using Section 6 of

the reference [110]. We consider a system with multiple energy states, each associated with a distinct probability of occurrence. Our objective is to characterize the thermodynamic behaviour of this system under constant temperature T, volume V, and number of particles N (referred to as a canonical ensemble or NVT ensemble). Given all conceivable states j, the probability of being in a quantum state i is computed as indicated.

$$p_i = \frac{e^{-\frac{E_i}{k_B T}}}{\sum_j e^{-\frac{E_j}{k_B T}}}. \tag{2.41}$$

In this equation, k_B represents Boltzmann's constant, T stands for absolute temperature, and p_i denotes the probability that a system within a given canonical ensemble occupies the quantum state i with quantum energy E_i. The total energy of a particle in the i^{th} state, denoted by E_i, is determined by the summation of p_i.

$$U = E = \sum_i p_i E_i. \tag{2.42}$$

By substituting equation (2.41) into equation (2.42) and connecting the thermodynamic parameter T with the statistical mechanical parameter β, we obtain the internal energy U in terms of the partition function Z:

$$U = \frac{\sum_i E e^{-\beta E_i}}{\sum_i e^{-\beta E_i}}, \tag{2.43}$$

where $\beta = 1/k_B T$. The statistical partition function $Z(N, V, \beta)$ is given by [111, 112]

$$Z(N, V, \beta) = \sum_i e^{-E_i/k_B T} = \sum_i e^{-\beta E_i}. \tag{2.44}$$

To connect Partition Function and Probability, the probability p_i can also be expressed in terms of the partition function Z as follows:

$$p_i = \frac{e^{-\frac{E_i}{k_B T}}}{Z(N, V, \beta)}. \tag{2.45}$$

This shows how the partition function encapsulates the statistical properties of the system.

For a collection of N distinguishable particles, the partition function is given by $Z_N = Z^N$, while for N indistinguishable particles, it becomes $Z_N = \frac{Z^N}{N!}$ in the limit of large N. Here, Z denotes the molecular partition function, which signifies the count of available states for a molecule at a specific temperature T. This function encapsulates all necessary information for computing the thermodynamic characteristics of a system composed of independent particles, rooted in quantum mechanics' wave function. From equation (2.44), it's evident that the partition function $Z(\beta)$ varies with temperature, where $\beta = 1/k_B T$. Consequently, the derivative of $\ln Z(\beta)$ can be taken as follows:

$$\left(\frac{\partial \ln Z(N,V,\beta)}{\partial \beta}\right)_{N,V} = -\sum_i \frac{(E_i(N,V))\, e^{-\beta E_i(N,V)}}{Z(N,V,\beta)}. \tag{2.46}$$

It can be observed that the right-hand-side of equation (2.46) is in the form of average energy,

$$\begin{aligned} \langle E \rangle &= -\sum_i \frac{(E_i(N,V))\, e^{-\beta E_i(N,V)}}{Z(N,V,\beta)} \\ &= -\sum_i p_i(N,V,\beta) E_i(N,V,\beta), \end{aligned} \tag{2.47}$$

which simplifies to

$$\langle E \rangle = -\left(\frac{\partial \ln Z}{\partial \beta}\right)_{N,V}. \tag{2.48}$$

In equation (2.46), we've shown the connection between a microscopic (molecular) quantity and the partition function, which relates to the macroscopic property of average energy, a thermodynamic property. Notably, as the systems are composed of molecules, the energy levels they occupy are quantum energy levels. Equation (2.44) also allows us to determine additional thermodynamic properties. Before we derive other thermodynamic functions, let us express equation (2.48) as a temperature derivative as follows;

$$\frac{\partial f}{\partial T} = \frac{\partial f}{\partial \beta}\frac{\partial \beta}{\partial T} = \frac{\partial f}{\partial \beta}\frac{d\,(1/k_B T)}{dT} = -kT^2 \frac{\partial f}{\partial T}. \tag{2.49}$$

Therefore, we now have

$$\langle E \rangle = \left(k_B T^2 \frac{\partial Z}{\partial T}\right)_{N,V} = -\left(\frac{\partial \ln Z}{\partial \beta}\right)_{N,V}. \tag{2.50}$$

Since the average energy $\langle E \rangle$ is related to the internal energy U by

$$U = N.\langle E \rangle = N\left(k_B T^2 \frac{\partial Z}{\partial T}\right)_{N,V} = -N\left(\frac{\partial \ln Z}{\partial \beta}\right)_{N,V}. \tag{2.51}$$

The internal energy U is often reported as a molar quantity

$$U = \langle E \rangle = k_B T^2 \frac{\partial \ln Z(T)}{\partial T} = -\frac{\partial \ln Z(\beta)}{\partial \beta}. \tag{2.52}$$

When the probabilities in equation (2.45) are not equal, the entropy is given by

$$S = -k_B \sum_i p_i \ln p_i. \tag{2.53}$$

Now, taking a logarithm of equation (2.45) yields

$$\ln(p_i) = -\frac{E_i}{k_B T} - \ln Z, \tag{2.54}$$

Substituting equation (2.54) into equation (2.53), we obtain

$$S = k_B \sum_i p_i \left(\frac{E_i}{k_B T} + \ln Z\right), \tag{2.55}$$

which simplifies to

$$S = \frac{U}{T} + k_B \ln Z, \tag{2.56}$$

using equation (2.42) was used. Note that equation (2.56) can also be rewritten as

$$U - TS = -k_B T \ln Z. \tag{2.57}$$

If we substitute equation (2.52) in equation (2.56) and simplifying, we obtain a partition function dependent entropy as

$$S = k_B T \frac{\partial \ln Z(T)}{\partial T} + k_B \ln Z(T) = -\frac{1}{\beta}\frac{\partial \ln Z(\beta)}{\partial \beta} + k_B \ln Z(\beta). \tag{2.58}$$

Having acquired the partition function Z, which depends on the mean energy U and entropy S of the system, we proceed to derive expressions for the free energy F and the specific heat capacity at constant volume C_V. Remembering that free energy is defined as

$$F = U - TS. \tag{2.59}$$

Substituting equation (2.57) into equation (2.59), we obtain

$$F = -k_B T \ln Z(T), \tag{2.60}$$

which can also written as function of β in the form

$$F = -k_B \frac{1}{\beta} \ln Z(\beta). \tag{2.61}$$

The specific heat capacity at constant volume C_V is defined as

$$C_V = \left(\frac{\partial U}{\partial T} \right)_V . \tag{2.62}$$

Inserting equation (2.51) into equation (2.62) yields

$$C_V = \left(\frac{\partial}{\partial T} \left(k_B T^2 \left(\frac{\partial}{\partial T} \ln Z \right)_{N,V} \right) \right)_V , \tag{2.63}$$

which can also be expressed as

$$C_V(\beta) = \frac{1}{T^2} \frac{\partial^2 \ln Z(T)}{\partial T^2} = k_B \beta^2 \frac{\partial^2 \ln Z(\beta)}{\partial \beta^2}. \tag{2.64}$$

These fundamental thermodynamic equations stem from the partition function Z, serving as the cornerstone of statistical mechanics. They establish a connection between the microscopic characteristics of a system and its macroscopic thermodynamic properties.

2.3.2 Magnetic properties

We also examine the thermodynamic properties of chosen diatomic molecules, while also subjecting their molecular structures to magnetic and Aharonov-Bohm (AB) flux fields. In pursuit of this, we assess the system's magnetization and magnetic susceptibility.

Magnetization (M)

Magnetization is the measure of the magnetic moment within a material relative to its volume. Essentially, it represents the concentration of permanent or induced dipole

moments within a magnetic substance, also known as magnetic polarization. The origin of magnetization is commonly attributed to the magnetic moments generated by the spin of electrons or nuclei, or the mobility of electrons within atoms [108, 109].
To obtain functions for M and χ, we begin with the Helmholtz free energy F and examine its application to a magnetic system. Given the Helmholtz free energy:

$$F = -k_B T \ln Z$$

The magnetization M can be obtained as:

$$M = -\frac{1}{\beta}\frac{\partial F}{\partial \boldsymbol{B}}$$

Differentiating F with respect to $\boldsymbol{B}$, we get:

$$M = -\frac{1}{\beta}\frac{\partial}{\partial \boldsymbol{B}}(-k_B T \ln Z)$$

$$M = \frac{1}{\beta}\frac{k_B T}{Z}\frac{\partial Z}{\partial \boldsymbol{B}}$$

$$M = \frac{1}{\beta}\frac{\partial E_{nm}}{\partial \boldsymbol{B}}$$

where E_{nm} is the magnetic energy and $\boldsymbol{B}$ is the magnetic field.

Magnetic Susceptibility (χ)

Magnetic susceptibility denotes a material's ability to become magnetized when subjected to an external magnetic field. In electromagnetism, it indicates the degree of magnetization a material undergoes in response to such a field. This trait facilitates the classification of materials' reactions to magnetic fields as either aligning with the field (paramagnetism) or aligning against it (diamagnetism) [108, 109].
Similarly, the magnetic susceptibility χ can be derived as:

$$\chi = \frac{\partial M}{\partial \boldsymbol{B}}$$

$$\chi = \frac{1}{\beta}\frac{k_B T}{Z}\frac{\partial^2 Z}{\partial \boldsymbol{B}^2}$$

These expressions provide the magnetization and magnetic susceptibility of the system in terms of the partition function Z and its derivatives with respect to the magnetic field $\boldsymbol{B}$.

Chapter 3

Thermo-magnetic Functions

3.1 Diatomic Molecular Potentials

In this work, will consider the Manning-Rosen plus a class of Yukawa potential, as well as the Hulthén plus Yukawa potential models. In the realm of nuclear physics, these potential models serve to analyze the interaction between pairs of distorted nuclei and the influence of spin-orbit coupling on particle motion within potential fields. Additionally, the oscillations occurring within the hadronic system's periphery can be described accurately by employing multiple potential models, as illustrated in the mathematical model [11,113–115]. The composite expression for the short-range Manning-Rosen plus a class of Yukawa potentials, is presented as follows [11]:

$$\begin{aligned} V_{\text{MRCY}}(r) &= V_{\text{MR}} + V_{\text{CY}} \\ &= \frac{\hbar^2}{2Md^2}\left[\frac{\alpha(\alpha-1)e^{-2r/d}}{(1-e^{-r/d})^2} - \frac{Ae^{-r/d}}{(1-e^{-r/d})}\right] - \frac{V_0 e^{-\delta r}}{r} - \frac{V_0' e^{-2\delta}}{r^2}. \end{aligned} \tag{3.1}$$

Here, A and α denote two dimensionless parameters, while d represents the potential range and $1/\delta$ signifies the potential strength. Given that the Schrödinger equation for short-range potential models can be accurately solved using an appropriate approximation method to circumvent the centrifugal term, it becomes imperative to approximate this centrifugal term for the Manning-Rosen plus a class of Yukawa potential model. This approximation is necessary to derive the eigensolution of the Schrödinger equation (2.14) for $\ell = 0$. Thus, when $\delta << 1$, employing an enhanced approximation scheme becomes crucial. In such conditions, the Greene-Aldrich approximation scheme, as referenced in [95, 96, 116], is utilized. Note that the above mentioned approximation

scheme is given by;

$$\frac{1}{r^2} \approx \frac{4\delta^2 e^{-2\delta r}}{(1-e^{-2\delta r})^2}; \quad \frac{1}{r} \approx \frac{2\delta e^{-\delta r}}{(1-e^{-2\delta r})}. \tag{3.2}$$

Now, substituting equation (3.2) into equation (3.1) we can now write the approximation for the Manning-Rosen plus a class of Yukawa potential in the form: [11]

$$\begin{aligned} V'_{\text{MRCY}}(r) &= V'_{\text{MR}} + V'_{\text{CY}} \\ &= \frac{(V_1+V_4)\,e^{-4\delta r}}{(1-e^{-2\delta r})^2} - \frac{(V_2+V_3)\,e^{-2\delta r}}{1-e^{-2\delta r}} \\ &= \frac{V_{14}e^{-4\delta r}}{(1-e^{-2\delta r})^2} - \frac{V_{23}e^{-2\delta r}}{1-e^{-2\delta r}}. \end{aligned} \tag{3.3}$$

The following parameters in equation (3.3) are defined as follows;

$$V_1 = \frac{2\hbar^2\delta^2\alpha(\alpha-1)}{M}, \quad V_2 = \frac{2\hbar^2\delta^2 A}{M}, \quad V_3 = 2\delta V_0, \quad V_4 = -4\delta^2 V'_0, \tag{3.4}$$

$$V_{14} = (V_1+V_4), \quad V_{23} = (V_2+V_3). \tag{3.5}$$

On the other hand the Hulthén plus Yukawa combined potential is of the form [33]:

$$\begin{aligned} V_{\text{HY}}(r) &= V_{\text{H}}(r) + V_{\text{Y}}(r) \\ &= -\frac{Ze^2\delta e^{-\delta r}}{1-e^{-\delta r}} - \frac{V_0 e^{-\delta r}}{r}, \end{aligned} \tag{3.6}$$

In this context, Ze^2 represents the potential strength parameter, while δ signifies the screening parameter, and their product, $Z\delta e^2 = V_0$. Moreover, by employing the Greene-Aldrich approximation scheme outlined in equation (3.2) within equation (3.6), we express an approximation for the Hulthén plus Yukawa potential

$$\begin{aligned} V'_{\text{HY}}(r) &= V'_{\text{H}} + V'_{\text{Y}} \\ &= -\frac{V_0 e^{-2\delta r}}{1-e^{-2\delta r}} - \frac{2V'_0\delta e^{-2\delta r}}{1-e^{-2\delta r}} \end{aligned} \tag{3.7}$$

as stated in [33]. The potentials $V(r)$ (MRCYP and HYP) and their corresponding approximations $V'(r)$ are depicted against the separation distance r in Figure 3.1 and Figure 3.2, respectively.

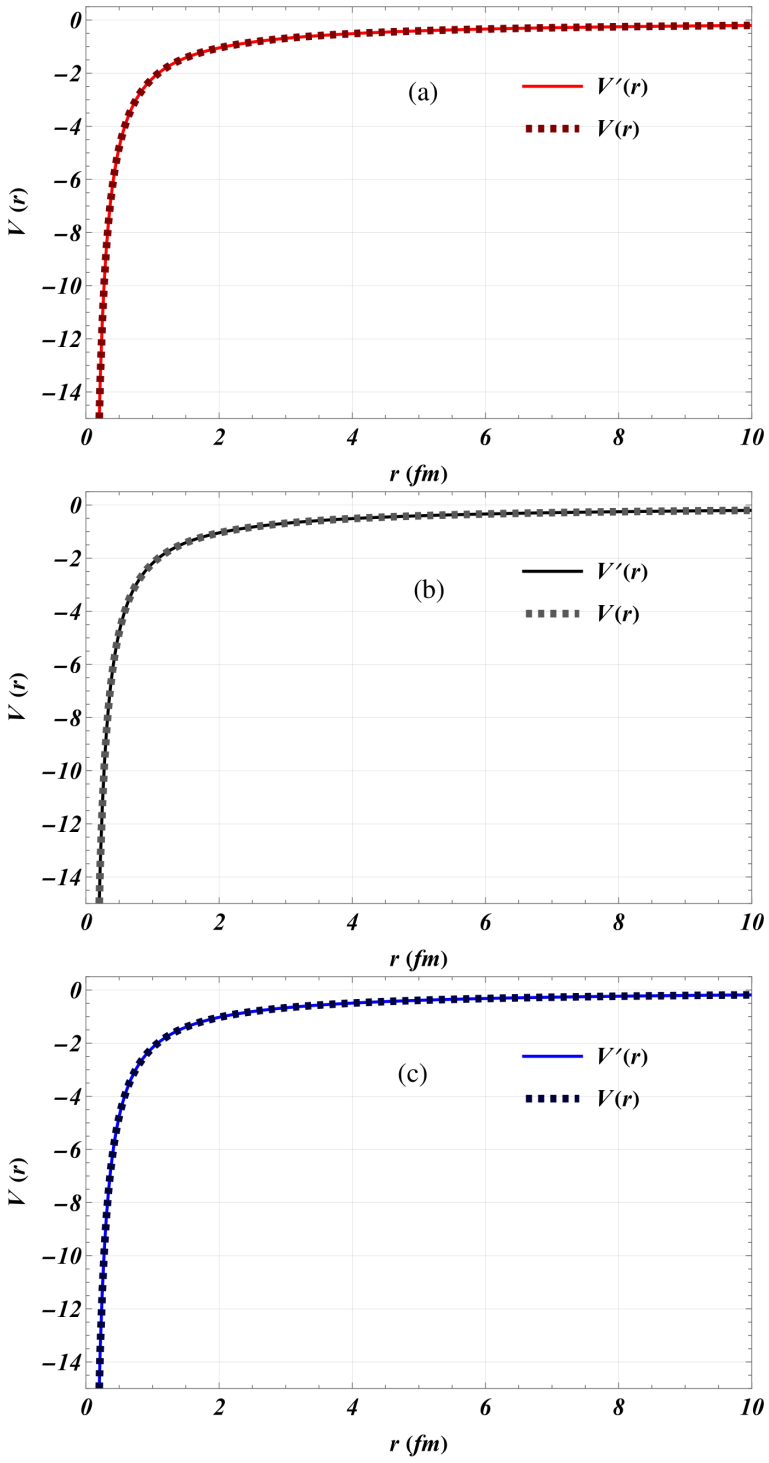

Figure 3.1: Comparison of the MRCYP $V(r)$ and its approximation $V'(r)$ against the separation distance r for (a) $\delta = 0.0001$; (b) $\delta = 0.001$; (c) $\delta = 0.01$.

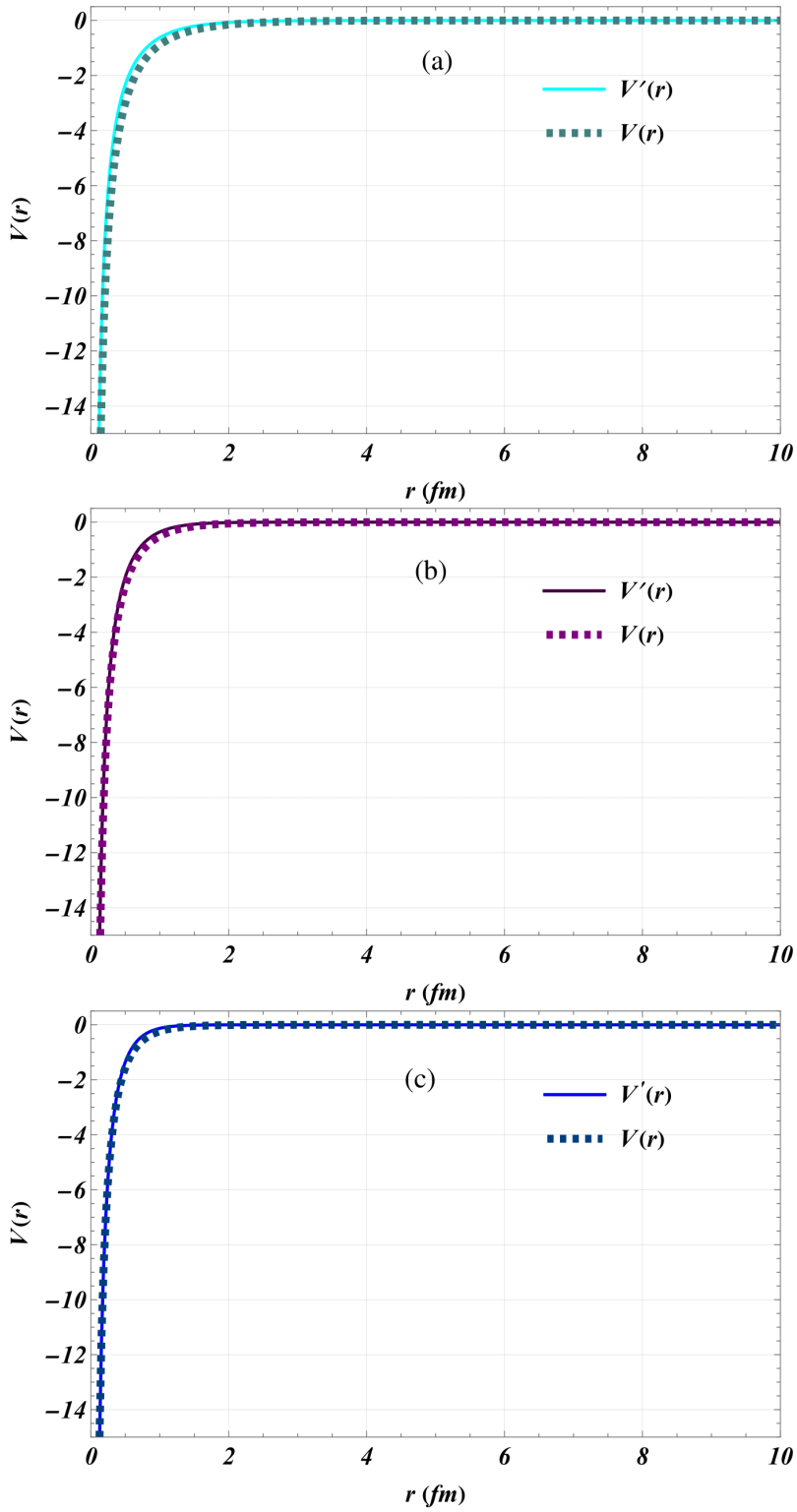

Figure 3.2: Comparison of the HYP $V(r)$ and its approximation $V'(r)$ against the separation distance r for (a) CuLi diatomic molecule; (b) CrH diatomic molecule; (c) for NiC diatomic molecule.

In Figure 3.3, we plotted the potential difference $\Delta V(r)$ between $V'(r)$ and $V(r)$ against the separation distance r for the MRCYP and HYP, respectively.

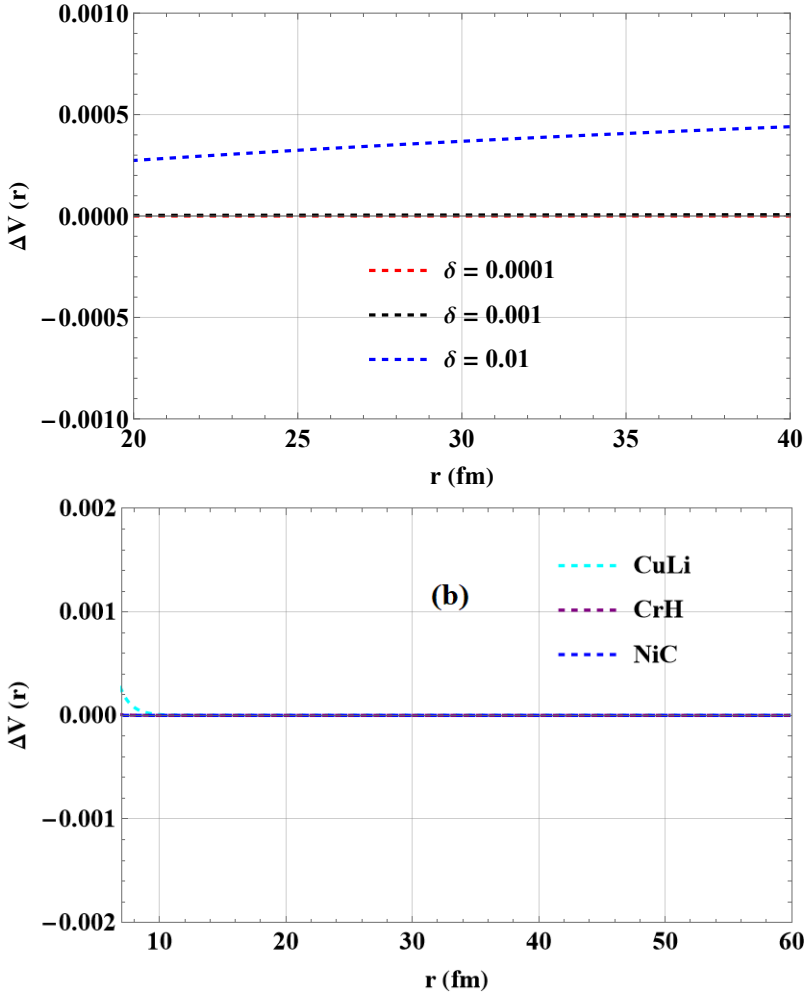

Figure 3.3: The difference $\Delta V(r)$ between $V'(r)$ and $V(r)$ against the separation distance r for (a) the MRCYP; (b) the HYP.

From Figure 3.3(a & b), it is evident that $\Delta V(r)$ is approximately on the order of 10^{-3} for a linear combination of Manning-Rosen and a class of Yukawa potential model, and around 10^{-2} for the Hulthén plus Yukawa potential model, depending on the specific parameters of the potentials. This implies that the total potential equations (3.3) and (3.7) serve as reliable approximations for the centrifugal term $\frac{1}{r^2}$. To further support this assertion, a comparison between the Greene-Aldrich approximation and the centrifugal term is presented in Figure 3.4.

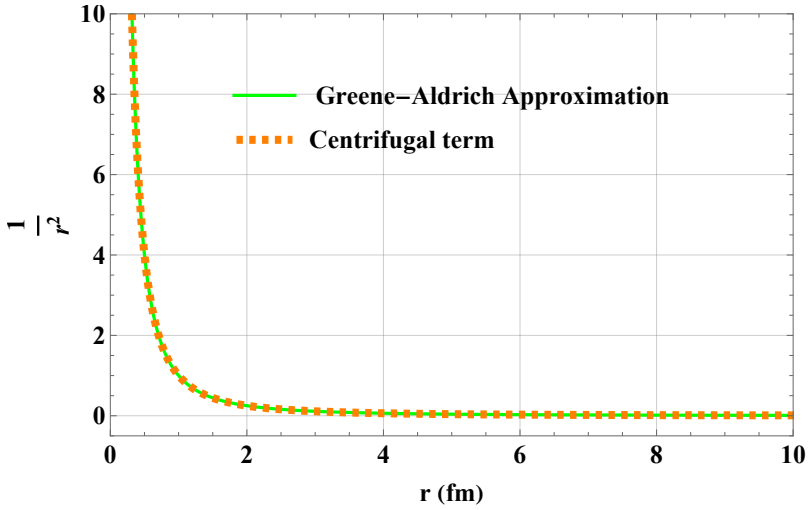

Figure 3.4: Comparison between the Centrifugal term $1/r^2$ with the Greene-Aldrich approximation against the separation distance r for $\delta = 0.0001$ for the Manning-Rosen plus the class of Yukawa potential.

It is evident from the plots in Figure 3.4 that the Greene-Aldrich approximation closely resembles the centrifugal term $1/r^2$. This confirms the appropriateness of the approximation scheme (3.2) for both combined potentials examined in this study.

3.2 Eigensolutions and thermodynamic functions with the MRCYP

3.2.1 Bound solutions for the MRCYP

To determine the partition function and other thermodynamic functions for different parameters δ, we first solve the Schrödinger equation using the Nikiforov-Uvarov method detailed in Chapter 2. Subsequently, we continue with our bounded solutions by incorporating equation (3.3) into Schrödinger equation (2.14) to obtain:

$$\frac{d^2\mathcal{R}_{n\ell}(r)}{dr^2}+\left[\frac{2\mu}{\hbar^2}E_{n\ell}-\frac{2\mu}{\hbar^2}\left(\frac{V_{23}e^{-2\delta r}}{(1-e^{-2\delta r})}-\frac{V_{14}e^{-4\delta r}}{(1-e^{-2\delta r})^2}\right)-\frac{2\mu\ell(\ell+1)}{\hbar^2r^2}\right]\mathcal{R}_{n\ell}(r)=0, \quad (3.8)$$

In order to accurately solve the radial Schrödinger equation, which includes the Manning-Rosen potential along with a class of Yukawa potential models, it becomes imperative to utilize a suitable approximation method to bypass the centrifugal term. The solution to equation (2.14) with $\ell = 0$ can be obtained by approximating the centrifugal term through the Greene and Aldrich method (3.2), yielding:

$$\frac{d^2\mathcal{R}_{n\ell}(r)}{dr^2} + \left[\frac{2\mu}{\hbar^2}E_{n\ell} - \frac{2\mu}{\hbar^2}\left(\frac{V_{23}e^{-2\delta r}}{(1-e^{-2\delta r})} - \frac{V_{14}e^{-4\delta r}}{(1-e^{-2\delta r})^2}\right) - \frac{4\ell(\ell+1)\delta^2 e^{-2\delta r}}{(1-e^{-2\delta r})^2}\right]\mathcal{R}_{n\ell}(r) = 0, \tag{3.9}$$

where V_{14} and V_{23} are given by equation (3.5). The algebraic simplifying of equation (3.9) yields

$$\frac{d^2\mathcal{R}_{n\ell}(r)}{dr^2} + \frac{1}{F^2}\left[-\varepsilon_{n\ell}^2 F^2 + \xi e^{-2\delta r}F - \gamma_1 e^{-4\delta r} - \ell(\ell+1)e^{-2\delta r}\right]\mathcal{R}_{n\ell}(r) = 0, \tag{3.10}$$

where $F = 1 - e^{-2\delta r}$. For bound solution to equation (3.9), we define the following parameters as follows;

$$\begin{aligned} \varepsilon_{n\ell}^2 &= -\frac{2\mu}{4\hbar^2\delta^2}E_{n\ell}; \\ \alpha = \frac{2\mu}{4\hbar^2\delta^2}V_{23}; \quad \gamma &= \frac{2\mu}{4\hbar^2\delta^2}V_{14}. \end{aligned} \tag{3.11}$$

Using the coordinate transformation $s = e^{-2\delta r}$ with $\mathcal{R}_{n\ell}(r) \to \mathcal{R}_{n\ell}(s)$, we obtain the hypergeometric differential equation of the form:

$$\frac{d^2\mathcal{R}_{n\ell}(s)}{ds^2} + \frac{(1-s)}{s(1-s)}\frac{d\mathcal{R}_{n\ell}(s)}{ds} + \frac{1}{s^2(1-s)^2}\left[-\chi_1 s^2 + \chi_2 s - \chi_3\right]\mathcal{R}_{n\ell}(s) = 0, \tag{3.12}$$

where

$$\chi_1 = \varepsilon_{n\ell}^2 + \alpha + \gamma; \quad \chi_2 = 2\varepsilon_{n\ell}^2 + \alpha - \ell(\ell+1); \quad \chi_3 = \varepsilon_{n\ell}^2. \tag{3.13}$$

With the Nikiforov-Uvarov method, we are required to compare equation (2.15) with equation (3.12), to obtain:

$$\tilde{\tau}(s) = 1 - s, \tag{3.14}$$

$$\sigma(s) = s(1-s), \tag{3.15}$$

$$\tilde{\sigma}(s) = -\chi_1 s^2 + \chi_2 s - \chi_3. \tag{3.16}$$

If one insert equations (3.14), (3.15) and (3.16) into equation (2.30), the following linear function is obtained

$$\pi(s) = -\frac{s}{2} \pm \sqrt{(\Upsilon - k)\, s^2 - (\chi_2 - k)\, s + \chi_3}, \tag{3.17}$$

where $\Upsilon = \chi_1 + \frac{1}{4}$. To find the constant k, we consider the discriminant of the expression under the square root of equation (3.17) such that

$$k_{\pm} = -\left(\ell(\ell+1) - \alpha\right) \pm 2\varepsilon_{n\ell}\sqrt{\ell(\ell+1) + \gamma}. \tag{3.18}$$

For bound-state solutions, the valid expression for k is in the form

$$k_{-} = -\left(\ell(\ell+1) - \alpha\right) - 2\varepsilon_{n\ell}\sqrt{\ell(\ell+1) + \gamma}. \tag{3.19}$$

In the view of that, our four possible functions of $\pi(s)$ are obtained by substituting equation (3.18) into equation (3.17) and are written as

$$\pi(s) = -\frac{s}{2} \pm \begin{cases} \left(\varepsilon_{n\ell} + \sqrt{\ell(\ell+1) + \gamma}\right) s - \varepsilon_{n\ell} : & k_{+}, \\ \left(\varepsilon_{n\ell} - \sqrt{\ell(\ell+1) + \gamma}\right) s - \varepsilon_{n\ell} : & k_{-}. \end{cases} \tag{3.20}$$

For the NU method, we select the expression $\pi(s)_{-}$ in order to obtain the polynomial $\tau(s) = \tilde{\tau}(s) + 2\pi(s)$ has a negative derivative. The selected expression is given by

$$\pi(s)_{-} = -\frac{s}{2} - \left[\left(\varepsilon_{n\ell} - \sqrt{\ell(\ell+1) + \gamma}\right) s - \varepsilon_{n\ell}\right]. \tag{3.21}$$

We now write the appropriate polynomial

$$\tau(s) = 1 - 2s - 2\left(\sqrt{\ell(\ell+1) + \gamma} + \varepsilon_{n\ell}\right) s + \varepsilon_{n\ell}, \tag{3.22}$$

which satisfies the bound-state condition $\tau' < 0$, such that

$$\tau'(s) = -2\left(1 + \sqrt{\ell(\ell+1) + \gamma} + \varepsilon_{n\ell}\right) < 0. \tag{3.23}$$

By employing equation (2.29), we define the λ parameter as

$$\lambda \;=\; -\ell(\ell+1) + \alpha - 2\varepsilon_{nl}\sqrt{\ell(\ell+1) + \gamma} - \frac{1}{2} - \sqrt{\ell(\ell+1) + \gamma} - \varepsilon_{n\ell}. \tag{3.24}$$

By determining $\sigma''(s) = -2$ and using equation (2.38), the constant λ_n can be defined as

$$\lambda_n = n^2 + 2n\left[\frac{1}{2} + \varepsilon_{n\ell} + \sqrt{\ell(\ell+1)+\gamma}\right]. \tag{3.25}$$

By letting $\lambda = \lambda_n$ in equation (3.24) and equation (3.25) and solving the resulting equation for $E_{n\ell}$, we obtain the discrete energy spectra for the Manning-Rosen plus a class of Yukawa potential

$$E_{n\ell} = -\frac{\hbar^2\delta^2}{2\mu}\left[\frac{\left(n+\frac{1}{2}+\sqrt{\ell(\ell+1)+\gamma}\right)^2 - (\alpha+\gamma)}{\left(n+\frac{1}{2}+\sqrt{\ell(\ell+1)+\gamma}\right)}\right]^2. \tag{3.26}$$

Next, we calculate the radial wave function $\mathcal{R}_{n\ell}$ in equation (3.9), we first evaluate $\phi(s)$ by substituting (3.15) and equation (3.21) into equation (2.18) and solving the first-order differential equation yields

$$\phi_n(s) = s^{\varepsilon_{n\ell}}\,(1-s)^{\frac{1}{2}+\sqrt{\ell(\ell+1)+\gamma}}. \tag{3.27}$$

The weight function $\rho(s)$ from equation (2.40) can be obtained using equation (2.39) as

$$\rho(s) = s^{2\left(\varepsilon_{n\ell}-\sqrt{\ell(\ell+1)+\gamma}\right)}\,(1-s)^{2\sqrt{\ell(\ell+1)+\gamma}}. \tag{3.28}$$

Implementing the Rodrigues relation of equation (2.39), we obtain

$$\begin{aligned} y_n(s) = B_n s^{-2\left(\varepsilon_{n\ell}-\sqrt{\ell(\ell+1)+\gamma}\right)}\,(1-s)^{-2\sqrt{\ell(\ell+1)+\gamma}}\,\frac{d^n}{ds^n} \\ \times\left[s^{n+2\left(\sqrt{\ell(\ell+1)+\gamma}-\varepsilon_{nl}\right)}\,(1-s)^{n+2\sqrt{\ell(\ell+1)+\gamma}}\right]. \end{aligned} \tag{3.29}$$

It is worthwhile to note that the function above can also be written in the form;

$$y_n(s) \equiv B_n P_n^{2\left(\sqrt{\ell(\ell+1)+\gamma}-\varepsilon_{n\ell}\right),2\left(\sqrt{\ell(\ell+1)+\gamma}\right)}\,(1-2s), \tag{3.30}$$

where P_n is the Jacobi polynomial [117,118]. The functions $y_{n\ell}$, up a numerical factor, are expressed in terms of Jacobi polynomials. and physically hold in the interval $(0 \leq r < \infty \rightarrow 0 \leq s \leq 1)$. Lastly, if one inserts equation (3.27) and equation

(3.30) into $\mathcal{R}_{n\ell}(s) = \phi_n(s)y_n(s)$, we obtain the normalized radial wave function for the MRCYP as

$$\mathcal{R}_{n\ell}(s) = B_{n\ell} s^{\varepsilon_{n\ell}} (1-s)^{\frac{1}{2}+\sqrt{\ell(\ell+1)+\gamma}} P_n^{2\left(\sqrt{\ell(\ell+1)+\gamma}-\varepsilon_{n\ell}\right),2\sqrt{\ell(\ell+1)+\gamma}} (1-2s), \quad (3.31)$$

where $B_{n\ell}$ is the normalization constant. Note that the wave function above satisfies the boundary conditions; $\mathcal{R}_{n\ell}(s) = 0 \quad \text{as} \quad s = 0(r \to \infty) \quad \text{and} \quad \mathcal{R}_{n\ell}(s) = 0 \quad \text{as} \quad s = 1(r = 0)$ [119]. Therefore the wave functions $\mathcal{R}_{n\ell}$ are physically valid for the closed interval $s \in [0,1] \quad \text{or} \quad r \in (0,\infty)$. In addition, the wave functions satisfy the normalization condition

$$\int_0^\infty \mid \mathcal{R}_{n\ell}(r) \mid^2 dr = 1 = b \int_0^1 s^{-1} |\mathcal{R}_{n\ell}(s)|^2 ds. \quad (3.32)$$

3.2.2 Thermodynamic functions for the MRCYP

The partition function is a widely recognized approach for acquiring all thermodynamic characteristics of a system. Once established, this function enables the calculation of all other thermal properties of the system under investigation. Determining the vibrational partition function involves summing the contributions from all attainable vibrational energy levels accessible to the system. The temperature-dependent partition function $Z(T)$ can be derived as outlined in the following references:

$$Z(\beta,\sigma) = \sum_{n=0}^{\sigma} \exp\left(-\beta\left(E_{n\ell} - E_{0\ell}\right)\right), \quad \beta = (k_B T)^{-1} \quad (3.33)$$

[112, 120, 121]. In this context, σ denotes the highest vibration quantum number, k_B represents Boltzmann's constant, and T signifies the absolute temperature. It is widely recognized that the partition function cannot be exactly computed through a closed form. Consequently, we can only obtain a satisfactory estimate for extremely high temperatures as $T \longrightarrow \infty$ and for extremely low temperatures as $T \longrightarrow 0$ [122]. To achieve our goal, we will calculate the partition function $Z(\beta)$ utilizing the Euler-MacLaurin formula [81, 123, 124]:

$$\sum_{n=0}^{\infty} f(x) = \frac{1}{2} f(0) + \int_0^\infty f(x)dx - \sum_{p=1}^{\infty} \frac{B_{2p}}{(2p)!} f^{(2p-1)}(0), \quad (3.34)$$

The Bernoulli numbers, denoted as B_{2p}, represent the values for the derivative of order $(2p-1)$. We consider values of p up to 3. Additionally, $B_2 = 1/6$ and $B_4 = -1/30$. To evaluate the partition function using equation (3.66), we can express the energy spectrum of the Manning-Rosen and a class of Yukawa potential model in the following manner:

$$E_{n\ell} = -h_2 \left[(n+\kappa) - \frac{h_1}{(n+\kappa)}\right]^2, \tag{3.35}$$

where

$$h_1 = \frac{2\mu}{4\hbar^2\delta^2}V_{23} + \frac{2\mu}{4\hbar^2\delta^2}V_{14}, \quad h_2 = \frac{\hbar^2\delta^2}{2\mu}, \quad \kappa = \frac{1}{2} + \sqrt{\frac{1}{4} + \ell(\ell+1) + \gamma}. \tag{3.36}$$

As a result, the Euler-Maclaurin formula vibrational partition function $Z(\beta, \sigma)$ simplifies to

$$\begin{aligned} Z(\beta,\sigma) &= \sum_{n=0}^{\sigma} \exp\left(-\beta\left(E_{n\ell} - E_{0\ell}\right)\right) \\ &= \frac{1}{2} + \int_0^{\sigma} f(n)dn - \sum_{p=1}^{\infty} \frac{B_{2p}}{(2p)!} f^{(2p-1)}(0), \end{aligned} \tag{3.37}$$

where

$$f(n) = \exp\left(-\beta\left[-h_2\left((n+\kappa) - \frac{h_1}{(n+\kappa)}\right)^2\right]\right), \tag{3.38}$$

$$\sigma = \sqrt{h_1} - \kappa. \tag{3.39}$$

Using Mathematica, we integrate equation (3.38) as follows:

$$\begin{aligned} I_1 = -\frac{\sqrt{\pi}}{4\sqrt{-h_2\beta}} \exp\Bigg(& E_{0\ell}\beta - 2h_1h_2\beta \\ & - 2\sqrt{-h_2\beta}\sqrt{-h_1^2h_2\beta}\Bigg)\left(\operatorname{erf}\left[\kappa\sqrt{-h_2\beta} - \frac{\sqrt{-h_1^2h_2\beta}}{\kappa}\right]\right. \\ & \left. + \operatorname{erf}\left[\frac{\sqrt{-h_1^2h_2\beta}}{(\kappa+\sigma)} - \sqrt{-h_2\beta}\,(\kappa+\sigma)\right]\right. \\ & + \exp\left(4\sqrt{-h_2\beta}\sqrt{-h_1^2h_2\beta}\right)\left(\operatorname{erf}\left[\kappa\sqrt{-h_2\beta} + \frac{\sqrt{-h_1^2h_2\beta}}{\kappa}\right]\right. \\ & \left.\left. - \operatorname{erf}\left[\frac{\sqrt{-h_1^2h_2\beta}}{(\kappa+\sigma)} + \sqrt{-h_2\beta}\,(\kappa+\sigma)\right]\right)\right), \end{aligned} \tag{3.40}$$

The standard error function, represented by $\mathrm{erf}(x)$, is defined as follows: $\mathrm{erf}(x) = \frac{2}{\sqrt{\pi}} \int_0^x e^{t^2} dt$ [12]. By substituting equation (3.40) into equation (3.37) and streamlining the process, we can obtain the temperature-dependent partition function $Z(\beta, \sigma)$ as indicated below:

$$\begin{aligned} Z(T,\sigma) = \frac{1}{2} - \frac{(\kappa^4 - h_1^2)\,\hbar^2\delta^2}{12\mu\kappa^3 T} - \frac{\sqrt{\pi}}{4\sqrt{-\frac{h_2}{T}}} \exp\Bigg(\frac{E_{0\ell}}{T} - \frac{2h_1h_2}{T} \\ - 2\sqrt{-\frac{h_2}{T}}\sqrt{-\frac{h_1^2h_2}{T}} \Bigg) \Bigg(\mathrm{erf}\left[\kappa\sqrt{-\frac{h_2}{T}} - \frac{\sqrt{-\frac{h_1^2h_2}{T}}}{\kappa} \right] \\ + \mathrm{erf}\left[\frac{\sqrt{-\frac{h_1^2h_2}{T}}}{(\kappa+\sigma)} - \sqrt{-\frac{h_2}{T}}\,(\kappa+\sigma) \right] \\ + \exp\left(4\sqrt{-\frac{h_2}{T}}\sqrt{-\frac{h_1^2h_2}{T}} \right) \Bigg(\mathrm{erf}\left[\kappa\sqrt{-\frac{h_2}{T}} + \frac{\sqrt{-\frac{h_1^2h_2}{T}}}{\kappa} \right] \\ - \mathrm{erf}\left[\frac{\sqrt{-\frac{h_1^2h_2}{T}}}{(\kappa+\sigma)} + \sqrt{-\frac{h_2}{T}}\,(\kappa+\sigma) \right] \Bigg) \Bigg) . \end{aligned} \tag{3.41}$$

Upon acquiring the partition function as depicted in equation (3.41), it becomes feasible to compute the thermodynamic properties of the system, including the free energy $F(T,\sigma)$, mean energy $U(T,\sigma)$, entropy $S(T,\sigma)$, and specific heat capacity $C_V(T,\sigma)$, utilizing the following relations, as referenced [80]:

1. **Free energy** $F(T,\sigma)$

   The equation below is used to calculate the free energy [80] ;

$$\begin{aligned} F(T,\sigma) &= -T\ln Z(T,\sigma) \\ &= -T\ln\Bigg(\frac{1}{2} - \frac{(\kappa^4 - h_1^2)\,\hbar^2\delta^2}{12\mu\kappa^3 T} \\ &\quad - \frac{\sqrt{\pi}}{4\sqrt{-\frac{h_2}{T}}} \exp\left(\frac{E_{0\ell}}{T} - \frac{2h_1h_2}{T} - 2\sqrt{-\frac{h_2}{T}}\sqrt{-\frac{h_1^2h_2}{T}} \right) \Lambda \Bigg) , \end{aligned} \tag{3.42}$$

where

$$\begin{aligned}\Lambda = \Bigg(& \operatorname{erf}\left[\kappa\sqrt{-\frac{h_2}{T}} - \frac{\sqrt{-\frac{h_1^2 h_2}{T}}}{\kappa}\right] + \operatorname{erf}\left[\frac{\sqrt{-\frac{h_1^2 h_2}{T}}}{(\kappa+\sigma)} - \sqrt{-\frac{h_2}{T}}\,(\kappa+\sigma)\right] \\ & + \exp\left(4\sqrt{-\frac{h_2}{T}}\sqrt{-\frac{h_1^2 h_2}{T}}\right)\left(\operatorname{erf}\left[\kappa\sqrt{-\frac{h_2}{T}} + \frac{\sqrt{-\frac{h_1^2 h_2}{T}}}{\kappa}\right]\right. \\ & \left. - \operatorname{erf}\left[\frac{\sqrt{-\frac{h_1^2 h_2}{T}}}{(\kappa+\sigma)} + \sqrt{-\frac{h_2}{T}}\,(\kappa+\sigma)\right]\right)\Bigg).\end{aligned} \tag{3.43}$$

2. **Mean energy** $U(T,\sigma)$

The following expression can be used to calculate the internal energy [125];

$$\begin{aligned}U(T,\sigma) &= -\frac{\partial \ln Z(T,\sigma)}{\partial T} \\ &= -\Bigg(\frac{1}{2} - \frac{(\kappa^4 - h_1^2)\,\hbar^2\delta^2}{12\mu\kappa^3 T} \\ &\quad - \frac{\sqrt{\pi}}{4\sqrt{-\frac{h_2}{T}}}\exp\left(\frac{E_{0\ell}}{T} - \frac{2h_1h_2}{T} - 2\sqrt{-\frac{h_2}{T}}\sqrt{-\frac{h_1^2h_2}{T}}\right)\Lambda\Bigg)^{-1}(\Gamma_1+\Gamma_2),\end{aligned} \tag{3.44}$$

where

$$\begin{aligned}\Gamma_1 = & \frac{(\kappa^4 - h_1^2)\,\hbar^2\delta^2}{12\mu\kappa^3 T} - \frac{\sqrt{\pi}}{4\sqrt{-\frac{h_2}{T}}}\exp\left(\frac{E_{0\ell}}{T} - \frac{2h_1h_2}{T} - 2\sqrt{\frac{h_2}{T}}\sqrt{-\frac{h_1^2h_2}{T}}\right)\left(-\frac{E_{0\ell}}{T^2}\right. \\ & \left. + \frac{2h_1h_2}{T^2} - \frac{h_2\sqrt{-\frac{h_1^2h_2}{T}}}{\sqrt{-\frac{h_2}{T}}T^2} - \frac{h_1^2h_2\sqrt{-\frac{h_2}{T}}}{\sqrt{-\frac{h_1^2h_2}{T}}}\right)\Lambda \\ & - \exp\left(\frac{E_{0\ell}}{T} - \frac{2h_1h_2}{T} - 2\sqrt{\frac{h_2}{T}}\sqrt{-\frac{h_1^2h_2}{T}}\right)\sqrt{\pi}h_2\Lambda,\end{aligned} \tag{3.45}$$

and

$$\begin{aligned}\Gamma_2 = \frac{2}{\sqrt{\pi}} \Bigg[& \exp\left(- \left(\kappa \sqrt{-\frac{h_2}{T}} - \frac{\sqrt{-\frac{h_1^2 h_2}{T}}}{\kappa} \right)^2 \right) \left(\frac{h_2 \kappa}{2\sqrt{-\frac{h_2}{T}} T^2} - \frac{h_1^2 h_2}{2\kappa \sqrt{-\frac{h_1^2 h_2}{T}} T^2} \right) \\ & + \exp\left(- \left(\frac{\sqrt{-\frac{h_1^2 h_2}{T}}}{(\kappa+\sigma)} - \sqrt{-\frac{h_2}{T}} (\kappa+\sigma) \right)^2 \right) \left(\frac{h_1^2 h_2}{2\sqrt{-\frac{h_1^2 h_2}{T}} T^2 (\kappa+\sigma)} \right. \\ & \left. - \frac{h_2(\kappa+\sigma)}{2\sqrt{-\frac{h_2}{T}} T^2} \right) \Bigg] + \frac{2}{\sqrt{\pi}} \Bigg[\exp\left(- \left(\kappa \sqrt{-\frac{h_2}{T}} - \frac{\sqrt{-\frac{h_1^2 h_2}{T}}}{\kappa} \right)^2 \right) \left(\frac{h_2 \kappa}{2\sqrt{-\frac{h_2}{T}} T^2} \right. \\ & \left. - \frac{h_1^2 h_2}{2\kappa \sqrt{-\frac{h_1^2 h_2}{T}} T^2} \right) \\ & - \exp\left(- \left(\frac{\sqrt{-\frac{h_1^2 h_2}{T}}}{(\kappa+\sigma)} - \sqrt{-\frac{h_2}{T}} (\kappa+\sigma) \right)^2 \right) \left(\frac{h_1^2 h_2}{2\sqrt{-\frac{h_1^2 h_2}{T}} T^2 (\kappa+\sigma)} \right. \\ & \left. - \frac{h_2(\kappa+\sigma)}{2\sqrt{-\frac{h_2}{T}} T^2} \right) \Bigg] + \exp\left(4\sqrt{-\frac{h_2}{T}} \sqrt{-\frac{h_1^2 h_2}{T}} \right) \left(\frac{2h_1^2 h_2 \sqrt{-\frac{h_2}{T}}}{\sqrt{-\frac{h_1^2 h_2}{T}} T^2} \right. \\ & \left. + \frac{2h_2 \sqrt{-\frac{h_1^2 h_2}{T}}}{\sqrt{-\frac{h_2}{T}} T^2} \right) \left(\operatorname{erf}\left[\kappa \sqrt{-\frac{h_2}{T}} + \frac{\sqrt{-\frac{h_1^2 h_2}{T}}}{\kappa} \right] \right. \\ & \left. - \operatorname{erf}\left[\frac{\sqrt{-\frac{h_1^2 h}{T}}}{(\kappa+\sigma)} + \sqrt{-\frac{h_2}{T}} (\kappa+\sigma) \right] \right). \end{aligned} \tag{3.46}$$

3. **Entropy** $S(T, \sigma)$

The expression provided below is used to calculate the entropy [126] ;

$$\begin{aligned} S(T,\sigma) &= \log Z(T,\sigma) + \frac{1}{T}\frac{\partial \log Z(T,\sigma)}{\partial T} \\ &= \log\left(\frac{1}{2} - \frac{\left(\kappa^4 - h_1^2\right)\hbar^2\delta^2}{12\mu\kappa^3 T}\right. \\ &\qquad \left. - \frac{\sqrt{\pi}}{4\sqrt{-\frac{h_2}{T}}}\exp\left(\frac{E_{0\ell}}{T} - \frac{2h_1h_2}{T} - 2\sqrt{-\frac{h_2}{T}}\sqrt{-\frac{h_1^2h_2}{T}}\right)\Lambda\right) \\ &\quad + \frac{1}{T}\left(\frac{1}{2} - \frac{\left(\kappa^4 - h_1^2\right)\hbar^2\delta^2}{12\mu\kappa^3 T}\right. \\ &\quad \left. - \frac{\sqrt{\pi}}{4\sqrt{-\frac{h_2}{T}}}\exp\left(\frac{E_{0\ell}}{T} - \frac{2h_1h_2}{T} - 2\sqrt{-\frac{h_2}{T}}\sqrt{-\frac{h_1^2h_2}{T}}\right)\Lambda\right)^{-1}(\Gamma_1+\Gamma_2)\,. \end{aligned} \tag{3.47}$$

4. **Specific heat capacity** $C_V(T,\sigma)$

The expression for this thermodynamic property is given by [108, 109] ;

$$\begin{aligned} C_V(\beta,\sigma) &= \frac{1}{T^2}\frac{\partial^2 \log Z(T,\sigma)}{\partial T^2} \\ &= \left(\frac{1}{T}\left(\frac{1}{2} - \frac{\left(\kappa^4 - h_1^2\right)\hbar^2\delta^2}{12\mu\kappa^3 T}\right.\right. \\ &\qquad \left.\left. - \frac{\sqrt{\pi}}{4\sqrt{-\frac{h_2}{T}}}\exp\left(\frac{E_{0\ell}}{T} - \frac{2h_1h_2}{T} - 2\sqrt{-\frac{h_2}{T}}\sqrt{-\frac{h_1^2h_2}{T}}\right)\Lambda\right)\right)^{-1}(\Gamma_1 \\ &\qquad + \Gamma_2)\,. \end{aligned} \tag{3.48}$$

3.3 Eigensolutions and thermodynamic functions for the HYP

3.3.1 Bound solutions for the HYP

In the same manner as discussed in subsection 3.2.1, we initiate the process of determining the partition function and thermodynamic properties of the diatomic molecules

CuLi, CrH, and NiC by solving the Schrödinger equation using the Hulthén plus Yukawa potential. The energy spectrum is obtained through the Nikiforov-Uvarov technique. Substituting equation (3.6) into equation (2.14), we derive the following expression:

$$\frac{d^2\mathcal{R}_{n\ell}(r)}{dr^2}+\frac{2\mu}{\hbar^2}\left[E_{n\ell}-\left(\frac{V_0e^{-2\delta r}}{1-e^{-2\delta r}}-\frac{V_0'e^{-\delta r}}{r}\right)-\frac{\ell(\ell+1)\hbar^2}{2\mu r^2}\right]\mathcal{R}_{n\ell}(r)=0. \quad (3.49)$$

Substituting equation (3.2) into (3.49), we have;

$$\frac{d^2\mathcal{R}_{n\ell}(r)}{dr^2}+\left[\frac{2\mu E_{n\ell}}{\hbar^2}-\frac{2\mu}{\hbar^2}\left(\frac{V_0e^{-2\delta r}}{1-e^{-2\delta r}}-\frac{V_0'\delta e^{-2\delta r}}{1-e^{-2\delta r}}\right)-\frac{4\delta^2\ell(\ell+1)e^{-2\delta r}}{(1-e^{-2\delta r})^2}\right]\mathcal{R}_{n\ell}(r)=0. \quad (3.50)$$

By changing the coordinate $s=e^{-2\delta r}$, we write the second derivative of $\mathcal{R}_{n\ell}$ in terms of the new coordinate s as

$$\frac{d^2}{dr^2}=4\delta^2s^2\frac{d^2}{ds^2}+4\delta^2s\frac{d}{ds}. \quad (3.51)$$

If we substitute equation (3.54) in (3.50), we rewrite the radial Schrödinger equation as follows;

$$\frac{d^2\mathcal{R}_{n\ell}(s)}{ds^2}+\frac{(1-s)}{s(1-s)}\frac{d\mathcal{R}_{n\ell}(s)}{ds}+\frac{1}{s^2(1-s)^2}\left[-\varrho_1s^2+\varrho_2s-\varrho_3\right]\mathcal{R}_{n\ell}(s)=0, \quad (3.52)$$

where

$$\varrho_1=\left(\varepsilon_{n\ell}+\alpha_1\right), \quad \varrho_2=\left(2\varepsilon_{n\ell}+\alpha_1-\gamma_1\right), \quad \varrho_3=\varepsilon_{n\ell}, \quad (3.53)$$

Here, subsequent dimensionless notations have been utilized to facilitate mathematics

$$\varepsilon_{n\ell}=-\frac{\mu E_{n\ell}}{2\hbar^2\delta^2}, \quad \alpha_1=\frac{\mu V_0}{2\hbar^2\delta^2}+\frac{\mu V_0'}{\hbar^2\delta}, \quad \gamma_1=\ell(\ell+1). \quad (3.54)$$

Equation (2.15) and (3.52) are compared, and the following parameters are defined:

$$\tilde{\tau}(s)=(1-s), \quad \sigma(s)=s(1-s), \quad \tilde{\sigma}(s)=-\varrho_1s^2+\varrho_2s-\varrho_3. \quad (3.55)$$

respectively. If we are to use equation (2.30), then polynomial equation π becomes

$$\pi(s)=-\frac{s}{2}\pm\sqrt{(\Pi-k)\,s^2-(\varrho_2-k)\,s+\varrho_3}, \quad (3.56)$$

where $\Pi = \varrho_1 + \frac{1}{4}$. To find the value of k, we equate the discriminant of equation (3.56) to zero, yielding the subsequent expression:

$$k_{\pm} = \alpha_1 - \gamma_1 \pm 2\sqrt{\varepsilon_{n\ell}}\sqrt{\frac{1}{4} + \gamma_1}. \tag{3.57}$$

For bound solutions, the valid expression for k is given by

$$k_{-} = \alpha_1 - \gamma_1 - 2\sqrt{\varepsilon_{n\ell}}\sqrt{\frac{1}{4} + \gamma_1}. \tag{3.58}$$

The substitution of k in equation (3.56) gives the possible functions of $\pi(s)$ as

$$\pi(s) = -\frac{s}{2} \pm \begin{cases} \left(\sqrt{\varepsilon_{n\ell}} + \sqrt{\frac{1}{4} + \gamma_1}\right) s - \sqrt{\varepsilon_{n\ell}}, & \text{for} \quad \alpha_1 - \gamma_1 + 2\sqrt{\varepsilon_{n\ell}}\sqrt{\frac{1}{4} + \gamma_1}, \\ \left(\sqrt{\varepsilon_{n\ell}} + \sqrt{\frac{1}{4} + \gamma_1}\right) s - \sqrt{\varepsilon_{n\ell}}, & \text{for} \quad \alpha_1 - \gamma_1 - 2\sqrt{\varepsilon_{n\ell}}\sqrt{\frac{1}{4} + \gamma_1}. \end{cases} \tag{3.59}$$

For the NU method, we select one function of $\pi(s)$ which gives a negative derivative for $\tau(s)$, which is

$$\pi(s) = -\frac{s}{2} - \left(\sqrt{\frac{1}{4} + \gamma_1} + \sqrt{\varepsilon_{n\ell}} + \right) s - \sqrt{\varepsilon_{n\ell}}. \tag{3.60}$$

Taking the derivative of equation (3.60), we obtain

$$\pi'(s) = -\frac{s}{2} - \left(\sqrt{\frac{1}{4} + \gamma_1} + \sqrt{\varepsilon_{n\ell}} + \right). \tag{3.61}$$

In order to get the polynomial $\tau(s)$, we employ equation (2.21) and obtain the following result:

$$\tau(s) = 1 - 2s - 2\left[\left(\sqrt{\frac{1}{4} + \gamma_1} + \sqrt{\varepsilon_{n\ell}} + \right) s - \sqrt{\varepsilon_{n\ell}}\right]. \tag{3.62}$$

The derivative of $\tau(s)$ in equation (3.62),

$$\tau^{'}(s) = -2\left[1 + \left(\sqrt{\frac{1}{4} + \gamma_1} + \sqrt{\varepsilon_{n\ell}}\right)\right] < 0. \tag{3.63}$$

The parameter λ is defined

$$\lambda = \alpha_1 - \gamma_1 - 2\sqrt{\varepsilon_{n\ell}}\sqrt{\frac{1}{4} + \gamma_1} - \frac{1}{2} - \left(\sqrt{\frac{1}{4} + \gamma_1} + \sqrt{\varepsilon_{n\ell}}\right), \tag{3.64}$$

and λ_n is expressed as,

$$\lambda_n = n^2 + n + 2n\sqrt{\varepsilon_{n\ell}} + 2n\sqrt{\frac{1}{4} + \gamma_1}. \tag{3.65}$$

The eigenvalue expression holds if $\lambda = \lambda_n$

$$\varepsilon_{n\ell} = \frac{1}{4}\left[\frac{\left(n + \frac{1}{2} + \sqrt{\frac{1}{4} + \gamma_1}\right)^2 - \alpha_1}{\left(n + \frac{1}{2} + \sqrt{\frac{1}{4} + \gamma_1}\right)}\right]^2. \tag{3.66}$$

Substituting equation (3.54) into (3.66), we obtain the energy as follows:

$$E_{n\ell} = -\frac{\hbar^2\delta^2}{2\mu}\left[\frac{(n+\kappa_1)^2 - \alpha_1}{(n+\kappa_1)}\right]^2, \tag{3.67}$$

where

$$\kappa_1 = \frac{1}{2} + \sqrt{\frac{1}{4} + \gamma_1}. \tag{3.68}$$

To compute the radial wave function $\mathcal{R}_{n\ell}(s)$ for the Hulthén plus Yukawa potential, we start by replacing $\pi(s)$ from equation (3.55) and $\sigma(s)$ from equation (3.60) in equation (2.18). This results in:

$$\frac{d\phi(s)}{\phi(s)} = \left[\frac{\sqrt{\varepsilon_{n\ell}}(1-s) - \kappa_1 s}{s(1-s)}\right] ds. \tag{3.69}$$

Integrating equation (3.69), we obtain

$$\phi(s) = s^{\sqrt{\varepsilon_{n\ell}}}(1-s)^{\kappa_1}. \tag{3.70}$$

From equation (2.39),

$$\frac{d\rho(s)}{\rho(s)} = \left[\frac{2\sqrt{\varepsilon_{n\ell}}(1-s) - 2s\left(\sqrt{\frac{1}{4} + \gamma_1}\right)}{s(1-s)}\right] ds. \tag{3.71}$$

Integrating equation (3.71), we obtain

$$\rho(s) = s^{2\sqrt{\varepsilon_{n\ell}}}(1-s)^{2\sqrt{\frac{1}{4}+\gamma_1}}. \tag{3.72}$$

By substituting equation (3.72) into equation (2.39), we get

$$\begin{aligned} y_n(s) &= B_n(s)s^{-2\sqrt{\varepsilon_{n\ell}}}(1-s)^{\sqrt{\frac{1}{4}+\gamma_1}}\frac{d^n}{ds^n}\left[s^{2\sqrt{\varepsilon_{n\ell}}+n}(1-s)^{\sqrt{\frac{1}{4}+\gamma_1}}\right] \\ &= P_n^{\left(2\sqrt{\varepsilon_{n\ell}}, 2\sqrt{\frac{1}{4}+\gamma_1}\right)}(1-2s). \end{aligned} \tag{3.73}$$

By substituting equations (3.70) and (3.73) into equation (2.16), we derive the comprehensive expression for the wave function of the Hulthén plus Yukawa potential in terms of the Jacobi polynomial:

$$\mathcal{R}_{n\ell}(s) = B_{n\ell} s^{\sqrt{\varepsilon_{n\ell}}}(1-s)^{\kappa_1} P_n^{\left(2\sqrt{\varepsilon_{n\ell}}, 2\sqrt{\frac{1}{4}+\gamma_1}\right)}(1-2s). \tag{3.74}$$

3.3.2 Thermodynamic functions for the HYP

Likewise, as demonstrated in subsection (3.2.2), we calculate the vibrational partition function and other thermal properties for various diatomic molecules. The overall impact of the bound state on the system's partition function $Z(\beta)$ can be assessed using Boltzmann's distribution as follows:

$$Z(\beta) = \sum_{n=0}^{n_{\max}} e^{-\beta E_{n\ell}}, \tag{3.75}$$

where $n = 0, 1, 2, ... < n_{\max}$, and $n_{\max}$ is the maximum quantum number. The maximum value $n_{\max}$ can be obtained by setting $dE_n/dn = 0$, to obtain

$$n_{\max} = -\kappa_1 \pm \sqrt{p_2}. \tag{3.76}$$

To evaluate the partition function $Z(\beta)$, the energy eigenvalue equation (3.67) can be written as follows;

$$E_{n\ell} = -p_1 \left[\frac{(n+\kappa_1)^2 - p_2}{(n+\kappa_1)}\right]^2, \tag{3.77}$$

where

$$\kappa_1 = \frac{1}{2} + \sqrt{\frac{1}{4}+\gamma_1}, \quad p_1 = \frac{\hbar^2\delta^2}{2\mu}, \quad p_2 = \frac{\mu V_0}{2\hbar^2\delta^2} + \frac{\mu V_0'}{\hbar^2\delta}. \tag{3.78}$$

Substituting equation (3.78) into equation (3.77) yields

$$Z(\beta) = \sum_{n=0}^{n_{\max}} \exp\left[-\beta p_1 \left(\frac{(n+\kappa_1)^2 - p_2}{(n+\kappa_1)}\right)^2\right]. \tag{3.79}$$

By replacing the summation in equation (3.79) by an integral, we obtain;

$$Z(\beta) = \int_{n=0}^{n_{\max}} \exp\left[-\beta p_1 \left(\frac{(n+\kappa_1)^2 - p_2}{(n+\kappa_1)}\right)^2\right] dn. \tag{3.80}$$

The integral in equation (3.80), can be evaluated as follows;

$$Z(\beta) = \int_{\kappa_1}^{n_{\max}+\kappa_1} \exp\left[-\beta p_1 \left(\rho^2 + \frac{p_2^2}{\rho^2} - 2p_2\right)^2\right] d\rho, \tag{3.81}$$

where $\rho = n + \kappa_1$, and the limits of the integral are: $\kappa_1 \leq \rho \leq n_{\max} + \kappa_1$. From here, we make use of Mathematica to evaluate the integral in equation (3.81), to obtain the partition function $Z(\beta)$ for the Hulthén plus Yukawa potential model as follows:

$$\begin{aligned} Z(\beta) = -\frac{\exp\left(2p_1p_2\beta - 2\sqrt{p_2\beta}\sqrt{p_1p_2^2\beta}\right)\sqrt{\pi}}{4\sqrt{p_2\beta}} \Bigg(& \operatorname{erf}\left[\frac{\sqrt{p_1p_2^2\beta}}{\kappa_1} - \sqrt{p_2\beta}\kappa_1\right] \\ & + \exp\left(4\sqrt{p_2\beta}\sqrt{p_1p_2^2\beta}\right)\operatorname{erf}\left[\frac{\sqrt{p_1p_2^2\beta}}{\kappa_1} + \sqrt{p_2\beta}\kappa_1\right] - \operatorname{erf}\left[\frac{\sqrt{p_1p_2^2\beta}}{\kappa_2} - \sqrt{p_2\beta}\kappa_2\right] \\ & - \exp\left(4\sqrt{p_2\beta}\sqrt{p_1p_2^2\beta}\right)\operatorname{erf}\left[\frac{\sqrt{p_1p_2^2\beta}}{\kappa_2} - \sqrt{p_2\beta}\kappa_2\right]\Bigg). \end{aligned} \tag{3.82}$$

The expression for κ_2 is given by $\kappa_2 = n_{\max} + \frac{1}{2} + \sqrt{\frac{1}{4} + \gamma_1}$ [111]. Following that, we present the free energy $F(\beta)$, mean energy $U(\beta)$, entropy $S(\beta)$, and specific heat capacity $C(\beta)$ for diatomic molecules CuLi, CrH, and NiC for the Hulthén plus Yukawa potential model.

1. **Free energy** $F(\beta)$

$$\begin{aligned} F(\beta) &= -\frac{1}{\beta}\ln Z(\beta) \\ &= \\ &\quad -\frac{1}{\beta}\Bigg(-\frac{\exp\left(2p_1p_2\beta - 2\sqrt{p_2\beta}\sqrt{p_1p_2^2\beta}\right)\sqrt{\pi}}{4\sqrt{p_2\beta}}\Bigg(-\operatorname{erf}\left[\frac{\sqrt{p_1p_2^2\beta}}{\kappa_1} - \sqrt{p_2\beta}\kappa_1\right] \\ &\qquad + \exp\left(4\sqrt{p_2\beta}\sqrt{p_1p_2^2\beta}\right)\operatorname{erf}\left[\frac{\sqrt{p_1p_2^2\beta}}{\kappa_1} + \sqrt{p_2\beta}\kappa_1\right] \\ &\qquad + \operatorname{erf}\left[\frac{\sqrt{p_1p_2^2\beta}}{\kappa_2} - \sqrt{p_2\beta}\kappa_2\right] \\ &\qquad + \exp\left(4\sqrt{p_2\beta}\sqrt{p_1p_2^2\beta}\right)\operatorname{erf}\left[\frac{\sqrt{p_1p_2^2\beta}}{\kappa_2} - \sqrt{p_2\beta}\kappa_2\right]\Bigg)\Bigg)^{-1}. \end{aligned} \tag{3.83}$$

2. **Mean energy** $U(\beta)$

$$
\begin{aligned}
&U(\beta)\\
&\quad= -\frac{\partial \ln Z(\beta)}{\partial \beta}\\
&\quad= \Bigg(\sqrt{\pi}\left(\operatorname{erf}\left[\frac{\sqrt{p_1 p_2^2 \beta}}{\kappa_1} - \sqrt{p_2\beta}\kappa_1\right]\right.\\
&\qquad\qquad + \exp\left(4\sqrt{p_2\beta}\sqrt{p_1 p_2^2\beta}\right)\operatorname{erf}\left[\frac{\sqrt{p_1 p_2^2\beta}}{\kappa_1} + \sqrt{p_2\beta}\kappa_1\right]\\
&\qquad\qquad - \operatorname{erf}\left[\frac{\sqrt{p_1 p_2^2\beta}}{\kappa_2} - \sqrt{p_2\beta}\kappa_2\right]\\
&\qquad + \exp\left(4\sqrt{p_2\beta}\sqrt{p_1 p_2^2\beta}\right)\operatorname{erf}\left[\frac{\sqrt{p_1^2 p_2\beta}}{\kappa_2} - \sqrt{p_2\beta}\kappa_2\right]\Bigg)\Bigg)^{-1}\left(4\exp\left(-2p_1p_2\beta\right.\right.\\
&\qquad\qquad \left.\left. + 2\sqrt{p_2\beta}\sqrt{p_1 p_2^2\beta}\right)\sqrt{p_2\beta}\right)(\Omega_1 - \Omega_2)\,,
\end{aligned}
\tag{3.84}
$$

where

$$
\begin{aligned}
\Omega_1 = \frac{\exp\left(2p_1p_2\beta - 2\sqrt{p_2\beta}\sqrt{p_1p_2^2\beta}\right)p_2\sqrt{\pi}}{8(p_2\beta)^{3/2}}&\left(-\operatorname{erf}\left[\frac{\sqrt{p_1p_2^2\beta}}{\kappa_1} - \sqrt{p_2\beta}\kappa_1\right]\right.\\
&+ \exp\left(4\sqrt{p_2\beta}\sqrt{p_1p_2^2\beta}\right)\operatorname{erf}\left[\frac{\sqrt{p_1p_2^2\beta}}{\kappa_1} + \sqrt{p_2\beta}\kappa_1\right]\\
&+ \operatorname{erf}\left[\frac{\sqrt{p_1p_2^2\beta}}{\kappa_2} - \sqrt{p_2\beta}\kappa_2\right]\\
&\left.+ \exp\left(4\sqrt{p_2\beta}\sqrt{p_1p_2^2\beta}\right)\operatorname{erf}\left[\frac{\sqrt{p_1p_2^2\beta}}{\kappa_2} - \sqrt{p_2\beta}\kappa_2\right]\right)\\
-\Pi_2\left(2p_1p_2 - \frac{p_1p_2^2\sqrt{p_2\beta}}{\sqrt{p_1p_2^2\beta}} - \frac{p_2\sqrt{p_1p_2^2\beta}}{\sqrt{p_2\beta}}\right)&\left(-\operatorname{erf}\left[\frac{\sqrt{p_1p_2^2\beta}}{\kappa_1} - \sqrt{p_2\beta}\kappa_1\right]\right.\\
&+ \exp\left(4\sqrt{p_1\beta}\sqrt{p_1p_2^2\beta}\right)\operatorname{erf}\left[\frac{\sqrt{p_1p_2^2\beta}}{\kappa_1} + \sqrt{p_2\beta}\kappa_1\right]\\
&+ \operatorname{erf}\left[\frac{\sqrt{p_1p_2^2\beta}}{\kappa_2} - \sqrt{p_2\beta}\kappa_2\right]\\
&\left.+ \exp\left(4\sqrt{p_2\beta}\sqrt{p_1p_2^2\beta}\right)\operatorname{erf}\left[\frac{\sqrt{p_1p_2^2\beta}}{\kappa_2} - \sqrt{p_2\beta}\kappa_2\right]\right)\Pi_1,
\end{aligned}
\tag{3.85}
$$

$$\Omega_2 = \Pi_2 \left[-\frac{2}{\sqrt{\pi}} \exp\left(-\left(\frac{\sqrt{p_1 p_2^2 \beta}}{\kappa_1} - \sqrt{p_2 \beta}\kappa_1 \right)^2 \right) \left(\frac{p_1 p_2^2}{2\sqrt{p_1 p_2^2 \beta}\kappa_1} - \frac{p_2 \kappa_1}{2\sqrt{p_2 \beta}} \right) \right.$$
$$+ \frac{2}{\sqrt{\pi}} \exp\left(4\sqrt{p_2 \beta}\sqrt{p_1 p_2^2 \beta} \right.$$
$$\left. - \left(\frac{\sqrt{p_1 p_2^2 \beta}}{\zeta_1} + \sqrt{p_2 \beta}\kappa_1 \right)^2 \right) \left(\frac{p_1 p_2^2}{2\sqrt{p_1 p_2^2 \beta}\kappa_1} + \frac{p_2 \kappa_1}{2\sqrt{p_2 \beta}} \right)$$
$$+ \frac{2}{\sqrt{\pi}} \exp\left(-\left(\frac{\sqrt{p_1 p_2^2 \beta}}{\kappa_2} - \sqrt{p_2 \beta}\kappa_2 \right)^2 \right) \left(\frac{p_1 p_2^2}{2\sqrt{p_1 p_2^2 \beta}\kappa_2} - \frac{p_2 \kappa_2}{2\sqrt{p_2 \beta}} \right)$$
$$+ \frac{2}{\sqrt{\pi}} \exp\left(4\sqrt{p_2 \beta}\sqrt{p_1 p_2^2 \beta} \right.$$
$$\left. \left. - \left(\frac{\sqrt{p_1 p_2^2 \beta}}{\kappa_2} + \sqrt{p_2 \beta}\kappa_2 \right)^2 \right) \left(\frac{p_1 p_2^2}{2\sqrt{p_1 p_2^2 \beta}\kappa_2} + \frac{p_2 \kappa_2}{2\sqrt{p_2 \beta}} \right) \right]$$
$$+ \exp\left(4\sqrt{p_2 \beta}\sqrt{p_1 p_2^2 \beta} \right) \left(\frac{2p_1 p_2^2 \sqrt{p_2 \beta}}{\sqrt{p_1 p_2^2 \beta}} + \frac{2p_2 \sqrt{p_1 p_2^2 \beta}}{\sqrt{p_2 \beta}} \right) \operatorname{erf}\left[\frac{\sqrt{p_1 p_2^2 \beta}}{\kappa_1} \right.$$
$$\left. + \sqrt{p_2 \beta}\kappa_1 \right] + \exp\left(4\sqrt{p_2 \beta}\sqrt{p_1 p_2^2 \beta} \right) \left(\frac{2p_1 p_2^2 \sqrt{p_2 \beta}}{\sqrt{p_1 p_2^2 \beta}} \right.$$
$$\left. + \frac{2p_2 \sqrt{p_1 p_2^2 \beta}}{\sqrt{p_2 \beta}} \right) \operatorname{erf}\left[\frac{\sqrt{p_1 p_2^2 \beta}}{\kappa_2} - \sqrt{p_2 \beta}\kappa_2 \right], \tag{3.86}$$

where

$$\Pi_1 = \left(4 \exp\left(-2p_1 p_2 \beta + 2\sqrt{p_2 \beta}\sqrt{p_1 p_2^2 \beta} \right) \sqrt{p_2 \beta} \right) \tag{3.87}$$

and

$$\Pi_2 = \frac{\exp\left(2p_1 p_2 \beta - 2\sqrt{p_2 \beta}\sqrt{p_1 p_2^2 \beta} \right) \sqrt{\pi}}{4\sqrt{p_2 \beta}}. \tag{3.88}$$

3. **Entropy** $S(\beta)$

$$
\begin{aligned}
S(\beta) &= \ln Z(\beta) - \beta \frac{\partial \ln Z(\beta)}{\partial \beta} \\
&= \left(\sqrt{\pi} \left(-\operatorname{erf}\left[\frac{\sqrt{-\frac{1}{\beta}\ln p_2^2 \beta}}{\kappa_1} - \sqrt{p_2 \beta}\kappa_1 \right] \right.\right. \\
&\qquad + \exp\left(4\sqrt{p_2\beta}\sqrt{-\frac{1}{\beta}\ln p_2^2\beta} \right) \operatorname{erf}\left[\frac{\sqrt{-\frac{1}{\beta}\ln^2 p_2\beta}}{\kappa_1} + \sqrt{p_2\beta}\kappa_1 \right] \\
&\qquad\qquad + \operatorname{erf}\left[\frac{\sqrt{-\frac{1}{\beta}\ln^2 p_2\beta}}{\kappa_2} - \sqrt{p_2\beta}\kappa_2 \right] \\
&\qquad \left.\left. + \exp\left(4\sqrt{p_2\beta}\sqrt{-\frac{1}{\beta}\ln^2 p_2\beta} \right) \operatorname{erf}\left[\frac{\sqrt{-\frac{1}{\beta}\ln^2 p_2\beta}}{\kappa_2} - \sqrt{p_2\beta}\kappa_2 \right] \right) \right)^{-1} \\
&\quad \times (\beta\Omega_1 - \Omega_2) - \ln\left(\Pi_2 \left(-\operatorname{erf}\left[\frac{\sqrt{p_1 p_2^2 \beta}}{\kappa_1} - \sqrt{p_2\beta}\kappa_1 \right] \right.\right. \\
&\qquad + \exp\left(4\sqrt{p_2\beta}\sqrt{p_1 p_2^2\beta} \right) \operatorname{erf}\left[\frac{\sqrt{p_1 p_2^2\beta}}{\kappa_1} + \sqrt{p_2\beta}\kappa_1 \right] \\
&\qquad\qquad + \operatorname{erf}\left[\frac{\sqrt{p_1 p_2^2\beta}}{\kappa_2} - \sqrt{p_2\beta}\kappa_2 \right] \\
&\qquad \left.\left. + \exp\left(4\sqrt{p_2\beta}\sqrt{p_1 p_2^2\beta} \right) \operatorname{erf}\left[\frac{\sqrt{p_1 p_2^2\beta}}{\kappa_2} - \sqrt{p_2\beta}\kappa_2 \right] \right) \right).
\end{aligned}
\tag{3.89}
$$

4. **Specific Heat Capacity** $C_V(\beta)$

$$
\begin{aligned}
C_V(\beta) &= \beta^2 \frac{\partial^2 \ln Z(\beta)}{\partial \beta^2} \\
&= -\left(\sqrt{\pi}\left(\exp\left(4\sqrt{p_2\beta}\sqrt{-\frac{1}{\beta}\ln^2 p_2\beta}\right)\operatorname{erf}\left[\frac{\sqrt{-\frac{1}{\beta}\ln^2 p_2\beta}}{\kappa_1}+\sqrt{p_2\beta}\kappa_1\right]\right.\right. \\
&\quad -\operatorname{erf}\left[\frac{\sqrt{-\frac{1}{\beta}\ln^2 p_2\beta}}{\kappa_1}-\sqrt{p_2\beta}\kappa_1\right]+\operatorname{erf}\left[\frac{\sqrt{-\frac{1}{\beta}\ln^2 p_2\beta}}{\kappa_2}-\sqrt{p_2\beta}\kappa_2\right] \\
&\quad \left.\left.+\exp\left(4\sqrt{p_2\beta}\sqrt{-\frac{1}{\beta}\ln^2 p_2\beta}\right)\operatorname{erf}\left[\frac{\sqrt{-\frac{1}{\beta}\ln^2 p_2\beta}}{\kappa_2}-\sqrt{p_2\beta}\kappa_2\right]\right)\right)^{-1}\left(\beta^3\Omega_1\right. \\
&\quad \left.-\Omega_2\right).
\end{aligned}
\tag{3.90}
$$

3.3.3 Bound solutions for the HYP with the magnetic and AB flux fields

To analyze how external magnetic and Aharonov-Bohm flux fields affect the thermodynamic properties of CuLi, CrH, and NiC diatomic molecules, we solve the Schrödinger equation. This equation incorporates the presence of magnetic and AB flux fields, as well as the Hulthén plus Yukawa potential. The expression for the Hamiltonian operator of a charged particle moving within the Hulthén plus Yukawa potential can be derived using cylindrical coordinates. This derivation considers the combined influence of an external magnetic field with a topological defect and AB flux. Reference [127] outlines the Schrödinger equation for this case as

$$
\left[\frac{1}{2\mu}\boldsymbol{P}^2-\left(\frac{V_0 e^{-2\delta r}}{1-e^{-2\delta r}}-\frac{V_0' e^{-\delta r}}{r}\right)\right]\psi(r,\varphi)=E_{nm}\psi(r,\varphi), \tag{3.91}
$$

where E_{nm} denotes the energy level, μ is the effective mass of the system. It is important to mention that when considering this, the momentum operator of the charged particle needs modification. For this purpose, we minimally associate a four-vector with the momentum operator in the following manner:

$$
\boldsymbol{P}=\left(i\hbar\boldsymbol{\nabla}-\frac{e}{c}\boldsymbol{A}\right),
$$

and $\boldsymbol{A}$ is the vector potential given by a superposition of two vectors can be expressed

$$\boldsymbol{A} = \boldsymbol{A}_1 + \boldsymbol{A}_2 = 0$$

with azimuthal components [127] and an external magnetic field represented by

$$\nabla \times \boldsymbol{A}_1 = \boldsymbol{B}, \quad \nabla \times \boldsymbol{A}_2 = 0,$$

where $\boldsymbol{B}$ is the magnetic field.

$$\boldsymbol{A}_1 = \frac{\boldsymbol{B}e^{-ar}}{(1-e^{-ar})}\hat{\varphi}$$

and

$$\boldsymbol{A}_2 = \frac{\varphi_{AB}}{2\pi r}\hat{\varphi}$$

give the additional magnetic flux φ_{AB} produced by a solenoid with

$$\nabla.\boldsymbol{A}_2 = 0$$

[127]. The vector potential in full is written in a simple form as [127];

$$\boldsymbol{A} = \left(0, \frac{\boldsymbol{B}e^{-\delta r}}{(1-e^{-\delta r})} + \frac{\varphi_{AB}}{2\pi r}, 0\right). \tag{3.92}$$

By utilizing equation (3.91), we deduce the subsequent radial second-order differential equation:

$$\mathcal{R}''_{nm}(r) + \frac{2\mu}{\hbar^2}\left[E_{nm} - V_{eff}(r)\right]\mathcal{R}_{nm}(r) = 0, \tag{3.93}$$

$$\begin{aligned} V_{eff}(r) = &-\frac{V_0 e^{-2\delta r}}{1-e^{-2\delta r}} - \frac{V\prime_0 e^{-\delta r}}{r} + \hbar\omega_c(m+\xi)\frac{e^{-\delta r}}{(1-e^{-\delta r})\,r} \\ &+ \left(\frac{\mu\omega_c}{2}\right)\frac{e^{-2\delta r}}{(1-e^{-\delta r})^2} + \frac{\hbar^2}{2\mu}\left[\frac{(m+\xi)^2 - \frac{1}{4}}{r^2}\right]. \end{aligned} \tag{3.94}$$

Here, $\xi = \varphi_{AB}$ is an integer with the flux quantum, $\varphi_0 = \frac{hc}{e}$, and the cyclotron frequency $\omega_c = \frac{e\boldsymbol{B}}{\mu c}$. The equation (3.93) becomes unsolvable due to the inclusion of a centrifugal element. To circumvent this centrifugal term, we employ the Greene-Aldrich approximation scheme (3.2). The approximate potential can then be expressed as follows [95, 116]:

$$V_{eff}(r) = C_1 + C_2 z + C_3 z^2. \tag{3.95}$$

Here, we have also introduced a new transformation defined as

$$z = \frac{e^{-\delta r}}{1 - e^{-\delta r}}.$$

To simplify matters, we will introduce dimensionless notations C_1, C_2, and C_3 in the following manner.

$$C_1 = \frac{\hbar^2\delta^2}{2\mu}\left((m+\xi)^2 - \frac{1}{4}\right), \tag{3.96}$$

$$C_2 = \hbar\omega_c(m+\xi)\delta - V_0 - V_0'\delta + 2\left(\frac{\hbar^2\delta^2}{2\mu}\left((m+\xi)^2 - \frac{1}{4}\right)\right), \tag{3.97}$$

$$C_3 = \frac{\hbar^2\delta^2}{2\mu}\left((m+\xi)^2 - \frac{1}{4}\right) + \hbar\omega_c(m+\xi)\delta + \frac{\mu\omega_c^2}{2}. \tag{3.98}$$

Please note that the study of the potential $V_{eff}(r)$ involves applying the quantization rule. This is accomplished by identifying the turning points z_a and z_b when solving $V(z) = E_{nm}$. Therefore, we can deduce that

$$z_a = -\frac{C_2}{2C_3} - \sqrt{\frac{C_2^2 - 4_{C_3}(C_1 - E_{nm})}{2C_3}}, \tag{3.99}$$

$$z_b = -\frac{C_2}{2C_3} + \sqrt{\frac{C_2^2 - 4C_3(C_1 - E_{nm})}{2C_3}}, \tag{3.100}$$

with

$$k(z) = \sqrt{\frac{2\mu C_3}{\hbar^2}}\left[(z - z_a)(z - z_b)\right]^{1/2}, \tag{3.101}$$

where $k(z)$ lies within the interval defined by z_a and z_b. Equation (3.93) can be expressed in the form of a Riccati equation

$$-\delta z(1+z)\varphi_0'(z) + (\varphi_0(z))^2 + \frac{2\mu}{\hbar^2}\left[E_{nm} - C_1 + C_2 z - C_3 z^2\right]\varphi_0(z) = 0. \tag{3.102}$$

The logarithmic derivative $\varphi_0(z)$ of the lowest energy state exhibits a consistent trend, intersecting zero at only one point and lacking singularities. Hence, it becomes imperative to utilize a linear equation involving z. As a result, we suggest a tentative solution represented as

$$\varphi_0(z) = A + Bz.$$

Upon substituting this solution into equation (3.102), we derive the non-linear Riccati equation, facilitating the computation of the lowest energy state's energy as follows:

$$E_{0m} = C_1 - \frac{\hbar^2 A^2}{2\mu}, \tag{3.103}$$

where A and B are given by

$$A = \frac{\delta}{2} + \frac{\mu C_2}{\hbar^2 B}, \quad B = \frac{\delta}{2} \pm \sqrt{\frac{\delta 2}{4} + \frac{2\mu C_3}{\hbar^2}}. \tag{3.104}$$

It is crucial to note that the issue can only be effectively addressed through a physical approach when

$$B = \frac{\delta}{2} + \sqrt{\frac{\delta^2}{4} + \frac{2\mu C_3}{\hbar^2}}.$$

Now, we'll calculate the quantum correction. To accomplish this, integrals were utilized, leading to

$$\begin{aligned}
\int_{z_a}^{z_b} k_0'(r)\frac{\varphi_0}{\varphi_0'}dr &= -\int_{z_a}^{z_b} \frac{k_0'(z)}{\delta z(1+z)}\frac{\varphi_0(z)}{\varphi_0'(z)}dz \\
&= \varpi \int_{z_a}^{z_b} \frac{\left(z - \frac{(z_a+z_b)}{2}\right)\left(\frac{A}{B}+z\right)}{z(1+z)\sqrt{(z-z_a)(z-z_b)}}dz \\
&= \varpi \int_{z_a}^{z_b} \frac{dz}{\sqrt{(z-z_a)(z-z_b)}}\left(\frac{\left(\frac{A}{B}-1\right)\left(1+\frac{z_a+z_b}{2}\right)}{z+1} - \frac{\frac{A}{B}\left(\frac{z_a+z_b}{2}\right)}{z} + 1\right),
\end{aligned} \tag{3.105}$$

where

$$\varpi = \frac{1}{\delta}\sqrt{\frac{2\mu C_3}{\hbar^2}}. \tag{3.106}$$

As a result, the quantum correction term is given as;

$$K_c = \frac{\pi}{\delta}\sqrt{\frac{2\mu C_3}{\hbar^2}}\left[\frac{1}{B}\sqrt{\frac{2\mu C_3}{\hbar^2}} + 1\right] \tag{3.107}$$

$$\begin{aligned}
\int_{z_a}^{z_b} k(r)dr &= -\int_{z_a}^{z_b} \frac{k(z)}{\delta z(1+z)}d\sigma \\
&= -\frac{1}{\delta}\sqrt{\frac{2\mu C_3}{\hbar^2}}\int_{z_a}^{z_b} \frac{\sqrt{(z-z_a)(z-z_b)}}{z(1+1)}dz \\
&= -\frac{\pi}{\delta}\sqrt{\frac{2\mu C_3}{\hbar^2}}\left[\sqrt{(z_a+1)(z_b+1)} - 1 - \sqrt{z_a z_b}\right] \\
&= -\frac{\pi}{\delta}\sqrt{\frac{2\mu C_3}{\hbar^2}}\left[\sqrt{\frac{C_3 - C_2 + C_1 - E_{nm}}{C_3}} - 1 - \sqrt{\frac{C_2 - E_{nm}}{C_3}}\right],
\end{aligned} \tag{3.108}$$

where appropriate standard integrals were used. Combining the results obtained by equation (3.107) and (3.108) we obtain

$$\begin{aligned} &-\frac{\pi}{\delta}\sqrt{\frac{2\mu C_3}{\hbar^2}}\left[\sqrt{\frac{C_3-C_2+C_1-E_{nm}}{C_3}}-1-\sqrt{\frac{C_1-E_{nm}}{C_3}}\right] \\ &=N\pi+\frac{\pi}{\delta}\sqrt{\frac{2\mu C_3}{\hbar^2}}\left[\frac{1}{B}\sqrt{\frac{2\mu C_3}{\hbar^2}}+1\right]. \end{aligned} \tag{3.109}$$

By employing fundamental algebraic operations and applying the formula from equation (3.95), we calculate the energy of the Hulthén plus Yukawa potential model in the presence of AB and magnetic flux fields with topological defects in the following manner:

$$E_{nm}=\frac{\hbar^2\delta^2}{2\mu}\eta-\frac{\hbar^2}{8\mu}\left[\frac{\frac{2\mu V_0}{\hbar^2}+\frac{2\mu V'}{\hbar^2}+\left(\frac{\mu\omega_c}{\hbar}\right)^2-\delta^2\eta-(n\delta+\boldsymbol{B})^2}{(n\delta+\boldsymbol{B})}\right]^2, \tag{3.110}$$

where

$$\eta=(m+\xi)-\frac{1}{4}.$$

3.3.4 Thermo-magnetic functions with the HYP

Once again, we will use a similar method to compute the vibrational partition function $Z(\beta)$ and other thermal characteristics, as explained in subsection 3.3.2. Our focus will be on analyzing the thermodynamic properties of CuLi, CrH, and NiC diatomic molecules under the influence of Aharanov-Bohm flux fields. Moreover, we will explore their magnetization and magnetic susceptibility. To begin, we start by restating the energy spectra in equation (3.110) as follows:

$$E_{n\ell}=\left[q_0-q_1\left(\frac{(n+\varkappa_1)^2-q_2}{(n+\varkappa_1)}\right)^2\right], \tag{3.111}$$

where

$$q_0=\frac{\hbar^2\delta^2}{2\mu}\eta,\quad q_1=\frac{\hbar^2\delta^2}{2\mu},\quad q_2=\frac{2\mu V_0}{\hbar^2}+\frac{2\mu V'}{\hbar^2}+\left(\frac{\mu\omega_c}{\hbar}\right)^2-\eta, \tag{3.112}$$

and

$$\varkappa_1 = \frac{1}{2} + \sqrt{(m+\xi)^2 + \left(\frac{\mu\omega_c}{\hbar\delta}\right)^2 + \frac{2\mu\omega_c}{\hbar\delta}(m+\xi)}. \tag{3.113}$$

To evaluate the partition function, we substitute equation (3.111) into equation (3.75), to obtain

$$Z(\beta) = \sum_{n=0}^{n_{\max}} \exp\left[-\beta\left(q_0 - q_1\left(\frac{(n+\varkappa_1)^2 - q_2}{(n+\varkappa_1)}\right)^2\right)\right], \tag{3.114}$$

where

$$n_{\max} = -\varkappa_1 \pm \sqrt{q_2}. \tag{3.115}$$

By replacing the summation in equation (3.75) by an integral, we obtain;

$$Z(\beta) = \int_{n=0}^{n_{\max}} \exp\left[-\beta\left(q_0 - q_1\left(\frac{(n+\varkappa_1)^2 - q_2}{(n+\varkappa_1)}\right)^2\right)\right] dn. \tag{3.116}$$

The integral in equation (3.80), can be evaluated as follows;

$$Z(\beta) = \int_{\varkappa_1}^{n_{\max}+\varkappa_1} \exp\left[-\beta\left(q_0 - q_1\left(\frac{(n+\varkappa_1)^2 - q_2}{(n+\varkappa_1)}\right)^2\right)\right] d\rho, \tag{3.117}$$

where $\rho = n + \varkappa_1$, and the limits of the integral are: $\varkappa \leq \rho \leq n_{\max} + \varkappa_1$. If we set

$$x = (n+\varkappa_1) - \frac{q_2}{(n+\varkappa_1)},$$

we can also rewrite the integral in equation (3.117) as follows:

$$\begin{aligned} &\int_{x_1}^{x_2} \exp\left(-\beta\left(q_0 - q_1\left(\frac{(n+\varkappa_1)^2 - q_2}{(n+\varkappa_1)}\right)^2\right)\right) dx \\ &= \frac{1}{2}\exp(-\beta q_0)\int_{x_1}^{x_2} \exp\left(\beta q_1 x^2\left(\frac{x}{\sqrt{x^2+4q_2}} - 1\right)\right) dx, \end{aligned} \tag{3.118}$$

where

$$x_1 = \varkappa_1 - \frac{q_2}{\varkappa_1}, \tag{3.119}$$

$$x_2 = (n_{\max} + \varkappa_1) - \frac{q_2}{(n_{\max}+\varkappa_1)}. \tag{3.120}$$

To proceed, we now calculate the integral stated in equation (3.118) with the aid of Mathematica. The partition function, denoted as $Z(\beta)$, for diatomic molecules CuLi, CrH, and NiC under the Hulthén plus Yukawa potential model will be evaluated in the presence of external magnetic and Aharanov-Bohm flux fields in the following manner:

$$\begin{aligned} Z(\beta,\eta) = -\frac{\exp\left(q_3\beta - 2\sqrt{-q_2\beta}\sqrt{-q_2^2q_1\beta}\right)\sqrt{\pi}}{4\sqrt{-q_2\beta}}\Bigg(&\operatorname{erf}\left[\frac{\sqrt{-q_2^2q_1\beta}}{\varkappa_1} - \sqrt{-q_2\beta}\varkappa_1\right] \\ &+ \exp\left(4\sqrt{-q_2\beta}\sqrt{-q_2^2q_1\beta}\right)\operatorname{erf}\left[\frac{\sqrt{-q_2^2q_1\beta}}{\varkappa_1} + \sqrt{-q_2\beta}\varkappa_1\right] \\ &- \operatorname{erf}\left[\frac{\sqrt{-q_2^2q_1\beta}}{\varkappa_2} - \sqrt{-q_2\beta}\varkappa_2\right] \\ &- \exp\left(4\sqrt{-q_2\beta}\sqrt{-q_2^2q_1\beta}\right)\operatorname{erf}\left[\frac{\sqrt{-q_2^2q_1\beta}}{\varkappa_2} - \sqrt{-q_2\beta}\varkappa_2\right]\Bigg), \end{aligned} \tag{3.121}$$

where

$$\varkappa_2 = n_{\max} + \frac{1}{2} + \sqrt{(m+\xi)^2 + \left(\frac{\mu\omega_c}{\hbar\delta}\right)^2 + \frac{2\mu\omega_c}{\hbar\delta}(m+\xi)}, \tag{3.122}$$

where $q_3 = q_2q_1 + q_0$. Using a method akin to that described in subsection 3.3.2, we can formulate thermo-magnetic properties such as the free energy $F(\beta)$, average energy $U(\beta)$, entropy $S(\beta)$, specific heat capacity $C(\beta)$, magnetization $M(\beta)$, and magnetic susceptibility $\chi_m(\beta)$ for CuLi, CrH, and NiC diatomic molecules. These expressions are outlined below:

1. **Free energy** $F(\beta)$

$$F(\beta) = -\frac{1}{\beta}\ln Z(\beta). \tag{3.123}$$

2. **Mean energy** $U(\beta)$

$$U(\beta) = -\frac{d\partial\ln Z(\beta)}{\partial\beta}. \tag{3.124}$$

3. **Entropy** $S(\beta)$

$$S(\beta) = \ln Z(\beta) - \beta\frac{\partial\ln Z(\beta)}{\partial\beta}. \tag{3.125}$$

4. **Specific Heat Capacity** $C_V(\beta)$

$$C_V(\beta) = \beta^2 \frac{\partial^2 \ln Z(\beta)}{\partial \beta^2}. \tag{3.126}$$

5. **Magnetisation** $M(\beta)$

   The following expression is used to calculate the magnetization is given by ;

$$M(\beta) = \frac{1}{\beta}\left(\frac{1}{Z(\beta)}\right)\left(\frac{\partial Z(\beta)}{\partial \boldsymbol{B}}\right). \tag{3.127}$$

6. **Magnetic susceptibility** $\chi_m(\beta)$

   The expression below is used to determine the magnetic susceptibility is written as follows;

$$\chi_m(\beta) = \frac{\partial M(\beta)}{\partial \boldsymbol{B}}. \tag{3.128}$$

In the following chapter, we present the numerical results generated by Mathematica along with their respective analyses.

Chapter 4

Results and Discussion

4.1 Results with the MRCYP

The numerical determination of energies for the MRCY potential under various screening parameters and quantum states was conducted using Mathematica software, and the results are displayed in Table 4.1. Our investigation was conducted with specific parameters: $\hbar = 1$, $V_0 = 1$, $M = 1$, $\mu = 1$, $a = 0.75$, and $V_0' = 0.1$.

Table 4.1 illustrates that as the number of quantum states n and ℓ increases, the energy $E_{n\ell}$ rises in correlation with the screening parameter δ. Furthermore, an increase in the screening parameter leads to a decrease in the energy $E_{n\ell}$ for a given quantum state. Figures 4.1, 4.2, and 4.3 visually represent the variations of energies $E_{n\ell}$ concerning different parameters δ, n, and ℓ. It is observed that energy decreases as δ increases across various quantum states, as demonstrated in Figure 4.1(a). Additionally, an increase in $E_{n\ell}$ is noticed when both n and ℓ are present at a specific δ, as depicted in Figure 4.1(b) for multiple quantum states.

At specific values of V_0, the energies $E_{n\ell}$ rise with an increase in the number of quantum states n and ℓ. Figure 4.2(a) shows a significant rise in energy at zero reduced mass. Moreover, a monotonic decrease in energy $E_{n\ell}$ is observed with a further increase in μ, particularly pronounced for $n = 2$ and $n = 1$ compared to other quantum states.

Figure 4.2(b) displays a steady increase in energies with an increase in ℓ for a given n, $E_{n\ell}$. Similarly, Figure 4.3 illustrates a monotonic increase in energy $E_{n\ell}$ as ℓ increases

for various n. It is noted that for a specific angular momentum quantum number ℓ, $E_{n\ell}$ increases as the principal quantum number n rises.

Table 4.1: Energy eigenvalues of the MRCYP for different screening parameters δ and quantum states n and ℓ.

n	l	$-E_{nl}$		
		$\delta = 0.0001$	$\delta = 0.001$	$\delta = 0.01$
0	0	−0.2047860794	−0.2056459966	−0.6940114985
1	0	0.1618605870	0.1607692012	0.5135365490
2	0	0.2659258174	0.2640362978	0.2454376935
	1	0.1405236150	0.01386819594	0.1209335323
3	0	0.1483481473	0.1465026002	0.1286106270
	1	0.08770339890	0.08588439030	0.06874269910
	2	0.05785981880	0.05605700625	0.03959817075
4	0	0.09306815480	0.09124584530	0.07394246325
	1	0.05987399025	0.05806990360	0.04154688244
	2	0.04218571795	0.04039467676	0.02462098684
	3	0.03178274934	0.03000293314	0.01502520083
5	0	0.06342586895	0.06161884650	0.04491373596
	1	0.04343734854	0.04164520098	0.02580015834
	2	0.03209761056	0.03031738282	0.01530837738
	3	0.02500506086	0.02323593189	0.009114176240
	4	0.02008839780	0.01833050216	0.005177749845

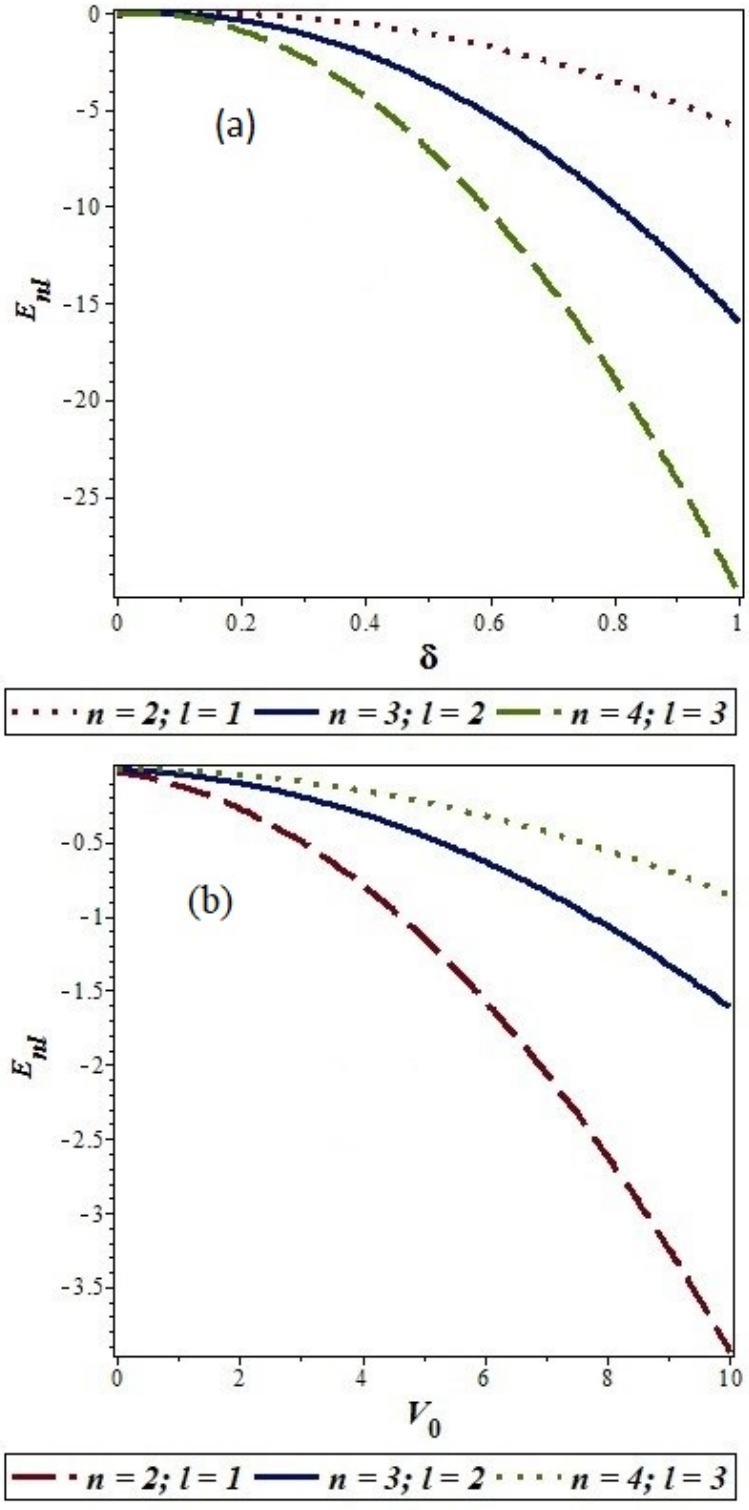

Figure 4.1: (a) Energy spectra $E_{n\ell}$ as a function of δ for various quantum states n and ℓ. (b) Energy spectra $E_{n\ell}$ as a function of potential strength V_0 for various quantum states n and ℓ.

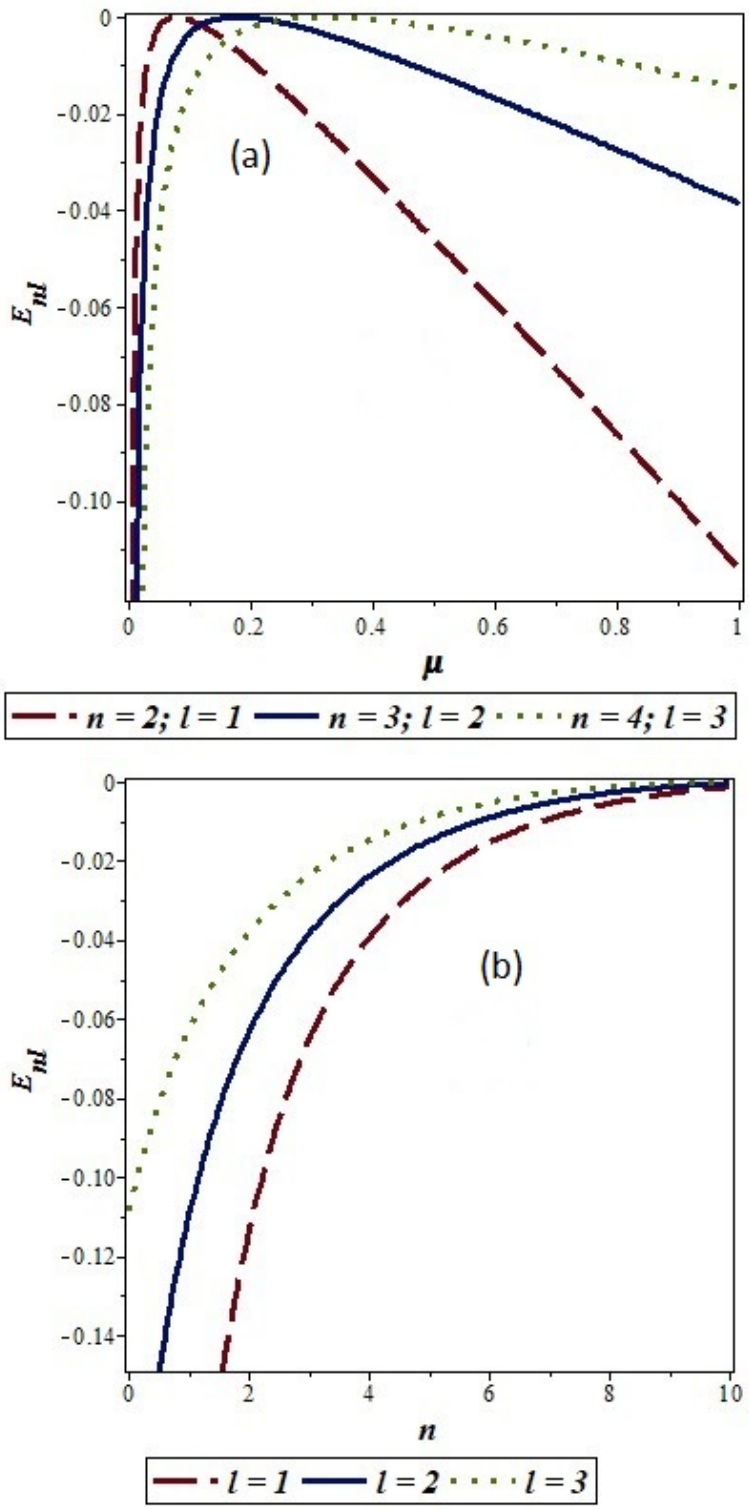

Figure 4.2: (a) Energy spectra $E_{n\ell}$ as a function of μ for various quantum states n and ℓ. (b) Energy spectra $E_{n\ell}$ as a function of n for various angular momentum quantum states ℓ.

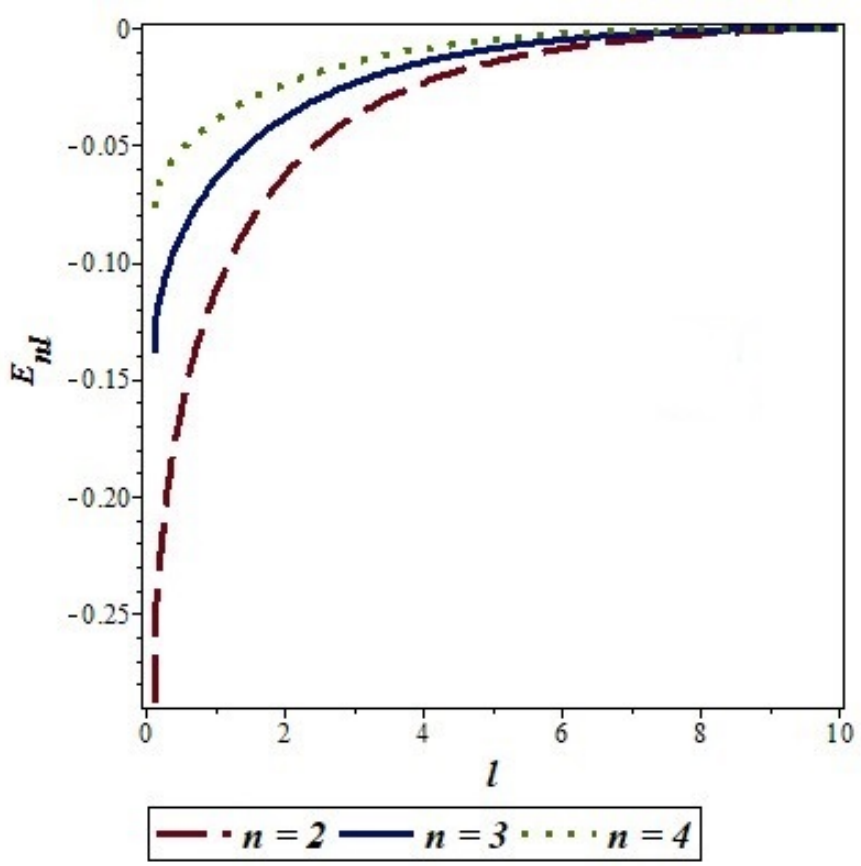

Figure 4.3: Energy spectra $E_{n\ell}$ as a function of ℓ for various principal quantum states n.

Utilizing the analytical expression for the bound energy $E_{n\ell}$ as indicated in equation (3.26), we derive the formulas for the partition function $Z(T)$ and other thermodynamic functions employing the Euler-MacLaurin formula. The expressions for the partition function and other thermodynamic functions are provided by equations (3.41) and (3.42), (3.44), (3.47), and (3.48), respectively. Figures 4.4(a) and 4.4(b) illustrate the variation of the partition function $Z(T)$ with temperature T for different screening parameters δ and quantum states n and ℓ, respectively.

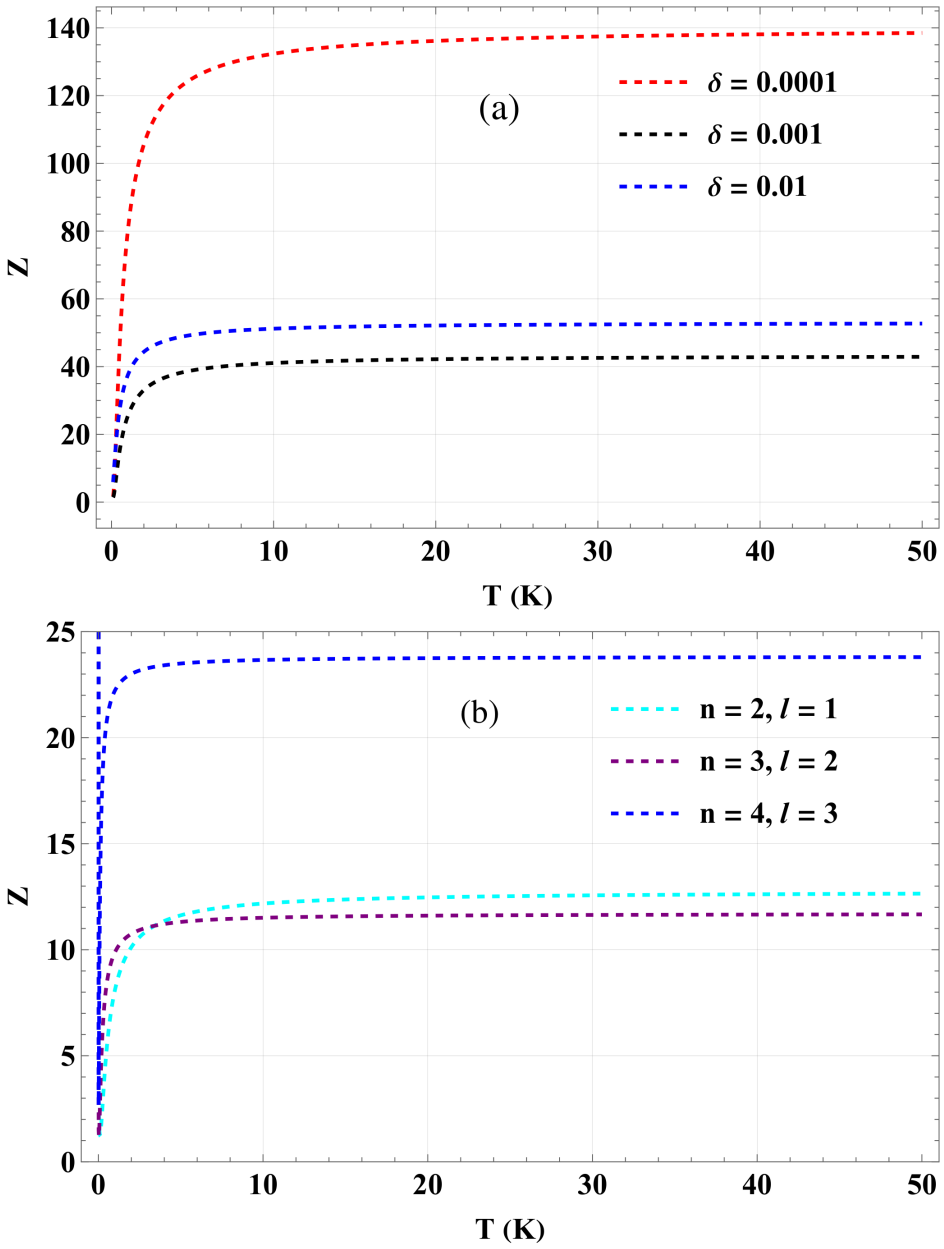

Figure 4.4: Variation of the vibrational partition function $Z(T)$ with temperature T for different values of (a) screening parameter δ; and (b) quantum states n and ℓ.

As the temperature T increases, it is observed that the partition function $Z(T)$ initially undergoes a sharp rise at zero temperature T and then stabilizes at specific values corresponding to the screening parameters δ and the quantum states n and ℓ under consideration.

In Figure 4.5(a) and Figure 4.5(b), we have depicted the variation of the free energy $F(T)$ with temperature T. As evident from the plots, the free energy $F(T)$ exhibits a linear decrease with increasing temperature T for the various screening parameters δ and quantum states n and ℓ examined.

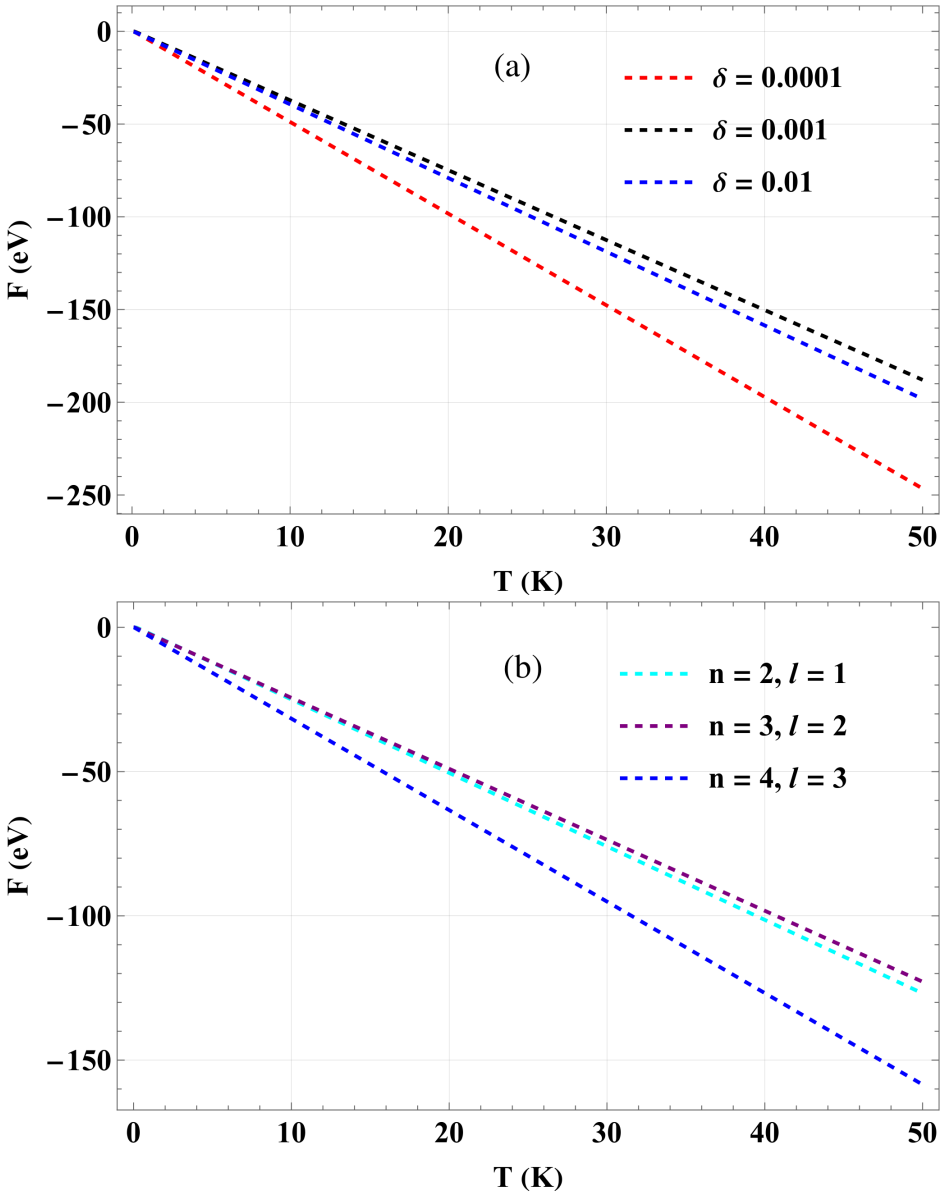

Figure 4.5: Variation of the vibrational free energy $F(T)$ with temperature T for different values of (a) screening parameter δ; and (b) quantum states n and ℓ.

The plots in Figure 4.6 depict the variation of the mean energy $U(T)$ concerning

temperature T. It is evident from Figure 4.6(a) and Figure 4.6(b) that there is a consistent increase in mean energy $U(T)$ with rising temperature T across various screening parameters δ and quantum states n and ℓ. Additionally, it is noted that in both graphs, as the temperature T increases, the mean energy $U(T)$ saturates at the origin.

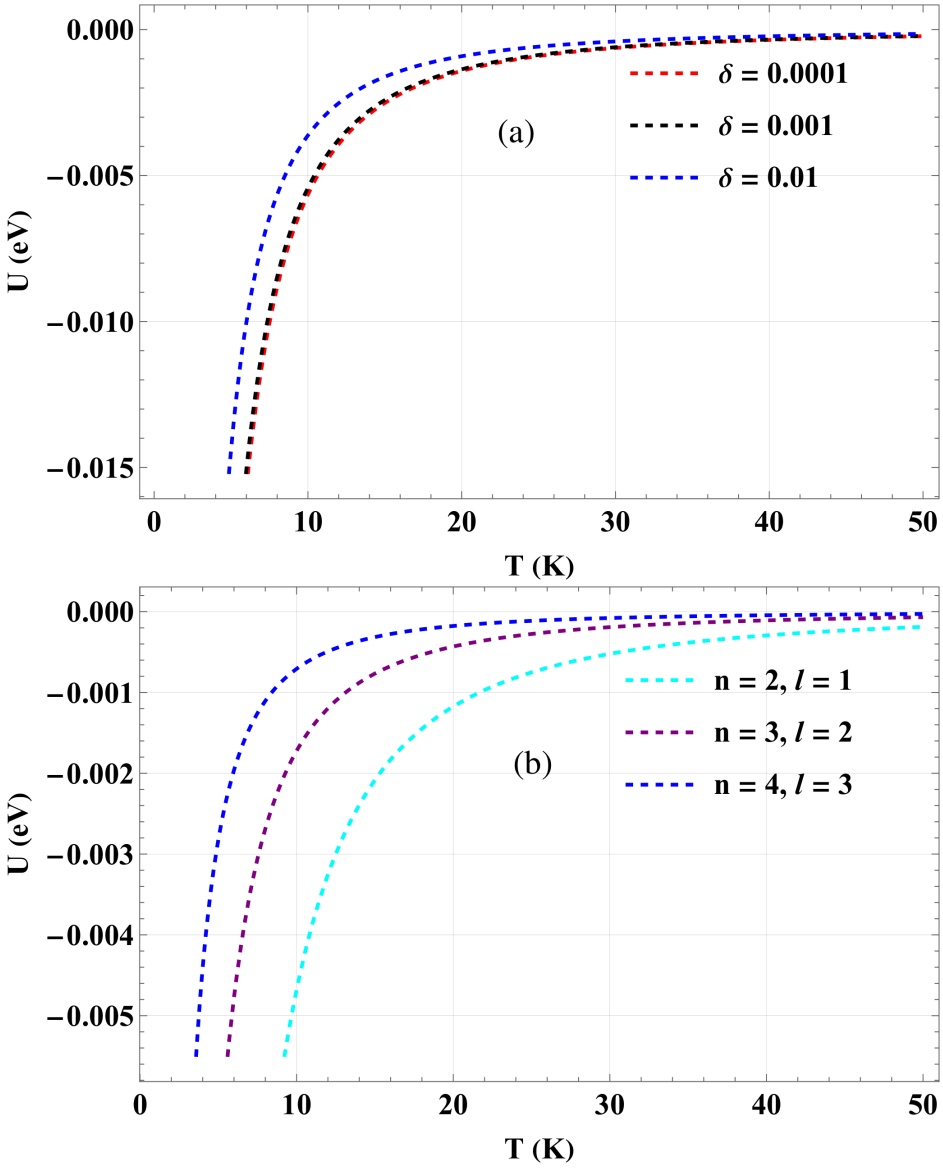

Figure 4.6: (a) Variation of the vibrational mean energy $U(T)$ with temperature for different values of (a) screening parameter δ; and (b) quantum states n and ℓ.

In Figures 4.7 and 4.8, we provide plots illustrating the entropy $S(T)$ and the specific

heat capacity $C(T)$ of the system.

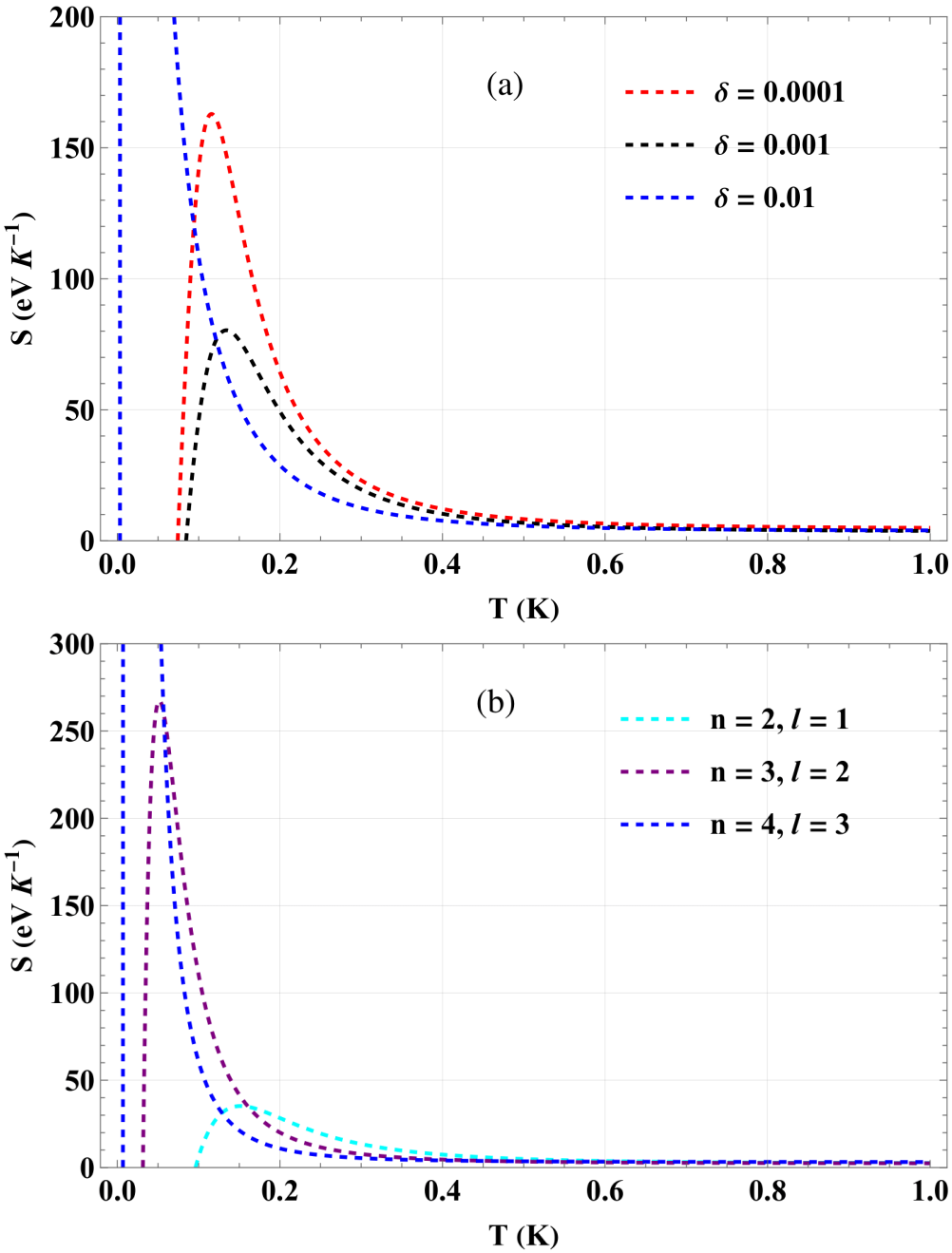

Figure 4.7: (a) Variation of the vibrational entropy $S(T)$ with temperature T for different values of (a) screening parameter δ; and (b) quantum states n and ℓ.

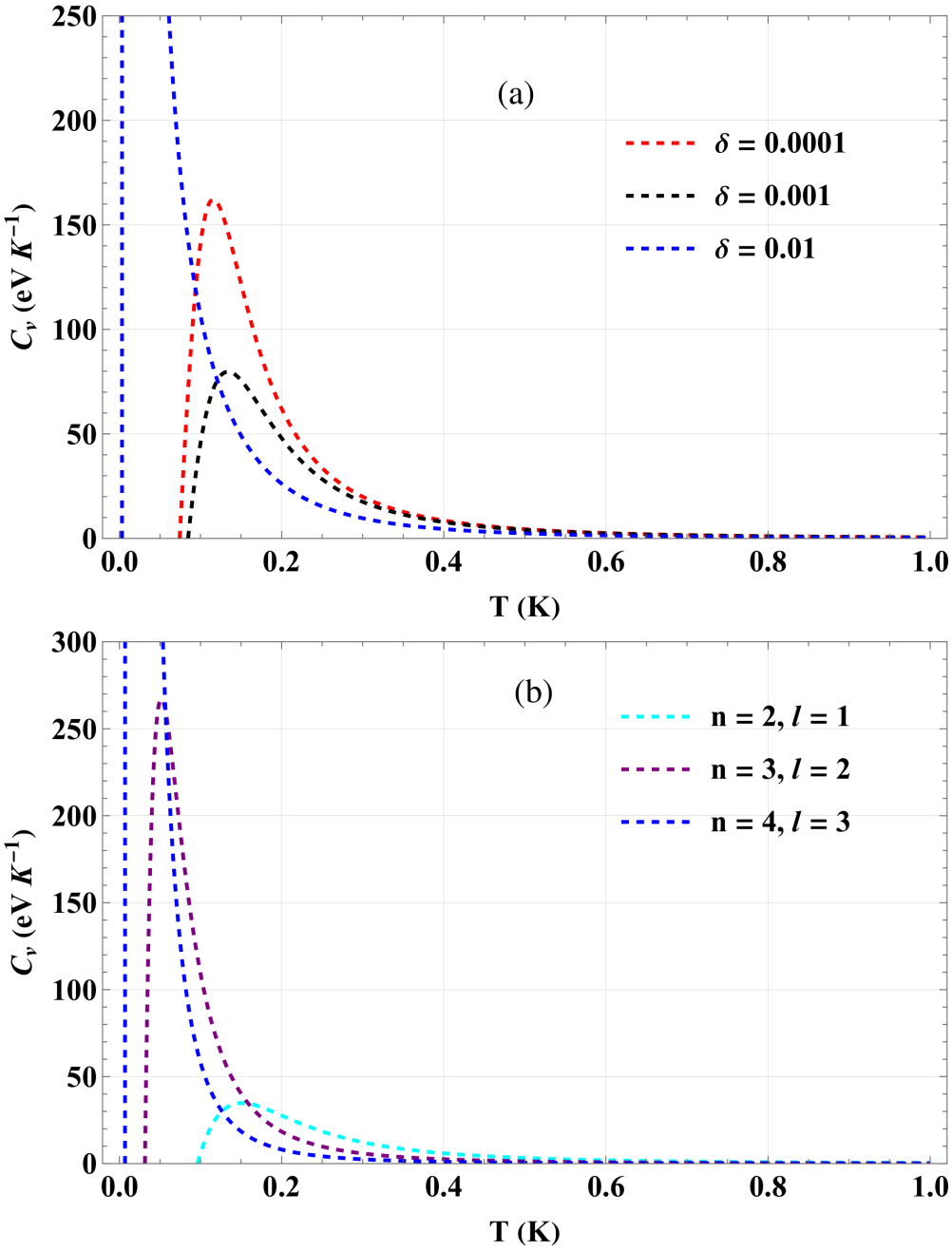

Figure 4.8: Variation of the specific heat capacity $C(T)$ with temperature T for different values of (a) screening parameter δ; and (b) quantum states n and ℓ.

We observe a pronounced increase in entropy, represented as $S(T)$, and specific heat capacity, denoted as $C(T)$, as temperature T rises towards a distinct value known as the critical temperature. This phenomenon holds true across various screening parameters and quantum states. Moreover, both entropy $S(T)$ and specific heat capacity $C(T)$

exhibit a steady decline as temperature T continues to rise. Once the temperature exceeds $0.4K$, the entropy $S(T)$ and specific heat capacity $C(T)$ for the considered screening parameters and quantum states reach a saturation point. At this juncture, the system can no longer absorb much energy due to the complete occupation of its excited states.

4.2 Results with the HYP.

4.2.1 Calculations without magnetic and AB flux fields

In this part of our study, we have focused on three diatomic molecules that have been extensively researched by numerous scientists: CuLi, CrH, and NiC. The standard molecular weights of these compounds are detailed in Table 4.2, derived from investigations in Source [128]. All computations employed the conversion factors: $\hbar c = 1973.269$ $eV\mathring{A}$ and 1 amu$= 931.5 \times 10^6$ $eV(\mathring{A})^{-1}$ [129].

Table 4.2: Spectroscopic parameters for CuLi, CrH, and NiC diatomic molecules.

Molecule [128]	$\delta(\mathring{A}^{-1})$	μ(amu)
CuLi	1.00818	6.259494
CrH	1.52179	0.988976
NiC	2.25297	9.974265

In Figures 4.9(a) and 4.9(b), we displayed the energy spectra $E_{n\ell}$ plotted against the angular momentum quantum number ℓ and the principal quantum number n, respectively. From the graphs, it is evident that the system's energy $E_{n\ell}$ rises steadily with increasing values of n and ℓ respectively. These molecules were studied in [131] with the shifted Deng-Fan potential model. The results presented in the reference are in good agreement with our results.

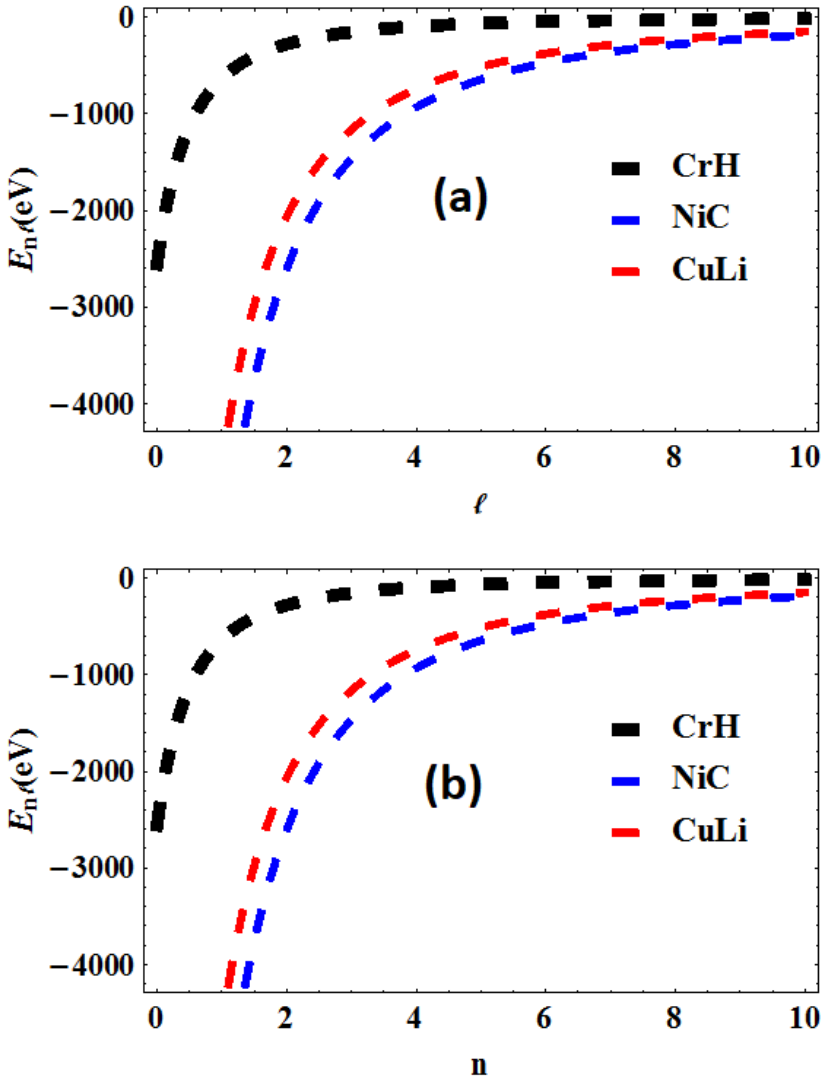

Figure 4.9: Energy spectra variation of the Hulthén plus Yukawa potential with (a) angular momentum quantum number ℓ, (b) principal quantum number n, for various diatomic molecules

In Figures 4.10, 4.11, 4.12, and 4.13, we present the vibrational partition function along with other thermodynamic properties for diatomic molecules CuLi, CrH, and NiC, derived from the energy spectra $E_{n\ell}$ of the Hulthén plus Yukawa potential. These thermodynamic characteristics are examined concerning discrete values of $\beta = \frac{1}{kT}$ and maximum quantum number $n_{\max}$. We have also depicted the partition function $Z(\beta)$, the free energy $F(\beta)$, and the mean energy $U(\beta)$ plotted against the temperature

$\beta = \frac{1}{kT}$ for CuLi, CrH, and NiC diatomic molecules in Figure 4.10(a, b, & c). The partition function $Z(\beta)$ increases with the temperature $\beta(K^{-1})$, while we also observe a monotonic rise in free energy $F(\beta)$ with increasing temperature $\beta(K^{-1})$. However, the mean energy $U(\beta)$ decreases as the temperature $\beta(K^{-1})$ rises. These thermodynamic properties for CrH and CuLi diatomic molecules were studied in [132] with the shifted Deng-Fan potential model. Our results agree with the results obtained in the reference.

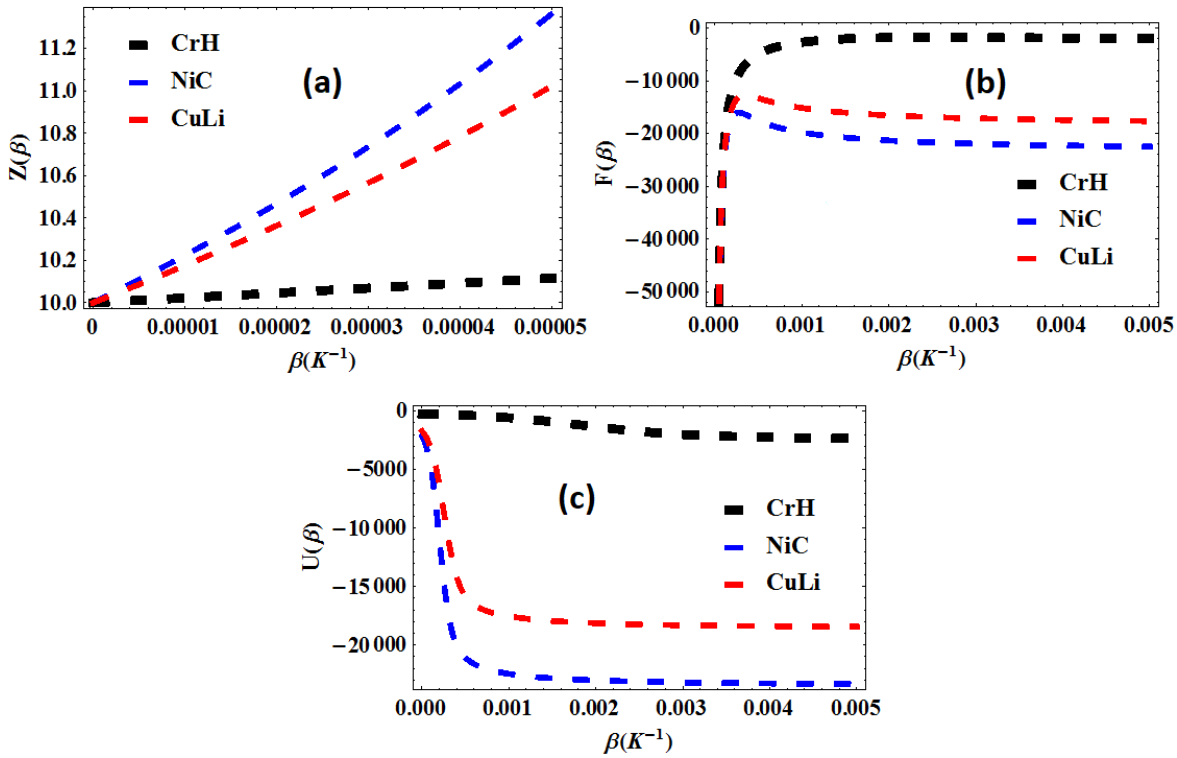

Figure 4.10: Variation of vibrational partition function $Z(\beta)$, (b) vibrational free energy $F(\beta)$ and (c) vibrational mean energy energy $U(\beta)$, with changing temperature $\beta(K^{-1})$, for different diatomic molecules with the Hulthén plus Yukawa potential.

In Figures 4.11(a) and 4.11(b), we observe plots depicting the entropy $S(\beta)$ and specific heat capacity $C(\beta)$ as functions of temperature $\beta(K^{-1})$ for CuLi, CrH, and NiC diatomic molecules. It is evident from the graphs that the entropy $S(\beta)$ decreases with increasing temperature $\beta(K^{-1})$. Moreover, as the temperature $\beta(K^{-1})$ increases, the specific heat capacity $C(\beta)$ for all molecules considered, initially reaches a peak

and then declines. The two thermodynamic properties for CrH and CuLi diatomic molecules were also studied in [132] with the shifted Deng-Fan potential model. Our results agree with the results obtained in the reference.

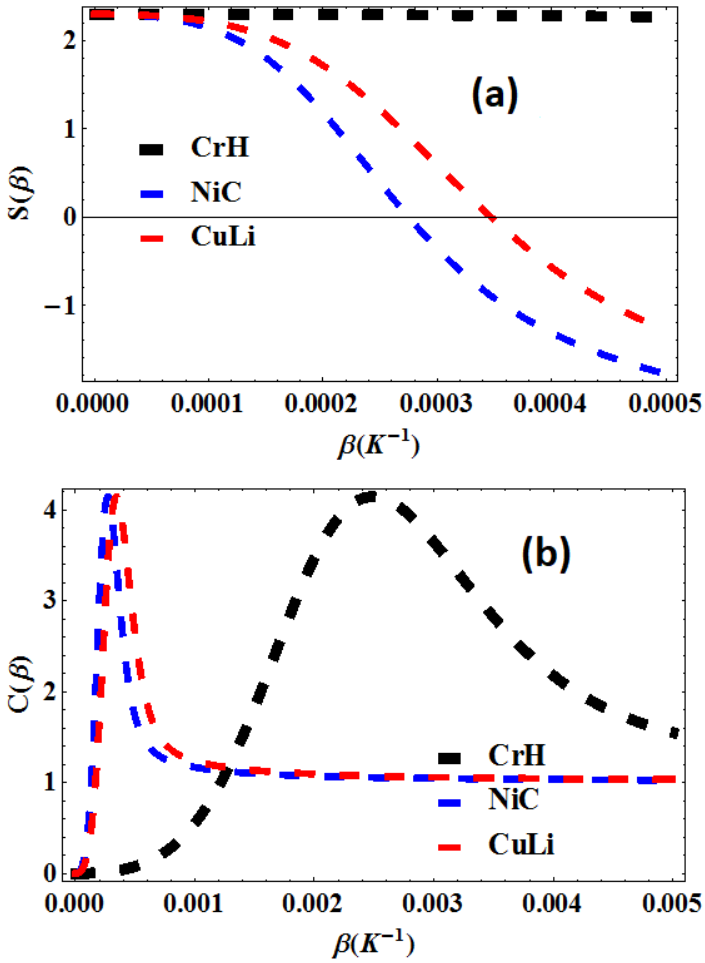

Figure 4.11: Variation of vibrational entropy $S(\beta)$ and (b) vibrational specific heat capacity energy $C(\beta)$, with changing temperature $\beta(K^{-1})$, for different diatomic molecules with the Hulthén plus Yukawa potential.

In Figures 4.12 and 4.13, we illustrate the variations of thermodynamic functions with respect to the maximum quantum number $n_{\max}$ at a constant $\beta = \frac{1}{kT}$. Figures 4.12(a), 4.12(b), and 4.12(c) portray the behavior of the partition function $Z(\beta)$, vibrational free energy $F(\beta)$, and vibrational mean energy $U(\beta)$, respectively, as functions of maximum quantum number $n_{\max}$ for different diatomic molecules. Observing the plots,

we note that the vibrational partition function $Z(\beta)$ increases with the rise in maximum quantum number $n_{\max}$, while the free energy $F(\beta)$ decreases with increasing maximum quantum number $n_{\max}$. The mean energy $U(\beta)$ shows a monotonic increase as the maximum quantum number $n_{\max}$ rises.

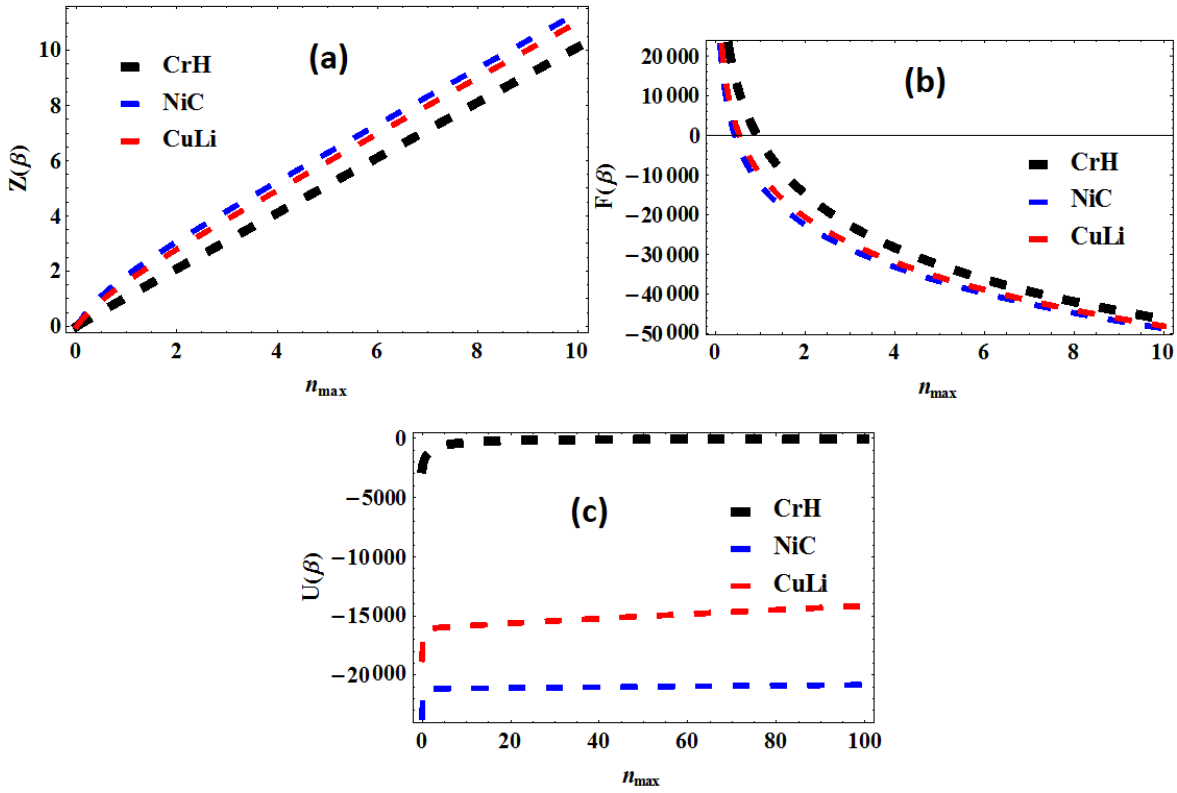

Figure 4.12: Variation of vibrational partition function $Z(\beta)$, (b) vibrational free energy $F(\beta)$ and (c) vibrational mean energy energy $U(\beta)$, with changing maximum quantum number $n_{\max}$, for different diatomic molecules with the Hulthén plus Yukawa potential.

The graphs in Figures 4.13 (a) and 4.13(b) illustrate the variations of vibrational entropy, $S(\beta)$, and vibrational specific heat capacity, $C(\beta)$, respectively, for the Hulthén plus Yukawa potential across different diatomic molecules as a function of the maximum quantum number, $n_{\max}$. As evidenced by the plots, the entropy $S(\beta)$ of the potential consistently rises as maximum quantum number $n_{\max}$ decreases, while the specific heat capacity $C(\beta)$ increases with increasing maximum quantum number $n_{\max}$. Notably,

$C(\beta)$ reaches a saturation point at higher maximum quantum number $n_{\max}$, with the value plateauing, particularly for CrH.

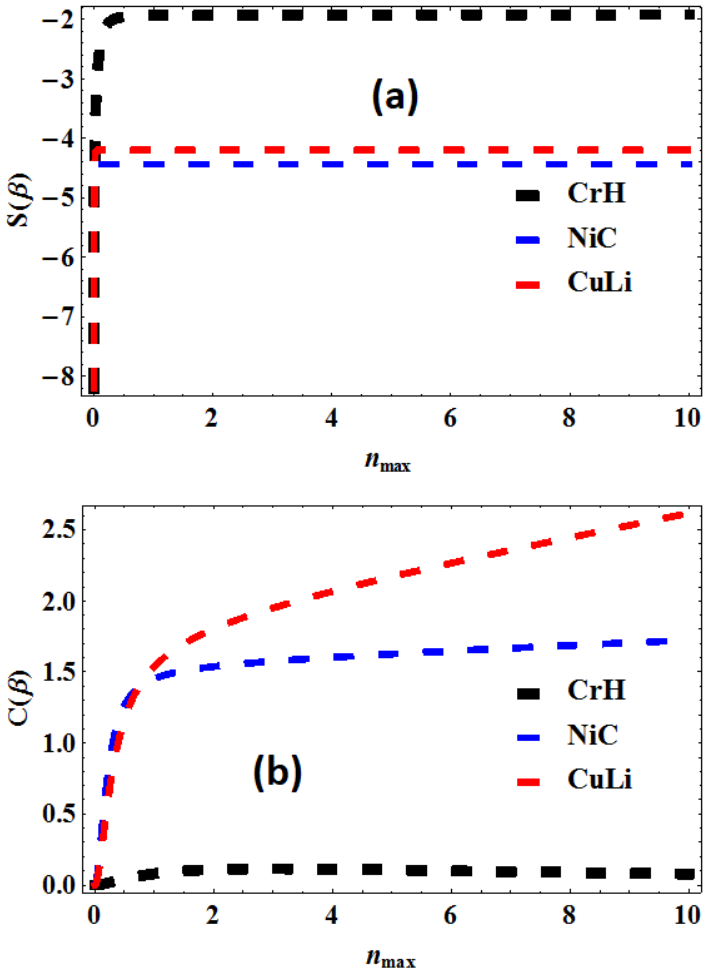

Figure 4.13: Variation of vibrational entropy $S(\beta)$ and (b) vibrational specific heat capacity energy $C(\beta)$, with changing maximum quantum number $n_{\max}$, for different diatomic molecules with the Hulthén plus Yukawa potential.

4.2.2 Calculations with magnetic and AB flux fields

In Figures 4.14, 4.15, 4.16, 4.18, 4.19, and 4.20, we depicted the vibrational partition function $Z(\beta, \boldsymbol{B}, \Phi_{AB})$, along with other thermodynamic functions, for CuLi, CrH, and NiC diatomic molecules derived from the Hulthén plus Yukawa potential energy spectra in the presence of external magnetic and Aharonov-Bohm flux fields. The plots

in Figures 4.14(a), 4.14(b), and 4.14(c) illustrate the partition function $Z(\beta, \boldsymbol{B}, \Phi_{AB})$, the free energy $F(\beta, \boldsymbol{B}, \Phi_{AB})$, and the mean energy $U(\beta, \boldsymbol{B}, \Phi_{AB})$ respectively, against the temperature $\beta(K^{-1})$. Observations reveal that the partition function $Z(\beta, \boldsymbol{B}, \Phi_{AB})$ decreases as the temperature $\beta(K^{-1})$ decreases, while the free energy $F(\beta, \boldsymbol{B}, \Phi_{AB})$ exhibits a monotonic increase with increasing temperature $\beta(K^{-1})$. However, the mean energy $U(\beta, \boldsymbol{B}, \Phi_{AB})$ decreases with rising temperature $\beta(K^{-1})$.

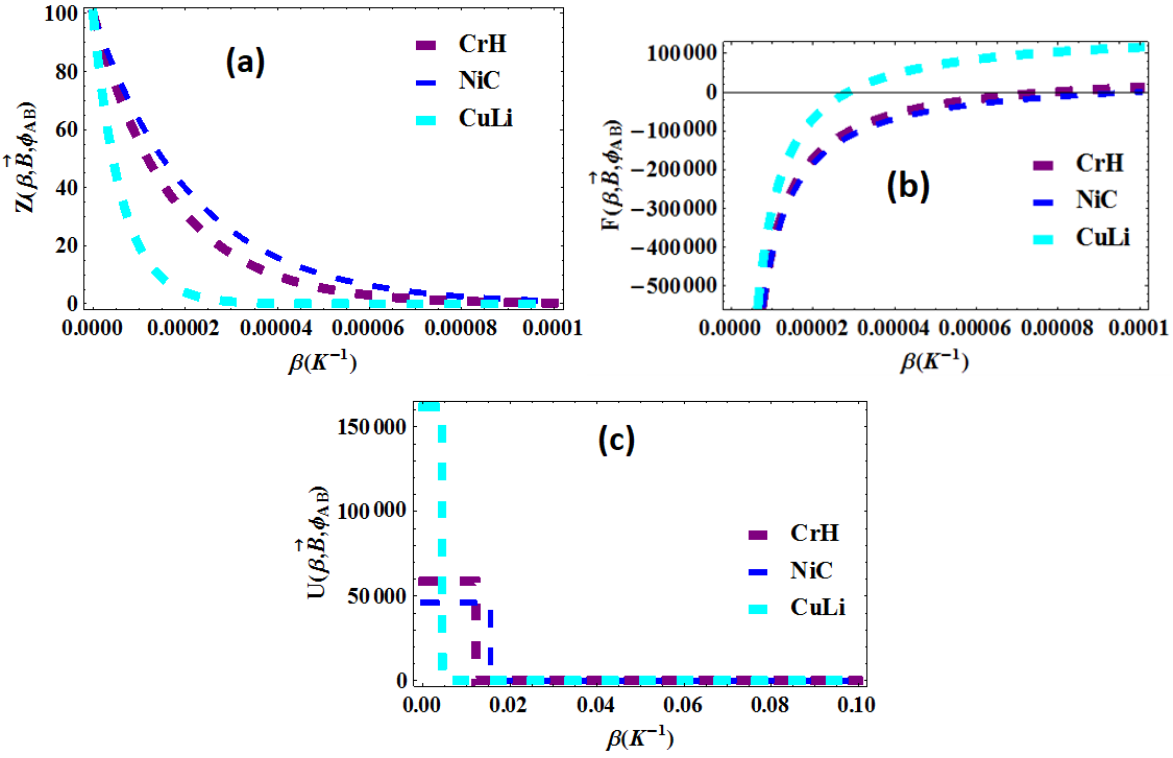

Figure 4.14: Variation of (a) vibrational partition function $Z(\beta, \boldsymbol{B}, \Phi_{AB})$, (b) vibrational free energy $F(\beta, \boldsymbol{B}, \Phi_{AB})$ and (c) vibrational mean energy energy $U(\beta, \boldsymbol{B}, \Phi_{AB})$, with changing temperature $\beta(K^{-1})$, for different diatomic molecules with the Hulthén plus Yukawa potential.

Figure 4.15(a) and Figure 4.15(b) display the entropy $S(\beta, \boldsymbol{B}, \Phi_{AB})$ and the vibrational specific heat capacity $C(\beta, \boldsymbol{B}, \Phi_{AB})$ as functions of temperature $\beta(K^{-1})$, respectively. The entropy $S(\beta, \boldsymbol{B}, \Phi_{AB})$ decreases slightly with increasing temperature $\beta(K^{-1})$, while the specific heat capacity $C(\beta, \boldsymbol{B}, \Phi_{AB})$ decreases for various diatomic molecules and

shows an attempt to increase for CrH.

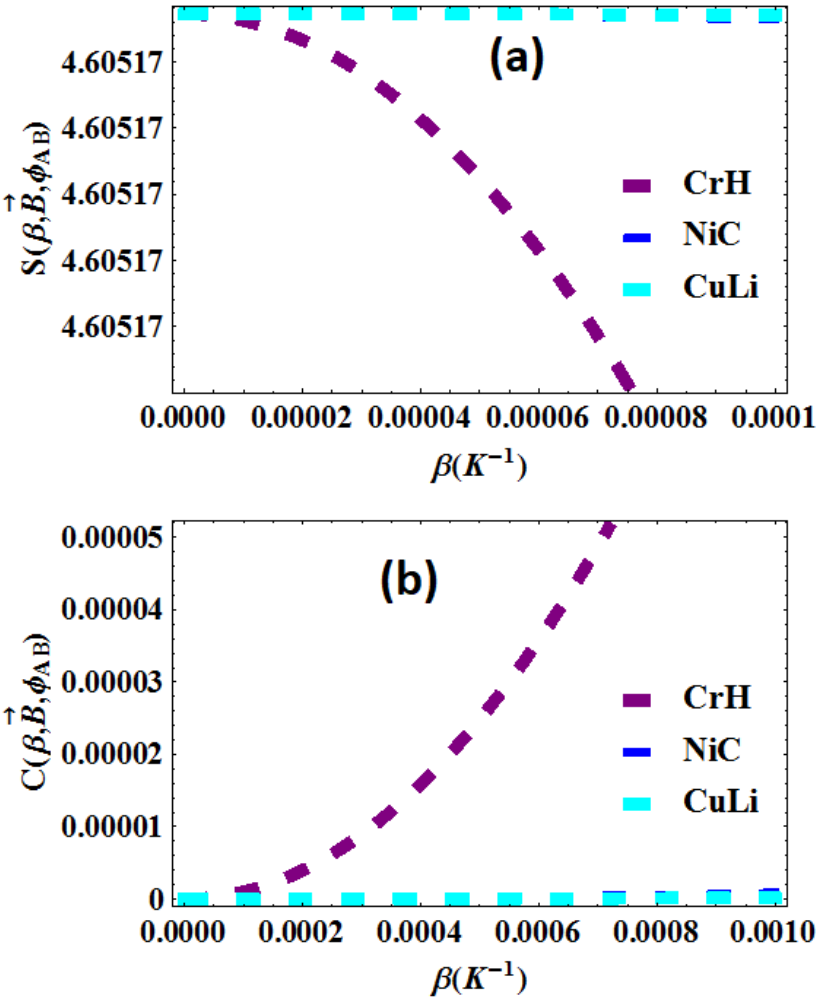

Figure 4.15: Variation of vibrational entropy $S(\beta, \boldsymbol{B}, \Phi_{AB})$ and (b) vibrational specific heat capacity energy $C(\beta, \boldsymbol{B}, \Phi_{AB})$, with changing temperature $\beta(K^{-1})$, for different diatomic molecules with the Hulthén plus Yukawa potential.

Figures 4.16(a), 4.16(b), and 4.16(c) depict the vibrational partition function $Z(\beta, \boldsymbol{B}, \Phi_{AB})$, free energy $F(\beta, \boldsymbol{B}, \Phi_{AB})$, and mean energy $U(\beta, \boldsymbol{B}, \Phi_{AB})$ as functions of the magnetic field $\boldsymbol{B}(T)$ for various diatomic molecules, respectively. It is evident that the partition function $Z(\beta, \boldsymbol{B}, \Phi_{AB})$ decreases with increasing magnetic field $\boldsymbol{B}(T)$, while the free energy $F(\beta, \boldsymbol{B}, \Phi_{AB})$ and mean energy $U(\beta, \boldsymbol{B}, \Phi_{AB})$ both increase with the magnetic field $\boldsymbol{B}(T)$.

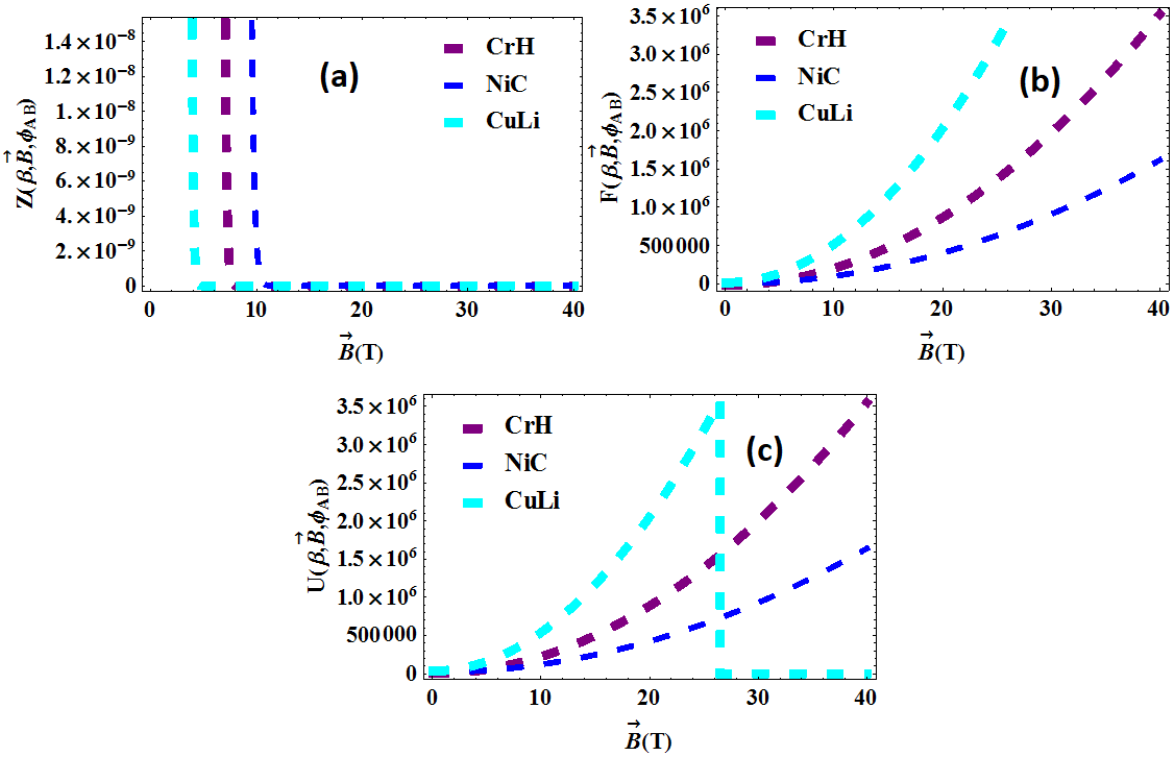

Figure 4.16: Variation of (a) vibrational partition function $Z(\beta, \boldsymbol{B}, \Phi_{AB})$, (b) vibrational free energy $F(\beta, \boldsymbol{B}, \Phi_{AB})$ and (c) vibrational mean energy energy $U(\beta, \boldsymbol{B}, \Phi_{AB})$, with changing magnetic field $\boldsymbol{B}$, for different diatomic molecules with the Hulthén plus Yukawa potential.

In Figures 4.17(a) and 4.17(b), we have depicted the vibrational entropy $S(\beta, \boldsymbol{B}, \Phi_{AB})$ and the specific heat capacity $C(\beta, \boldsymbol{B}, \Phi_{AB})$ as functions of $\boldsymbol{B}(T)$, respectively. It is evident that the entropy $S(\beta, \boldsymbol{B}, \Phi_{AB})$ increases with a slight rise in the magnetic field $\boldsymbol{B}(T)$, while the specific heat capacity $C(\beta, \boldsymbol{B}, \Phi_{AB})$ decreases and shows a tendency to increase for CrH.

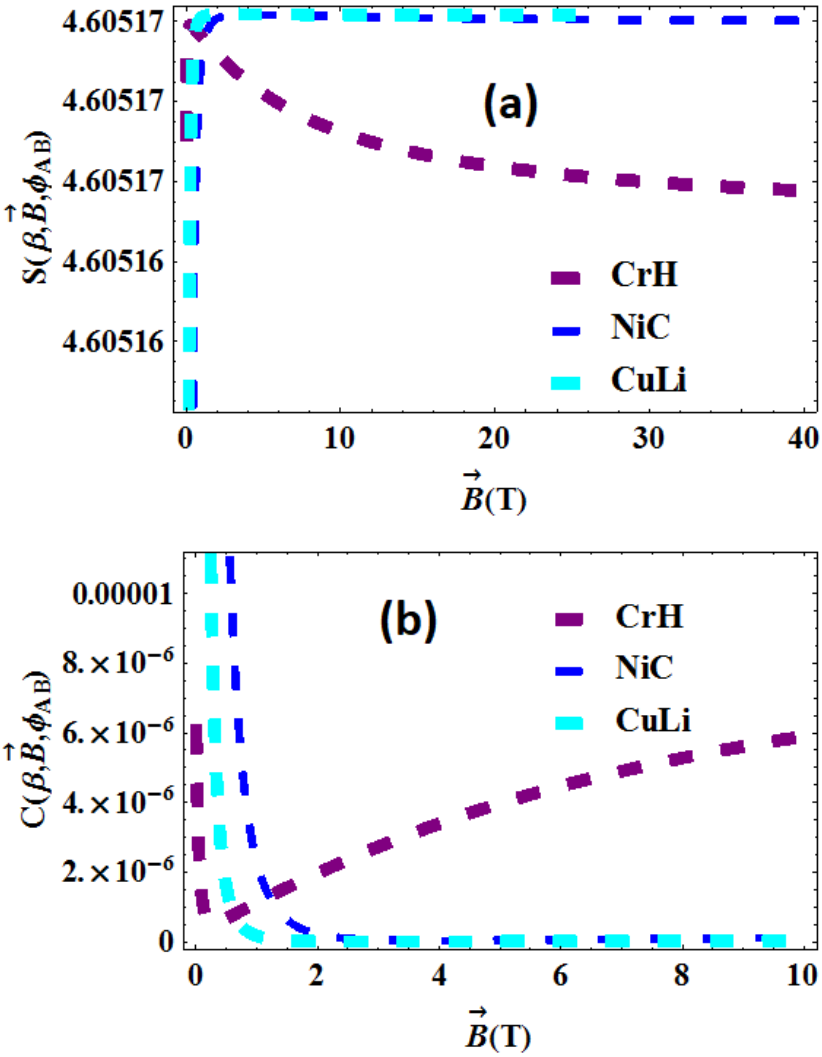

Figure 4.17: Variation of vibrational entropy $S(\beta, \boldsymbol{B}, \Phi_{AB})$ and (b) vibrational specific heat capacity energy $C(\beta, \boldsymbol{B}, \Phi_{AB})$, with changing magnetic field $\boldsymbol{B}$, for different diatomic molecules with the Hulthén plus Yukawa potential.

Figures 4.18(a), 4.18(b), and 4.18(c) depict the vibrational partition function $Z(\beta, \boldsymbol{B}, \Phi_{AB})$, free energy $F(\beta, \boldsymbol{B}, \Phi_{AB})$, and mean energy $U(\beta, \boldsymbol{B}, \Phi_{AB})$ as functions of the Aharanov–Bohm field ξ for various diatomic molecules. As the AB field ξ increases, the partition function $Z(\beta, \boldsymbol{B}, \Phi_{AB})$ rises, while the free energy $F(\beta, \boldsymbol{B}, \Phi_{AB})$ decreases. Moreover, the mean energy $U(\beta, \boldsymbol{B}, \Phi_{AB})$ decreases as the AB field ξ increases.

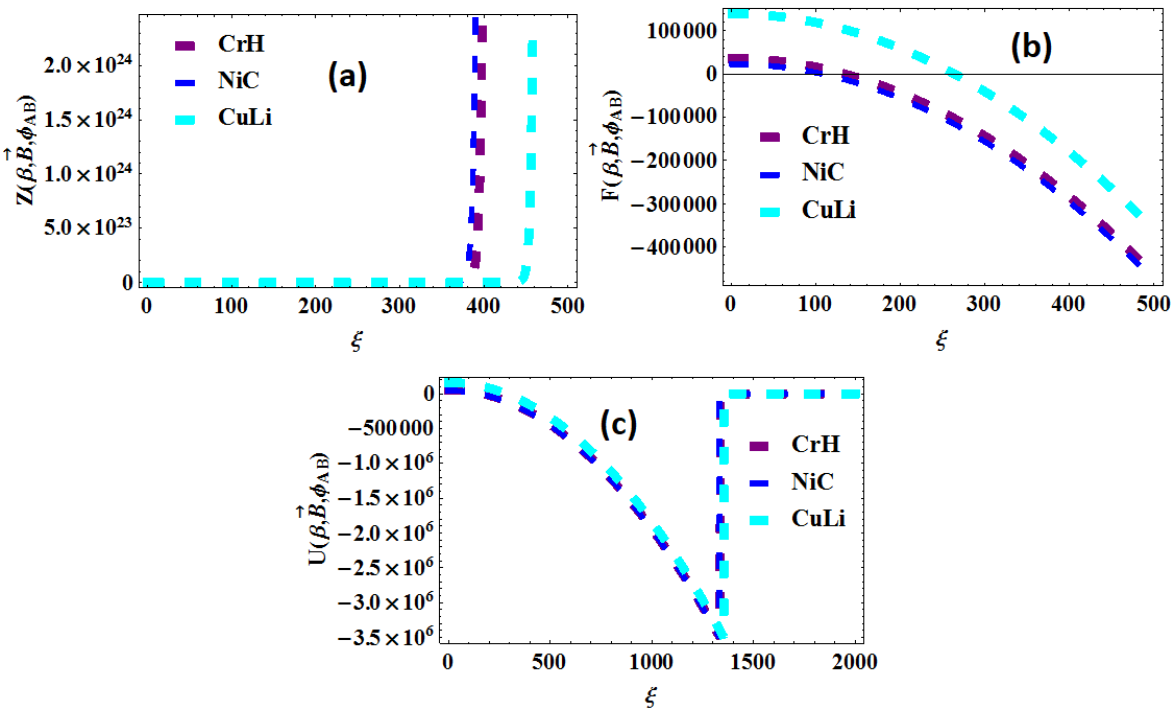

Figure 4.18: Variation of (a) vibrational partition function $Z(\beta, \boldsymbol{B}, \Phi_{AB})$, (b) vibrational free energy $F(\beta, \boldsymbol{B}, \Phi_{AB})$ and (c) vibrational mean energy energy $U(\beta, \boldsymbol{B}, \Phi_{AB})$, with changing AB field ξ, for different diatomic molecules with the Hulthén plus Yukawa potential.

In Figures 4.19(a) and 4.19(b), we have graphed the entropy $S(\beta, \boldsymbol{B}, \Phi_{AB})$ and the specific heat capacity $C(\beta, \boldsymbol{B}, \Phi_{AB})$ as functions of the Aharanov–Bohm field ξ, respectively. It appears that there is a decrease in entropy $S(\beta, \boldsymbol{B}, \Phi_{AB})$ as the AB field ξ increases slightly, but it exhibits a quasi-linear or invariant pattern for different diatomic molecules, respectively. Additionally, we observe that for all three diatomic molecules studied, the specific heat capacity $C(\beta, \boldsymbol{B}, \Phi_{AB})$ does not demonstrate a completely discernible pattern in the variation trend for CuLi and NiC, and it also shows attempts to increase for CrH.

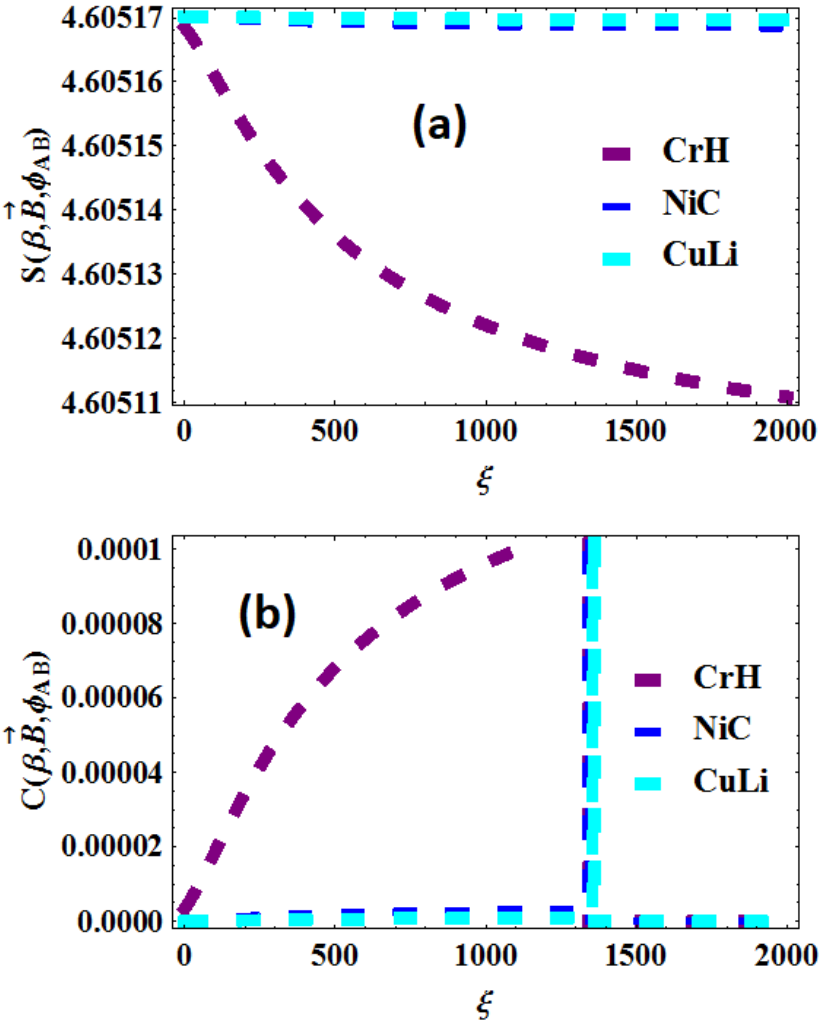

Figure 4.19: Variation of vibrational entropy $S(\beta, \boldsymbol{B}, \Phi_{AB})$ and (b) vibrational specific heat capacity energy $C(\beta, \boldsymbol{B}, \Phi_{AB})$, with changing AB field ξ, for different diatomic molecules with the Hulthén plus Yukawa potential.

The magnetization $M(\beta, \boldsymbol{B}, \Phi_{AB})$ and magnetic susceptibility $\chi_m(\beta, \boldsymbol{B}, \Phi_{AB})$ for various diatomic molecules with the Hulthén plus Yukawa potential are presented in Figure 4.20 and Figure 4.21, respectively. Figures 4.20(a), 4.20(b), and 4.20(c) depict the magnetization $M(\beta, \boldsymbol{B}, \Phi_{AB})$ plotted against temperature $\beta(K^{-1})$, magnetic field $\boldsymbol{B}(T)$, and the Aharanov–Bohm field ξ, respectively, for different diatomic molecules with the Hulthén plus Yukawa potential. It is evident, from these fugues that the magnetization $M(\beta, \boldsymbol{B}, \Phi_{AB})$ increases with temperature $\beta(K^{-1})$, while it linearly decreases with

the rise in magnetic field $\boldsymbol{B}(T)$. Moreover, the magnetization $M(\beta, \boldsymbol{B}, \Phi_{AB})$ remains constant as the Aharanov–Bohm field ξ increases.

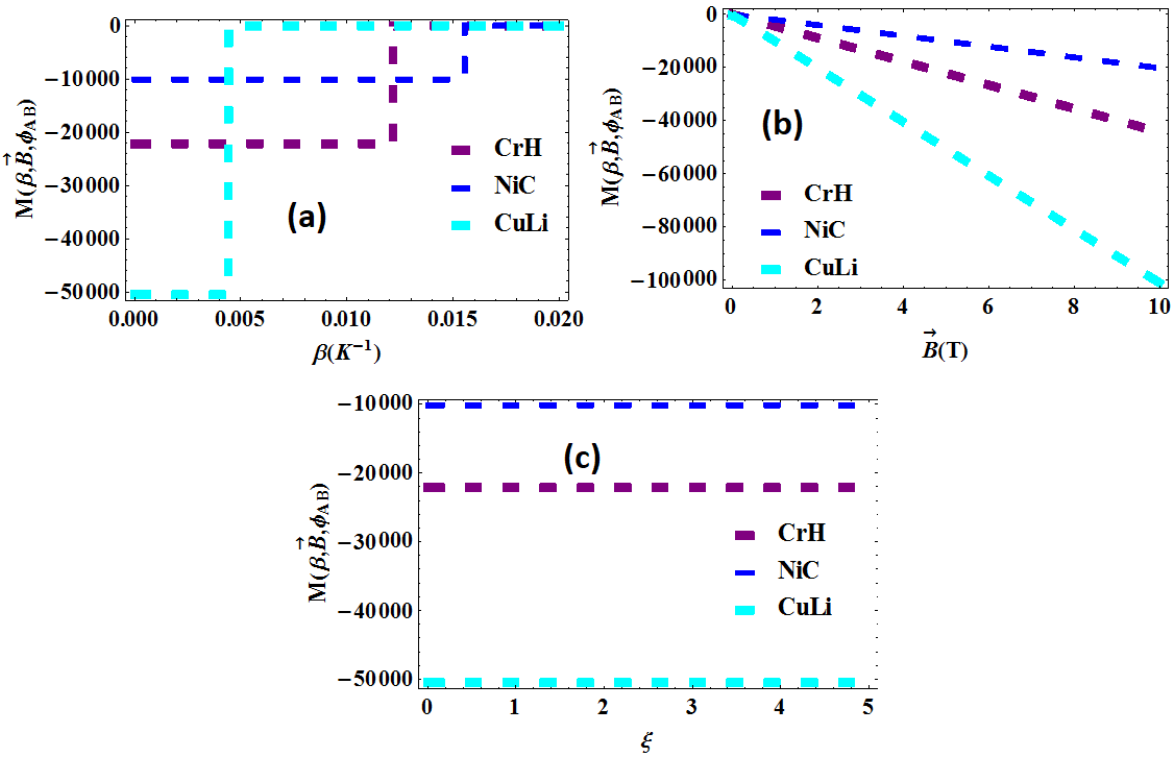

Figure 4.20: The magnetization $M(\beta, \boldsymbol{B}, \Phi_{AB})$ of the Hulthén plus Yukawa potential with (a) temperature $\beta(K^{-1})$, (b) magnetic field $\boldsymbol{B}(T)$ (c) AB field ξ, for different diatomic molecules.

In Figures 4.21(a), 4.21(b), and 4.21(c), we have depicted the variation of magnetic susceptibility $\chi_m(\beta, \boldsymbol{B}, \Phi_{AB})$ with respect to temperature $\beta(K^{-1})$, magnetic field $\boldsymbol{B}(T)$, and the Aharanov–Bohm field ξ for different diatomic molecules, modeled using the Hulthén plus Yukawa potential. It is evident that magnetic susceptibility $\chi_m(\beta, \boldsymbol{B}, \Phi_{AB})$ increases with temperature $\beta(K^{-1})$, decreases with magnetic field $\boldsymbol{B}(T)$, and exhibits an upward trend with increasing Aharanov–Bohm field ξ.

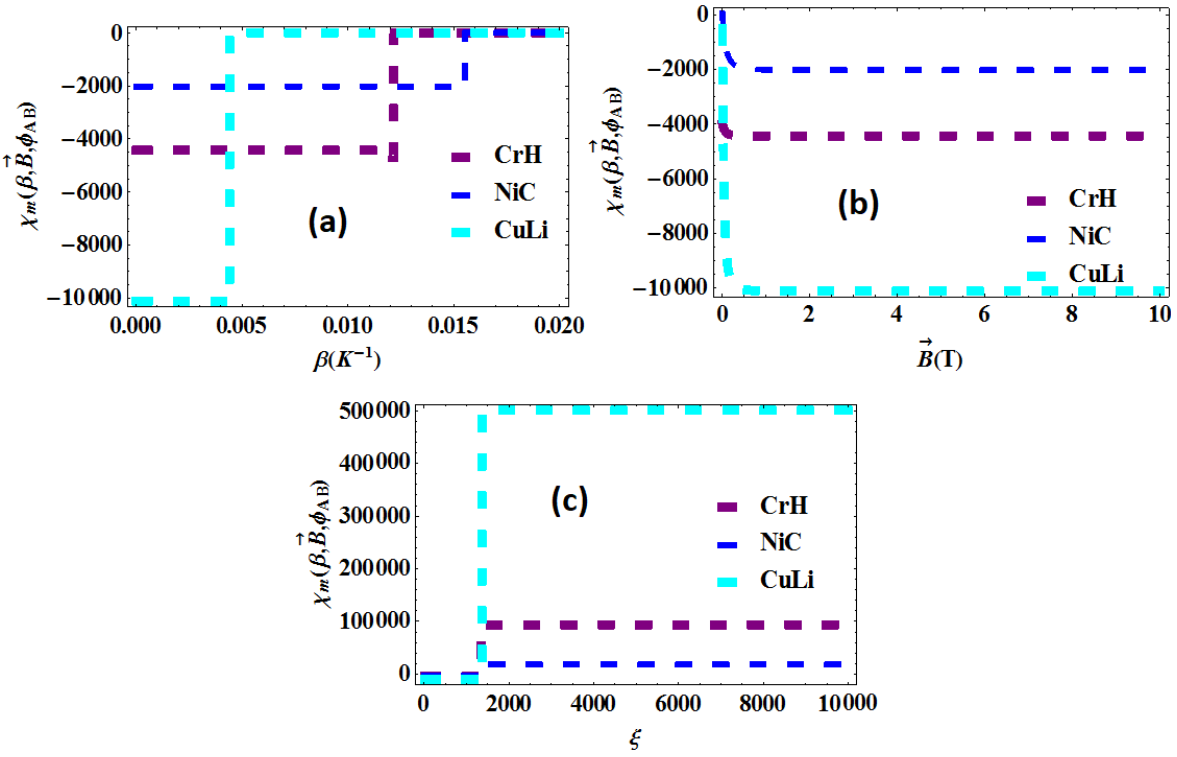

Figure 4.21: The variation of the magnetic susceptibility $\chi_m(\beta, \boldsymbol{B}, \Phi_{AB})$ of the Hulthén plus Yukawa potential with (a) temperature $\beta(K^{-1})$, (b) magnetic field $\boldsymbol{B}(T)$, (c) AB field ξ, for different diatomic molecules.

Chapter 5

Concluding Remarks

In the first part of this study, we applied the Nikiforov-Uvarov technique to solve the radial the time-independent Schrödinger equation within the context of the Manning-Rosen plus a class of Yukawa potential model. We obtained expressions for the energy eigenvaluesand the wave function corresponding to this composite potential model. By utilizing the closed-form Euler-Maclaurin formula, we computed the vibrational partition function as well as other thermodynamic functions including the vibrational free energy, mean vibrational energy, vibrational entropy, and specific heat capacity for the system. The energy eigenvalues, partition function, and other thermodynamic functions were evaluated with respect to different parameters such as the screening parameter, potential strength, reduced mass, principal quantum number, and angular momentum quantum number. Our numerical analysis involved plotting the results and engaging in a comprehensive discussion on how temperature affects these thermodynamic properties with respect to different screening parameters and quantum states. Our graphical representations indicated a decrease in energy with increase in the screening parameter, reduced mass, and potential strength, while energy exhibited an increasing trend with higher quantum states. This analysis underscores the significant influence of the screening parameter and quantum states on the energy and thermodynamic characteristics of the Manning-Rosen combined with the Yukawa potential model.

We also solved the Schrödinger equation by employing the Hulthén plus Yukawa potential model through the Nikiforov-Uvarov approach. We derived both the energy

equation and the wave function. Using the resultant energy spectra, we calculated the vibrational partition function and various thermodynamic functions such as the vibrational free energy, mean vibrational energy, vibrational entropy, and vibrational specific heat capacity for CuLi, CrH, and NiC diatomic molecules. Our numerical computations on the energy spectra were performed by adjusting the quantum states. Simultaneously, we calculated the partition function and other thermodynamic functions at different temperatures and the maximum quantum number. The analysis of the results showed that the energy increased with the rise in quantum states. Additionally, except for CrH, the specific heat capacity for the selected diatomic molecules reached saturation for large values of the principal quantum number in the classical limit.

To investigate the influence of external magnetic and Aharonov-Bohm flux fields on thermodynamic properties, we utilized the exact quantization rule to solve the 2-dimensional Schrödinger equation incorporating the Hulthén plus Yukawa potential. Subsequently, the energy spectra derived were employed to compute various thermomagnetic functions including the vibrational partition function, as well as the vibrational free energy, mean energy, entropy, and specific heat capacity, alongside magnetization and magnetic susceptibility, for diatomic molecules CuLi, CrH, and NiC. Numerical computations were conducted while varying temperature, magnetic field, and Aharonov-Bohm field, respectively. Graphical representations were utilized to elucidate the impact of external fields on the thermodynamic characteristics of the aforementioned diatomic molecules. Our results unveiled comparable behaviour in the magnetic susceptibility of the system at both zero and finite temperatures. We illustrated that the system exhibits an irregular response to magnetic fields and is notably sensitive to the Aharonov-Bohm field. As seen from our analysis, it is evident that as temperature rises, magnetization increases, while it decreases linearly with an increase in magnetic field. Additionally, magnetization remains steady with the increase of the

Aharanov–Bohm field. Our study also revealed that when the Aharonov-Bohm field varies with a constant magnetic field, the magnetic susceptibility of CuLi, CrH, and NiC diatomic molecules increases, corroborating previous research. These discoveries offer exciting prospects for applications in chemical, atomic, and condensed matter physics.

Bibliography

[1] S M Ikhdair, and B J Falaye, *Chem. Phys* **421**, 84 (2013)

[2] C Berkdemir, *J. Math. Phys* **46** , 13 (2009)

[3] M M Nieto, *Am. J. Phys* **47** , 1067 (1979)

[4] S M Ikhdair, and R Sever, *J. Mol. Struc* **806**, 155 (2007)

[5] C Berkdemir, *Application of the Nikiforov-Uvarov Method in Quantum Mechanics*, The Pennsylvania State University, Usa, (2012)

[6] P M Morse, *Phys. Rev* **34**, (1929)

[7] Gh E Drăgănescu, and N M Avram, *Can. J. Phys* **76**, 4 (1998)

[8] T A Akanbi, C A Onate, and O Y Oludoun, *AIP Adv.* **11** 045213 (2021)

[9] R J Leroy, and R B Bernstein, *J. Chem. Phys* **52**, 8 (1970)

[10] J M Cai, P Y Cai, and A Inomata, *Physicall Rev. A.* **34**, 6 (1986)

[11] A I Ahmadov, M Demirci, S M Aslanova, M Sh Orujova, and M F Mustamin, *Phys. Lett A* **384**, 12 (2020)

[12] C -S Jia, L -H Zhang, C -W Wang, *Chem. Phys. Lett* **667**, 211 (2017)

[13] A Hesam, H Nikoofard, M Sargolzaei, *Chem. Phys. Lett* **764** 138276 (2021)

[14] G Pöschl, E Teller, *Z. Phys.,* **83**, 143 (1933)

[15] W A Yahya, and K J Oyewumi, *Journal of the Association of Arab Universities for Basic and Applied Sciences* **21**, 53 (2016)

[16] C O Edet, P O Amadi, U S Okorie, A Tas, A N Ikot, and G J Rampho, *Rev. Mex. Fis***66**, 824 (2020)

[17] E Omugbe, O E Osafile, I B Okon, *Eur. Phys. J. Plus,* **136** 740 (2021)

[18] Z H Deng, Y P Fan, *Shandong Univ. J* **7**, 162 (1957)

[19] P -Q Wang, L -H Zhang, C -S Jia and J -Y Liu, *J. Mol. Spect* **274** , 5 (2012)

[20] H. Hassanabadi, B. H. Yazarloo, S. Zarrinkamar, and H. Rahimov, *Commun. Theor. Phys.,* **57**, 339 (2012)

[21] D Nath, and A K Roy, *Quantum Chem* **121** 10 (2021)

[22] H Yukawa, *proc. phys. math. Soc. Jpn* **17**, 48 (1935)

[23] M Hamzavi, M Movahedi, K -K Thylwe, and A A Rajabi, *Chin. Phys. Lett* **29**, 8 (2012)

[24] M Napsuciale, and S Rodríguez, textitPhys. Lett. B., **816** 136218 (2021)

[25] L Hulthen, *Ark. mat. astron. Fys A* **28**, 5 (1942)

[26] L Hulthen, *Ark. mat. astron. Fys. B* **29**, 1 (1942)

[27] S M Ikhdair, and R Sever, *J. Math. Chem* **42** 461 (2007)

[28] A N Ikot, B C Lutfuoglu, M I Ngweke, M E Udoh, S Zare and H Hassanabadi, *Eur. Phys. J. Plus* **131**, 419 (2016)

[29] H. I. Ahmadov, S. I. Jafarzade, and M. V. Qocayeva, *Int. J. M Phys. A* **30** 32 (2015)

[30] A I Ahmadov, M Naem, M V Qocayeva, and V A Tarverdiyeva, *int. J. Mod. Phys. A,* **33** , 1850021 (2018)

[31] M F Manning, *Phys. Rev* **44**, 951 (1933)

[32] M F Manning, N Rosen, *Phys. Rev.,* **44**, 953 (1933)

[33] A I Ahmadov, S M Aslanova, M S Orujova, S V Badalov, S -H Dong, *Phys Lett A* **383**, 24 (2019)

[34] S H Dong, *Factorization method in Quantum Mechanics*, Armsterdam: Springer, (2007)

[35] H Ciftci, R L Hall, and N Saad, *J. Phys. A: Math Gen* **36** , 11807 (2003)

[36] B J Falaye, *Cent. Euro. J. Phys* **10**, 960 (2012)

[37] G Chen *Phys. Lett. A* **326** , 55 (2004)

[38] A N Ikot, H P Obong, T M Abbey, S Zare, M Ghafourian and H Hassanabadi, *Few-Body Systems (Berlin: Springer)*, (2016)

[39] A Suparmi, C Cari, and B N Pratiwi, *J. Phys: Conf. Series* **710**, 012026 (2016)

[40] C A Onate, M C Onyeaju, A N Ikot and J O Ojonubah, *Chin. J. Phys* **000**, 1 (2016)

[41] A N Ikot, O A Awoga, A D Antia, H Hassanabadi and E Maghsodi, *Few-Body Syst* **54** 2041 (2013)

[42] M R Setare, and E Karimi, *Phys. Scri* **75**, 90 (2007)

[43] S M Ikhdair, and R Sever, *J. Math. Chem* **45**, 1137 (2009)

[44] A N Ikot, U S Okorie, P O Amadi, C O Edet, G Rampho, and R Sever, *Few-Body Syst* **62**, 9 (2021)

[45] E Witten, *Nucl. Phys. B* **188** , 513 (1981)

[46] F Cooper, and B Freedman, *Ann. Phys* **146**, 262 (1983)

[47] M Aktaş, and R Sever, *J. Mol. Str* **710**, (2004)

[48] L Infeld, and T E Hull, *Hull, Rev. Mod. Phys* **23**, 21 (1951)

[49] H Ciftci, R L Hall, and N Saad, *J. Phys. A: Math. Gen* **36**, 11807 (2003)

[50] H Ciftci, R L Hall, N Saad, *J. Phys. A: Math. Gen* **38**, 1147 (2005)

[51] R E Moss, *Am. J. Phys* **55**, 397 (1987)

[52] G Esposito, and P Santorelli, *J. Phys. A. Gen* **32**5643 (1999)

[53] M Hamzavi, A A Rajabi, and H Hassanabadi, *Phys. Let. A* **374**, (2010)

[54] E Olğar, H Dhahir, and H Mutaf, *Open Physics* **12**, 4 (2014)

[55] A J SOUS, *J. App. Math. Phys* **3**, 1406 (2015)

[56] A N Ikot, U Okorie, A T Ngiangia, C A Onate, C O Edet, I O Akpan, P O Amadi, *Ecl. Quím. J.* **45**, 1 (2020)

[57] E Schrödinger, *Ann. Phys* **384**, 4 (1926)

[58] M J Englefield, *J. Math. An. Appl* **48** 270 (1974)

[59] S Miraboutalebi, and L Rajaei, *J. Mat Chem* **134** , 60 (2019)

[60] S Miraboutalebi, *Eur. Phys. J. Plus* **135**, 16 (2020)

[61] F Iachello, *Chem. Phys. Lett* **78** 581 (1981)

[62] F Iachello, and S Oss, *J. Chem. Phys* **104**, 6954 (1996)

[63] O S Van Roosmalen, A E Dieperink, and F Iachello, *Chem. Phys. Lett* **85**, 52 (1982)

[64] F Iachello, and M Ibrahim, *J. Phys. Chem. A* **102** 9427 (1998)

[65] J Choudhury, *Chin. J. Phys* **51**, 3 (2013)

[66] I Prigogine and S A Rice, *Frontmatter. Adv. in Chem. Phys.*, (1974)

[67] Z Q Ma, and B W Xu, *Int. J. Mod. Phys. E* **14**, 599 (2005)

[68] Z Q Ma, and B W Xu, *Europhys. Lett* **69**, 685-691 (2005)

[69] S H Dong, D Morales, J Garćıa-Ravelo, *Int. J. Mod. Phys. E,* **16** 189 (2007)

[70] P. R. Kumar, and S.H. Dong, *Phys. Lett. A* **417**, 127700 (2021)

[71] U S Okorie, A N Ikot, M C Onyeaju, and E O Chukwuocha, *J. Mol. Mod* **24**, 289 (2018)

[72] J Y Liu, X T Hu, and CS Jia, *Can. J. Chem* **92**, (2014)

[73] A N Ikot, U S Okorie, G J Rampho, P O Amadi, C O Edet, I O Akpan, H Y Abdullah and R Horchani, *J. Low Temp. Phys* **202** , 269 (2021)

[74] A F Nikifirov and V B Uvarov, *Special Functions of Mathematical Physics* Birkhäuser: Basel (1988)

[75] C O Edet, U S Okorie, A T Ngiangia and A N Ikot, *Ind. J. Phys* **94** , 425 (2019)

[76] S A Ekong, U S Okorie, A N Ikot, I B Okon, L F Obagboye, H Y Abdullah, R Sever, and K. W Qadir, *Eur. Phys. J. Plus***138** 364 (2023) *Bulg. J. Phys* **45** 323 (2018)

[77] E B Ettah, *Eur. J. App. Phys***3** 5 (2021)

[78] M E Udoh, P O Amadi, U S Okorie, A D Antia, L F Obagboye, R Horchani, N Sulaiman, and A N Ikot, *Pramana* **96**, 222 (2022)

[79] R Khordad, and A Ghanbari, *Comp. Theor. Chem* (2019)

[80] A N Ikot, E O Chukwuocha, M C Onyeaju, C A Onate, B I Ita and M E Udoh, *Pramana J. Phys* **90**, 22 (2018)

[81] K Chabi, and A Boumali, *Rev. Mex. Fis* **66**, 1 (2020)

[82] H R Rastegar-Sedehi, *Eur. Phys. J. Plus* **136**, 514 (2021)

[83] C Tavares, S Oliveira, V Fernandes, A Postnikov, and M I Vasilevskiy, *Soft Comput* **25**, 6807–6830 (2021)

[84] SK Tokunaga, J M Dyne, E A Hinds, and M R Tarbutt, *New J. Phys.* **11**, 055038 (2009)

[85] A N Ikot, C O Edet, P O Amadi, U S Okorie, G J Rampho, and H Y Abdullah, *Eur. Phys. J. D* **74** , 159 (2020)

[86] C O Edet, and A N Ikot, *Eur. Phys. J. Plus* **136**, 1–11 (2021)

[87] O Negrete, F Peña, and P Vargas, *Entropy* **20**, 888 (2018)

[88] S M Ikhdair, B J Falaye, M Hamzavi, *Ann. Phys.* **353**, 282–298 (2015)

[89] B J Falaye, K J Oyewumi†, F Sadikoglu, M Hamzavi, and S M Ikhdair, *J. Theo. Comp. Chem.* **14**, 5 (2015)

[90] L G M Pettersson, S R Langhoff, D P Chong, *J. Chem. Phys.* **85**, 2836 (1986)

[91] C W Bauschlicher Jr., S R Langhoff, H Partridge, S P Walch, *J. Chem. Phys.* **86**, 5603 (1987)

[92] C W Bauschlicher Jr., P E M Siegbahn, *Chem. Phys. Lett.* **104**, 331 (1984)

[93] I Shim, K A Gingerich, *Chem. Phys. Lett.* **303**, 87 (1999)

[94] C L Tang, *Fundamentals of Quantum Mechanics: For Solid State Electronics and Optics*, Cambridge University Press, Cambridge, (2005)

[95] C O Edet, and P O Okoi, *Rev. Mex. Fis* **65**, 333 (2019)

[96] C O Edet, P O Okoi, S O Chima, *Rev. Bras. Ens. FÃs* **42**, e20190083 (2019)

[97] C O Edet, K O Okorie, H Louis, and N A Nzeata-Ibe, *Ind. J. Phys.* **94**, 243 (2020)

[98] P O Okoi, C O Edet, and T O Magu, *Rev. Mex. Fis.* **66**, 1 (2020)

[99] U S Okorie, A N Ikot, C O Edet, I O Akpan, R Sever and G J Rampho, *J. Phys. Comm* **3**, 095015 (2019)

[100] H Louis, B I Ita, O U Akakuru, N A Nzeata-Ibe, A I Ikeuba, T O Magu, P I Amos, and C O Edet, *Oriental J. Phys. Sci* **3**, 1 (2018)

[101] C O Edet, P O Okoi, A S Yusuf, P O Ushie, and P O Amadi, *Ind. J. Phys* **95**, 471 (2021)

[102] I N Levine, *Quantum Chemistry*, Prentice Hall, (2008)

[103] S Flügge, *Practical Quantum Mechanics II*, Springer, Berlin, (1971)

[104] G Sezgo, *Orthogonal Polynomials*, American Mathematical Society, New York, (1939)

[105] J Wang, C -S Jia, C -J Li, X -L Peng, L -H Zhang, J -Y Liu, *ACS Omega*, **4** 19193–19198 (2019)

[106] C -S Jia, R Zeng, X -L Peng, L -H Zhang, Y -L Zhao, *Chem. Eng. Sci.*, **190** 1–4 (2018)

[107] C O Edet, A N Ikot, M C Onyeaju, U S Okorie, G J Rampho, M L Lekala, S Kaya, *Phys. E*, **131** 114710 (2021)

[108] H R Sedehi, and Khordad, R, *Physica E*, **134** 114886 (2021)

[109] M Habibinejad, A Ghanbari, *Eur. Phys. J. Plus* **136** , 400 (2021)

[110] B Keller *Statistical Thermodynamics*

[111] O Edet, P O Amadi, M C Onyeaju, U S Okorie, R Sever, G J Rampho, H Y Abdullah, I H Salih and A N Ikot, *J. Low Temp. Phys.* **202** , 83 (2021)

[112] M L Strekalov, *Chem. Phys. Lett* **439** , 209 (2007)

[113] L D Blokhintsev, V O Eremenko, B F Irgaziev, *Yu.V. Orlov. Bull. Russ. Acad. Scie., Phys* **75**, 4 (2011)

[114] V I Kovalchuk, V K Tartakovsky, I V Koslovsky, *Ukr. J. Phys* **53**, 8 (2008)

[115] L D Blokhintsev, V O Eremenko, B F Irgaziev, *Yu.V. Orlov. Bull. Russ. Acad. Scie., Phys* **71**, 3 (2007)

[116] R L Greene, and C Aldrich, *Phys Rev A.,* **14** , 2363 (1976)

[117] A Boumali, and H Hassanabadi, *Eur. Phys. J. Plus.* **128** 124 (2013)

[118] G Andrews, R Askey, and R Roy, *"Special Functions"*, Cam- bridge University Press, Cambridge, (1999)

[119] M Abramowitz and I A Stegun, *Handbook of Mathematical Functions,* Dover, New York, NY, USA, (1964)

[120] C O Edet, A N Ikot, *J. Low Temp. Phys* (2021)

[121] R Horchani, and H Jelassi, *Chem. Phys* **532**, 110692 (2020)

[122] R Khordad, and A Ghanbari, *J. Low Temp. Phys* **199**, 1198 (2020)

[123] A Boumali, *J. Math. Chem.* **56**, 1656 (2018)

[124] G Arfken, *Mathematical Methods for Physicists* 3rd Ed., Academic Press, Orlando, 327, (1985)

[125] C -S Jia, L -H Zhang, X -L Peng, J -X Luo, Y -L Zhao, J -Y Liu, J -J Guo, and L -D Tang *Chem. Eng. Sci.* **202**, 70–74 (2019)

[126] C O Edet, P O Amadi, M C Onyeaju, U S Okorie, R Sever, G J Rampho, H Y Abdullah, I H Salih and A N Ikot, *J. Low Temp. Phys* **202**, 83–105 (2021)

[127] G J Rampho, A N Ikot , C O Edet and U S Okorie, *Mol. Phys.* (2020)

[128] K J Oyewumi, B J Falaye, C A Onate, O J Oluwadare and W A Yahya, *Molecular Phys.* **112** , 127 (2014)

[129] K J Oyewumi, O J Oluwadare, K D Sen and O A Babalola, *J. Math. Chem.* **51**, 976 (2013)

[130] C O Edet, and P O Okoi, *Rev. Mex. Fis* **65**, 333 (2019)

[131] O J Oluwadare, K J Oyewumi, *Eur. Phys. J. Plus* **133,** 422 (2018)

[132] Co Edet, and A N Ikot, *BRIAC* **12,** 3 (2022)4126